A Trace Element Study of Sediments from the Olifants River Estuary, the Berg River Estuary, and the Off-Shore Mud Belt

A Dissertation
Presented to
The Science Faculty

By,

Arthur Taylor

In Partial Fullfillment
Of the Requirements for the Degree

Master of Science in Environmental Geochemistry

Department of Geological Sciences

University of Cape Town
November 2004

Acknowledgements

Thank you to my two supervisors, Dr. John Compton and Dr. Alakendra Roychoudhury for guidance, advice, sampling assistance, and knowledge transfer; and most importantly, support.

Thank you to Meris Smith for always keeping your door open and answering my endless questions.

Thank you to Heather Sessions for allowing me to use the C:H:N analyzer at MCM.

Thank you to Ernest for fusing many an XRF disc for me and keeping me company in the lab while I prepared sulfur pellets.

Thank you to Fayrooza Rawoot for assistance with the ICP-MS digestions.

Thank you to Amy Mackowski for helping me get through this project.

Thank you to Roisin DeBurca, Conrad Savy and Dana Rosenstein for assistance proofreading this work.

Thank you to everyone else who helped along the way.

ABSTRACT

Trace elements have received increased attention since the mid-1900's. Although some studies have investigated trace element accumulation as a result of urban expansion in the Western Cape, South Africa, few have catalogued the accumulation and behavior of trace elements resulting from agricultural practices. This study investigates the distribution and behavior of trace elements for the Olifants and Berg river catchments by focusing on the sediments of the estuaries. The dominant industry in both catchments is agriculture and the there exists relatively little urban sprawl. Two sediment samples taken from the offshore mud belt in the vicinity of the two river mouths were also analyzed.

The sediments were analyzed for trace elements using inductively coupled plasma mass spectrometry (ICP-MS), major elements using X-ray fluorescent spectroscopy (XRF), total sulfur using XRF, total and organic carbon using a C:H:N analyzer, and grain size analysis was performed (>62 μm, 38-63 μm, 2-38 μm, <2μm). The mud belt cores were dated using ^{14}C dating. Estuarine surface waters were analyzed for trace elements, pH, dissolved oxygen (DO), electrical conductivity (EC), and temperature. The trace elements arsenic (As), cadmium (Cd), copper (Cu), lead (Pb), and zinc (Zn) were focused on.

The trace element concentrations in the sediments were compared with those of soils that occur in the study area, as well as their parent materials, to determine background concentrations. The concentration profiles of elements with respect to depth are compared with natural deposition rates to recognize signs of recent enrichment of individual trace elements. Inter-element comparisons are made in an attempt to determine speciation. Comparison between the estuarine and mud belt sediments were made to assess the estuaries ability to filter fluvial trace elements, as well as to determine the sediment contributions of the Olifants and Berg rivers to the mud belt. Statistical analysis was performed to group sediment populations.

Trace element and organic matter concentrations showed strong positive correlations with fine-sized particles. The mud belt sediments displayed considerably more OC than the

estuarine sediments. The trace elements appear to associate predominantly with clay minerals (alumino-silicates), Fe/Mn oxides, and organic matter. Trace element correlations with S and carbonate carbon were also observed. Comparison with estimates of natural deposition rates and compositions of soils occurring in the catchments did not suggest an anthropogenic pollution input. From the data available the estuarine and Mud Belt sediments appear enriched in Cd, Cu and Zn in comparison to the background soils. The estuaries seem to effectively trap Zn and Pb, but do not capture As well. Statistical analysis suggest that, of the rock types considered, the sediments of the Olifants and Berg river estuaries and those of the off shore mud belt are most similar to sediments derived from the Malmesbury and Ecca Groups.

The Olifants and Berg rivers are important sources of water for the farming community, as well as for municipal use in the Western Cape. Based on this investigation of the estuarine waters and sediments the rivers appear to be in good health in regards to trace element concentrations.

Table of Contents

List of Tables

List of Tables and Figures

1 Introduction

All metals occur in the environment naturally, varying from high to minute concentrations. The latter are often referred to as "trace metals" or "trace elements" and will be the focus of this study. The number and scope of investigations of the chemical properties and environmental interactions of trace elements have increased dramatically since the mid-1900s (Davies, 1980, Shacklette, 1985). The increased attention to trace elements is a result of the discovery that some are essential to life at low concentrations (e.g. Adriano, 2001; Jenkin & Wyn Jones, 1980), but at elevated concentrations they prove toxic to living things, including humans (e.g. Fergusson, 1990; Thomspon, 1990). The bioavailability of metals is dependent on quantity as well as speciation. Therefore in order to recognize the health risks associated with trace elements it is necessary to identify the quantities they exist in as well as their speciation.

The inputs of many trace elements from terrestrial and atmospheric sources to the aquatic environment have increased in recent years (Baut-Mènard, 1984). This is largely attributed to human activity. Since the industrial revolution, humans have increasingly polluted the environment with trace elements through the burning of fossil fuels, waste dumping, agricultural run-off, sewage effluent, urban run-off and industrial practices such as mining, smelting and numerous other production processes that involve metals. These activities have put bodies of water under increased pressure from pollution. In South Africa, rivers of the Western Cape receive a considerable amount of mineral pollution from urban and rural sources, mainly in the form of factory effluents, purified sewage and run-off from farmlands (Fourie & Steer, 1971). Some studies have investigated trace element accumulation as a result of urban expansion in the Western Cape (e.g. Haniff, 2002), but few have catalogued the accumulation and behavior of trace elements resulting from agricultural practices. The Olifants and Berg River catchments in the Western Cape, South Africa, were chosen as a focus for study because the major industry of the area is agriculture and the catchments contain relatively little urban sprawl (Basson, et al., 1998; Fourie & Steer, 1971).

Trace elements are found in pesticides, insecticides, herbicides, silvisides, and fertilizers used in agricultural practices (Adriano, 2001). For example, cadmium (Cd) concentrations in phosphate

fertilizers range from 7 to 170 ppm (Kabata-Pendias and Pendias, 1985). Some of the more common trace elements utilized in the farming industry are arsenic (As), cadmium (Cd), copper (Cu), lead (Pb), and zinc (Zn). Thus these trace elements will be focused on in this investigation. The trace elements added to soils through farming practices can be leached from the soils into surface or ground water, especially where intensive irrigation is practiced. In addition to the anthropogenic input, soils naturally contain trace elements inherited from the parent material the relative concentrations of which vary (Adriano, 2001; Kabata-Pendias and Pendias, 1985; Jenkins & Wyn Jones, 1980). The mobility of trace elements in soils are largely determined by the stability of the host mineral in the particular weathering environment (Jenkins & Wyn Jones, 1980). Farming practices can also result in increased trace element inputs to surface and ground waters by increasing erosion. On a per mass basis sediments are the principle carriers of heavy metals in the hydrosphere (Salomons & Förstner, 1984). Estuaries act as sediment traps for suspended particles carried by rivers (Schubel, J.R. & Kennedy, V.S., 1984). For this reason the focus of this investigation will be on the sediments of the Olifants and Berg river estuaries. The state of an estuary often tells a great deal about the state of the rivers and groundwater that feed it. Monitoring of an estuary can help determine the optimum water management practices for sustaining a healthy river.

1.1 Project Aims

The Berg River is of particular importance in the Western Cape as it is the major source of municipal and industrial water (Hall and Gorgens, 1978). The major industry in the Olifants and Berg river catchments is agriculture. Since the majority of the Olifants and Berg river catchments fall in a semi-arid region the livelihood of the farms are highly dependent on surface water resources. In addition, the Olifants River is considered ecologically important. The Olifants River contains eight species of endemic fish, the highest number of any river south of the Zambezi; 2 species considered vulnerable, 3 endangered and 3 others considered critically endangered (Basson, et al., 1998). In addition, the Olifants and Berg river estuaries are of international importance for birds. Thus, water quality is of supreme importance to the entire region. An important aspect of water quality is the level of trace elements, which in elevated concentrations can prove toxic to living things (Fergusson, 1990; Thomspon, 1990).

The goals of this investigation are to:

- Determine the extent to which the Olifants and Berg river systems are polluted with trace elements.
- Evaluate the estuaries ability to trap trace elements.
- Assess where the trace elements input to the estuary originate.
- Determine the speciation and potential mobility of trace elements in the estuarine sediments and how it changes with depth.

To this end, the total concentrations of trace and major elements in sediments of the Olifants and Berg river estuaries were investigated. Trace element analysis of the estuarine surface waters was also performed. The trace element concentrations in the sediments were compared with those of soils that occur in the study area, as well as their parent materials, to determine background concentrations. The concentration profiles of elements with respect to depth are compared with natural deposition rates to recognize signs of recent enrichment of individual trace elements. In addition, inter-element comparisons are made in an attempt to determine speciation. Grain size analysis is performed to give insight to estuarine sedimentation dynamics as well as trace element-particle size distribution.

Major and minor elemental analysis was performed on two sediments samples taken from the coastal shelf in the vicinity of the Olifants and Berg river mouths. Comparison with the estuarine sediments were made to assess the estuaries ability to filter fluvial trace elements, as well as to determine the sediment contribution of the Olifants and Berg rivers to the near shore mud belt off the west coast of southern Africa. Statistical analysis was performed to group sediment populations.

1.2 Literature Review

For the purposes of assessing the source, behavior and fate of trace metals in the near coastal environment it is necessary to understand the transport mechanisms of sediments and waters in the riverine and offshore environments, as well as the chemical reactions that occur within waters, sediments and at the water-sediment interface. In investigating an area it is also necessary to gather estimates of the natural levels of trace metals in the region in assessing the possible sources, both anthropogenic and natural, of trace elements to surface waters. The ability of an estuary to trap trace metals as well as their ability to tolerate disturbances vary from estuary to estuary. Although comparisons will be made with other estuarine studies and assumptions

will be made of the Olifants and Berg River estuaries based on these studies, it is important to note that estuaries behave individually.

1.2.1 Trace Element Inputs In the Near-Coast Environment

The primary source of trace elements in the ocean is considered to be the atmosphere (Buat-Mènard, 1984). Fergusson (1990) suggests that 90% of lead and 50% of cadmium in the ocean come from the atmosphere. However, in the coastal environment the riverine inputs may outweigh those of the atmosphere, especially when the particulate material is considered. There are numerous sources of trace elements in the offshore environment (Fig. 1.2.1.A). The two atmospheric inputs are aerosols and wind blown dust. The former generally come from anthropogenic sources and can have lifetimes of minutes to 40 days depending on particle size (Fergusson, 1990). Because of the strong winds characteristic of the study area (Heydorn & Tinley, 1980) this can equate to substantial travel distances. Trace element concentrations in the atmosphere increase significantly in urban areas. The upwelling of deep-sea waters enriched in trace elements (Burton & Statham, 1990), characteristic of the west coast of southern Africa (Shannon, 1990), act as a source of trace elements to the nearshore environment. For example, Cd concentrations show significant increases in areas of upwelling (Burton & Statham, 1990). The riverine contribution of trace elements to the estuary is largely dependent on geology of the catchment and the human activities influencing trace element fluxes into waters.

The primary natural source of trace elements to surface waters is from rocks and the soils formed from those parent materials. Trace metals make it into surface waters either via leaching of the rocks and soils or as sediments via erosion of rocks and soils. The leachability and erodibility of the geological formations contribute significantly to the sediment load of a river. Anthropogenic habits, such as land clearing, irrigation, and construction increase erosion; in turn increasing sediment loads of the rivers. In a study by Wolman (1967), clearing a forested area increased the sediment yield 4 to 8 times. High levels of rainfall or irrigation increase the potential for metals to reach surface waters in both dissolved and particulate form. Flooding often has a dramatic effect on the sediment yield of a river. The Potomac River, USA, deposited 70% of its annual sediment in 10 days of heavy flow during two consecutive years (Wark & Keller, 1963). The bulk of the suspended sediments carried by rivers are eventually trapped in their estuaries (Schubel, 1971).

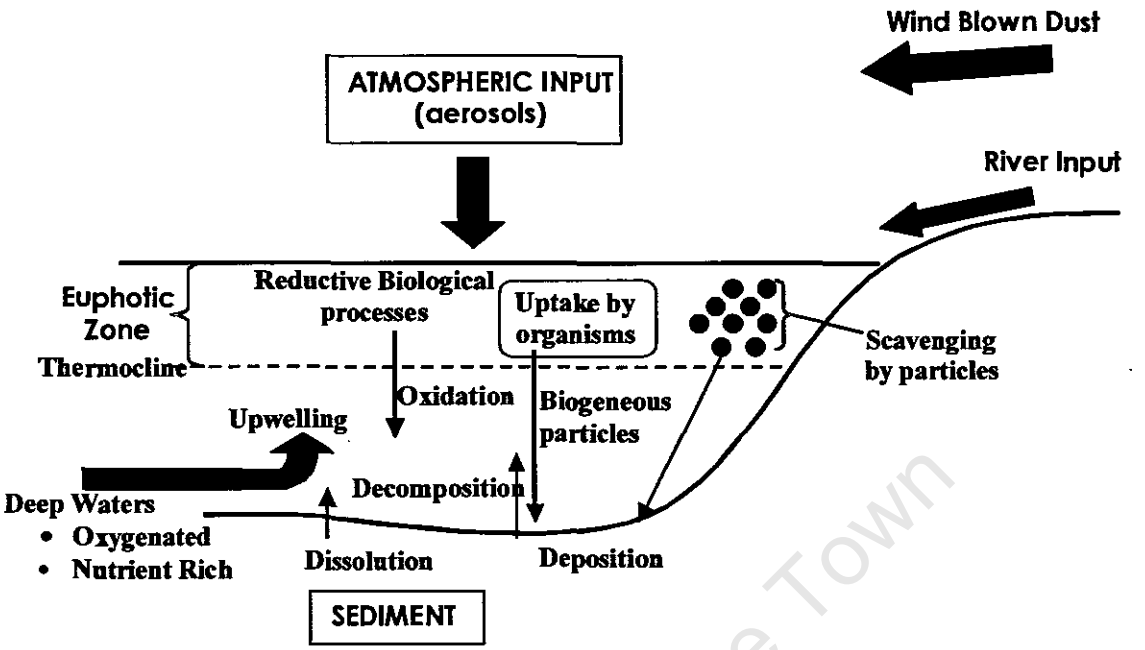

Figure 1.2.1.A. Trace Element Dynamics in the Offshore Environment– inputs, processes, and recycling

There is considerable trace element cycling in the near shore environment (Shannon, 1990). Trace elements are taken up by organisms and brought to depth with decaying matter. Upon decomposition the trace elements are released back into the water column or repartitioned in the sediment (Burton & Statham, 1990). Dissolved trace elements are scavenged by particles and deposited on the sea floor. Dissolution of trace elements from sediments can then occur as witnessed for Zn in the Chesapeake Bay, USA (Bradford, 1972).

Some of the common anthropogenic sources of select trace elements are given in Table 1.2.1.A. Adriano (2001) gives a good account of the uses of many trace elements. Some of the agricultural uses of As, Cd, Cu, Pb and Zn are summarized here. Until the development of organic pesticides in the 1940s Ca-arsenate and Pb-arsenate were the backbone of the insecticide industry. The As containing herbicides MSMA and DSMA are some of the largest volume pesticides in use and account for more than 90% of As used in the farming industry (Adriano, 2001). Lead is also used in herbicides, but has been banned in some countries, but remains in use in South Africa. Arsenic and Cu are both used as feed additives, mainly for poultry.

Cadmium, Cu and Zn are all used in fertilizers, although environmental concerns regarding Cd have resulted in decreased use.

Table 1.2.1.A. Some common uses of select trace elements, the populations affected by elevated concentrations and the human health risks (taken from Brady & Weil, 1999).

Element	Major uses and sources	Population effected	Human health effects
Arsenic	Pesticides, plant desiccants, animal feed additives, coal and petroleum, mine tailings, and detergents.	Humans, land animals, fish, birds	Cumulative poison, possibly cancer.
Cadium	Electroplating, pigments for plastics and paints, plastic stabilizers, batteries, and phosphate fertilizers.	Humans, land animals, fish, birds, plants	Heart & Kidney disease, bone embrittlement.
Copper	Mine tailings, fly ash, fertilizers, windblown copper-containing dust, water pipes.	Fish, plants	Rare
Lead	Combustion of oil, gasoline and coal; iron and steel production; and solder on water-pipe joints	Humans, land animals, fish, birds	Brain damage, convulsions
Zinc	Galvanized iron & steel, alloys, batteries, brass, rubber manufacturer, mining and old tires	Fish, plants	Rare

1.2.2 Trace Element Behavior

Trace elements exist in the environment in aqueous or solid forms. Some factors that determine partitioning of trace elements between the solution and solid phases are speciation, uptake by biota, redox conditions, and precipitation as insoluble species (Fergusson, 1990). In sediments trace elements exist in five fractions (generally most readily mobile to least): exchangeable, bound to carbonates, bound to iron and manganese oxides, bound to organic matter and the residual fraction (Akcay et al., 2003). Förstner (1982) has ranked the relative trace element capacities of major soil components as:

Manganese Oxides > Organic Matter > Iron Oxides > Clay Minerals

Which type of compound a metal is associated with depends on a number of factors, including but not limited to the valance state of the metal, redox conditions, and exchange capacity. Soil components have stronger affinities for some trace elements than for others. For example, humic acid's affinity series for divalent metal ions has been reported as Cu > Pb >> Fe > Ni = Co = Zn > Mn = Ca (Bloom, 1981). Whereas that of hydrous iron oxides is Pb ≥ Cu >> Zn = Cd

(Adriano, 2001). Trace elements preferentially form certain types of complexes under different redox potentials. For example, Cd is partial to forming carbonates over a range of redox potentions, whereas As tends to associate with Fe/Mn-oxides (Tingzong et al., 1997).

Clays and organic matter play an important role in trace metal chemistry. A mechanism by which clays bind to metals is:

$$nClay\text{-}OH + Metal^{n+} \Leftrightarrow (Clay\text{-}O)_n\text{-}M + nH^+ \text{ (Fergusson, 1990)}$$

The above reaction causes a drop in pH, contributing to the development of reducing conditions in sediments. Due to the numerous functional groups and complex structure of organic materials they are capable of binding strongly to trace elements and dissolved organic matter can mobilize metals by bringing them into solution (Fergusson, 1990). Some researchers suggest that organic matter is the controlling factor in trace metal chemistry regardless of the quantity of organic molecules (Yen, 1977).

1.2.3 Estuarine & Offshore Environment

Estuaries are of geochemical significance as they are where the fresh water of rivers mix with the saline, high ionic strength waters of the ocean. The major cations and anions in sea water are: $Na^+ >> Mg^{2+} > Ca^{2+} > K^+ = Cl^- >> SO_4^{2-} > HCO_3^- > Br^-$, whereas in fresh water the order is: $Ca^{2+} >> Na^+ > Mg^{2+} > K^+ = HCO_3^- > SO_4^{2-} > Cl^- > Br^-$ (Fergusson, 1990). The high ionic strength, due particularly to the high sodium concentration, in sea water causes compression of the double layer which can cause destabilization of particulate suspensions in fresh water, which may result in flocculation (Fergussen, 1990). Conversely, metals may be released into solution in estuaries. One proposed mechanism is the release of metals from clay particles by cation exchange (Fergusson, 1990). Using sodium as an example:

$$M^{n+}\text{-clay} + nNa^+(aq) \Leftrightarrow nNa^+\text{-clay} + M^{n+}(aq)$$

Estuaries are areas of high productivity and the decay of organic material in the estuary produces organic ligands, which can extract metals from sediments into solution. Estuaries are dynamic environments where mixing of waters promote reactions.

The mixing waters in estuaries have a suspended sediment population associated with them. Sediment inputs to an estuary include fluvial sediments, shore erosion, biological activity and the

sea, each capable of being the dominant input. The relative strengths of the sediment input sources of most estuaries are poorly known (Schubel, 1971).

1.2.3.1 Estuarine Dynamics

Estuarine dynamics are extremely complex. The variables include climate, width of mouth, depth, size and geometry of the estuary, strength of river flow, strength of ocean current, direction the river mouth is facing, and catchment and marine geology. Therefore it is difficult to predict how mixing will occur and what will be the fate of suspended particles in both the ocean and river waters. According to the classification system used by Pritchard and Carter (1971) the Olifants and Berg rivers are type B, partially mixed estuaries. There are three main types of circulation patterns associated with type B estuaries, although others have been observed (Schubel & Carter, 1984). The first occurs when the river flow is so strong as to overpower the tidal effect of the sea and flow in the estuary is unidirectional toward the sea. The secondoccurs when the river flow is weak and the water in the estuary, or even lower reaches of the river, change direction with the tide. The third (Figure 1.2.3.A) occurs somewhere in between these two cases. In this circulation pattern, the fresh river water flows mainly seaward on the top layer

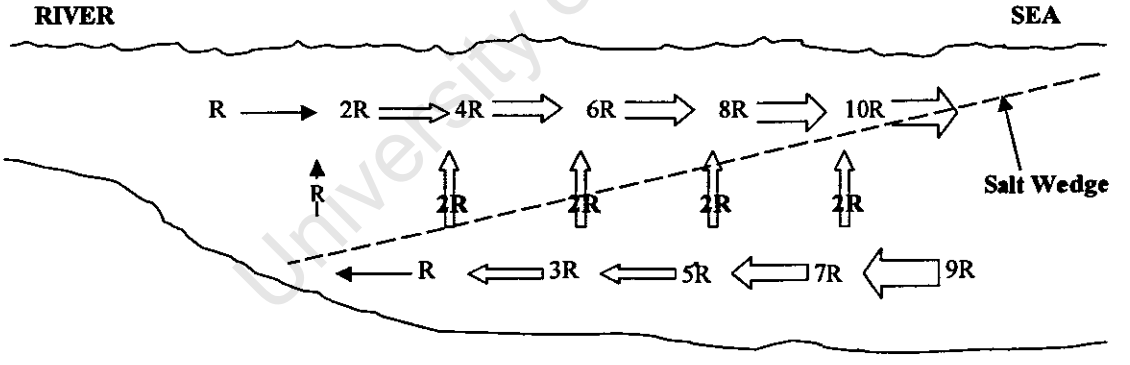

Figure 1.2.3.A. Circulation Dynamics for Partially Mixed Estuary. Using the example where the sea penetration is 9 times that of the river flow rate (R). Arrows denote the net flows.

of the water. The denser, saline ocean water flows landward on the bottom. Depending on the strength of the tide and of the river the ocean water penetrating the estuary can be over 10 times the normal flow rate of the river (R) (Pritchard & Carter, 1971). Vertical mixing sends seawater to the top layer and river water to the bottom, the net flow being in the upward direction. This results in a reduction of the landward bottom flow in the upstream direction until a point is

reached where the river flows only seaward. These flows are often difficult to measure because they are superimposed on a large tidal fluctuation (Dyer, 1979). In some estuaries sediment build up at the mouth restricts flow in and out of the estuary increasing its retention time.

During winter the strong flow of the Olifants River limits seawater penetration, while in the summer the river almost ceases and seawater penetrates far upstream (Morant, 1984). In the interim the mixed flow circulation pattern depicted (Figure 1.2.3.A) is the likely scenario. Although the lower reaches of the Olifants River estuary are only 5-7 m deep the development of a salt wedge, as in the above circulation pattern, is supported by Morant's (1984) observation of stratification with higher salinity at depth. In such a circulation pattern there is a good degree of mixing between sea and river water that make it difficult to determine the fate of suspended particles. As particles settle out of the top layer they are taken back upstream by the bottom flow and are capable of returning to the surface layer via vertical mixing. The area in which the suspended particles are concentrated is referred to as the "turbidity maxima." This is one aspect that make estuaries "sediment traps." Filter feeding activities (Schubel & Kennedy, 1984), aquatic plants that trap suspended sediments (Short & Short, 1984), and the development of salt marshes are among the other mechanisms by which estuaries trap suspended sediments.

Dams, which stop water flow allowing suspended particles to settle out, on both the Olifants and Berg rivers are used to regulate flow, especially during the dry summer months. During summer the Berg River dam water is periodically released to push back the encroaching ocean water. Thus the circulation profile swings from the low river flow scenario toward the river dominant and back again in a regular basis.

1.2.3.2 Sedimentation

The particles with settling velocities greater than the vertical mixing velocity have the greatest probability of depositing on the estuary floor. Settling velocity, as calculated via Stoke's Law, is based on diameter (McBride, 1994), thus the larger particles are more likely to settle out, while the smaller fraction is more likely to be carried further downstream or out to sea. Particles that are deposited are often resuspended as the water changes direction due to the tide or flow velocity as a result of changes in run-off. Waves can play an important role in the resuspension of bottom sediments (Schubel, 1971). In a partially mixed estuary there exists a population of

sediments in suspension for long periods of time as their settling velocities are approximately equal to the mean vertical mixing velocity. There also exists a second population of particles which are constantly deposited and resuspended

As discussed in Section 1.2.3, the high ionic strength of seawater promotes flocculation of suspended particles. This is magnified in the turbidy maxima where mixing promotes particle collisions. Flocculation also results from the electrostatic forces of clay particles; bacteria and filter feeds have also been shown to play an important role in producing agglomerates (Morales-Alamo & Haven, 1966). The aggregates formed have a larger diameter than the individual particles, thus a faster settling velocity. In a study of the Chesapeake Bay Schubel (1971) found that agglomerates made up 97% of the total volume of bottom sediments.

1.3 Site Description

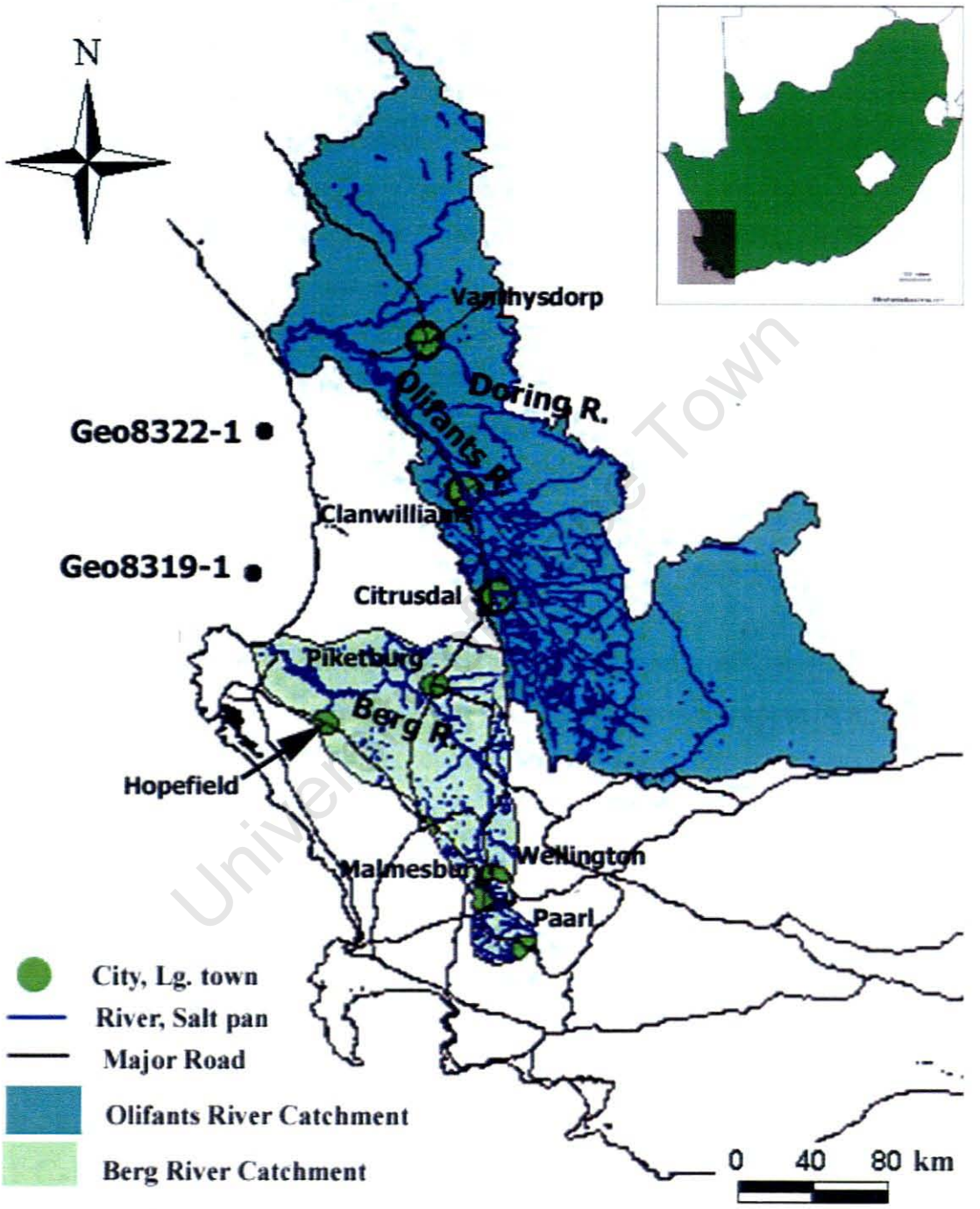

Figure 1.3.A. Catchment areas of the Olifants and Berg rivers. The Berg River Catchment is approximated from the topography and maps from other publications. The Mud Belt sample sites, Geo8322 and Geo8319, are shown.

1.3.1 Olifants River

The Olifants River catchment (Figure 1.3.A) is the second largest in South Africa, with an area of approximately 46 000 km^2 (Morant, 1984). The long axis of the catchment runs north to north-west, along the north-south axis of the Cape Fold Belt. The catchment forms the southern boundary of the Namaqualand region and in the past acted as the main route to the copper mines of Namaqualand (Bulpin, 1980). European settlement of the area began in the early 1700s (Morant, 1984). The early farmers grew rice, but the area has become one of the main citrus growing areas of South Africa (Langhhout, 1998). As of 1998 approximately 56 000 people live in towns and communities within the catchment (Basson et al., 1998). There is no significant industrial development in the area and the infrastructure consists of two major roads and a rail line, which is used mainly to transport ore between the Namaqua Sands mine in Saldana and their smelting plant to the north west of the catchment (Langhout, 1998). Marine diamond mining takes place on the shore to the north (Morant, 1984). A well developed irrigation scheme exists along the length of the Olifants River, with approximately 11 500 hectares under irrigation (Basson, et al., 1998). Forty-four percent of the irrigation water is retrieved from the Clanwilliams dam, built in 1932 and raised in 1966, with a capacity of 127 x 10^6 m^3 (Morant, 1984). The second major dam, the Bulshoek, is 23 km downstream of Clanwilliams and has a capacity of 7.5 x 10^6 m^3 (Morant, 1984). Return to the river through seepage from irrigation in the Olifants River is estimated to be 20% (Fourie & Steer, 1971).

The Olifants River system consists of 1 100 km of major rivers and tributaries (Morant, 1984). The major tributary of the Olifants River is the Doring River, with a length of 270 km, compared with the 260 km of the Olifants (Morant, 1984). At the confluence the Olifants contributes 279.2 million $m^3 \cdot a^{-1}$, whereas the Doring contributes 403.9 million $m^3 \cdot a^{-1}$ (Basson, et al., 1998). Under natural conditions the estuary receives 1055.4 million $m^3 \cdot a^{-1}$ to 737.5 million $m^3 \cdot a^{-1}$ (Basson, et al., 1998).

1.3.1.1 Catchment Area Description

The topography of the Olifants River catchment can be separated into two distinct areas. The south west area containing much of the Olifants basin and some of the Doring has significant relief, whereas the north eastern region has much less relief, typical of the Western Karoo

(Langhout, 1998). The Olifants River valley begins at an elevation of 700 meters, passes through a narrow gorge and emerges into a wider valley near Keerom after which the river flows northward for 100 km, passing through the Clanwilliams and Bulshoek dams. The Doring rises in the eastern slopes of the Cedarberg Mountains (Morant, 1984). Twenty km past the Bulshoek Dam, the Olifants River meets up with the Doring River and the topography flattens as the river makes it way to the sea (Langhout, 1998; Morant, 1984; Basson et al, 1998). The bridge at Lutzville, 32 km from the river mouth, marks the head of the tidal effect, but it is estimated that the tidal prism does not penetrate further than Ebenhaeser, approximately 14 km from the mouth (Morant, 1984).

The vegetation of the catchment consists of fynbos in the south west region, some False Karoo in the far north and scattered along the eastern basin boundary, with Karoo and Karrois occurring in most of the remainder (Langhout, 1998). The sparse vegetation, especially in the east, combined with the impermeable bedrock leads to rapid run-off in the catchment, especially in areas which have not been developed for agriculture. Most soils in the area have low amounts of organic material, but high fine sand and silt contents (Lambrechts and Schloms, 1998). The soils in the low rainfall areas of the catchment are poorly leached and base saturated, with pH values greater or equal to seven (Lambrechts and Schloms, 1998).

1.3.1.2 Geology

The geology of the Olifants River catchment (Figure 1.3.1.A) has been extensively studied (Coward, 1981; Morant, 1984; Langhout, 1998, Basson, et al., 1998; Heydorn & Tinley, 1980). The southwest portion of the catchment consists of predominantly quartizic sandstone of the Table Mountain Group (TMG), with minor inter-bedded shale horizons. Halfway through the major succession of the quartizic sandstone exists a shale marker known as the Cedarberg Formation, above which the sandstone belongs to the Nardouw Subgroup and below which to the Peninsula Formation. Further north is overlain by basal Karoo Dwyka tillites. The lower Olifants River valley, below Ebenhauser, was cut more deeply into the surrounding plateau, which consists of Table Mountain sandstone, Malmesbury shale and Pre-Cambrian limestone and is covered by superficial Tertiary and Quaternary deposits of limestone, sandstone and gravel. Both sides of the estuary are steep rocky shorelines with Malmesbury sandstone on the north bank and Table Mountain sandstone on the south. North of Lutzville the catchment drains

off sandstones and quartzites of the Table Mountain Group, Bokkeveld Group shales and Witteberg Group quarzites and shales. The north eastern part of the catchment is underlain by rocks of the Karoo Sequence, mainly Ecca Group shales and sandstones, Beaufort Shale and the tillites of the Dwyka Formation. The central portion of the Hantams/Doring/Sout/Hol river complex consists of shales, greywakes, and limestones of the Malmsebury Group. The northwestern portion of the complex consists of schists, gneisses and migmatites of the Namaqua Province.

The majority of the Olifants River drains off the resistant quartizic sandstone of the Table Mountain Group resulting in it carrying almost no silt (Morant, 1984). In addition, the Clanwilliam and Bulshoek dams act as silt traps. The Doring river carries the bulk of the Olifants River's silt load as it drains off the easily weathered tillites and shales. Basson et al. (1998) reported the estimated silt load of the Olifants River to range from 140-250 tons$km^{-2}a^{-1}$, whereas in parts of the Doring River catchment it would reach a maximum of 600 tons$km^{-2}a^{-1}$.

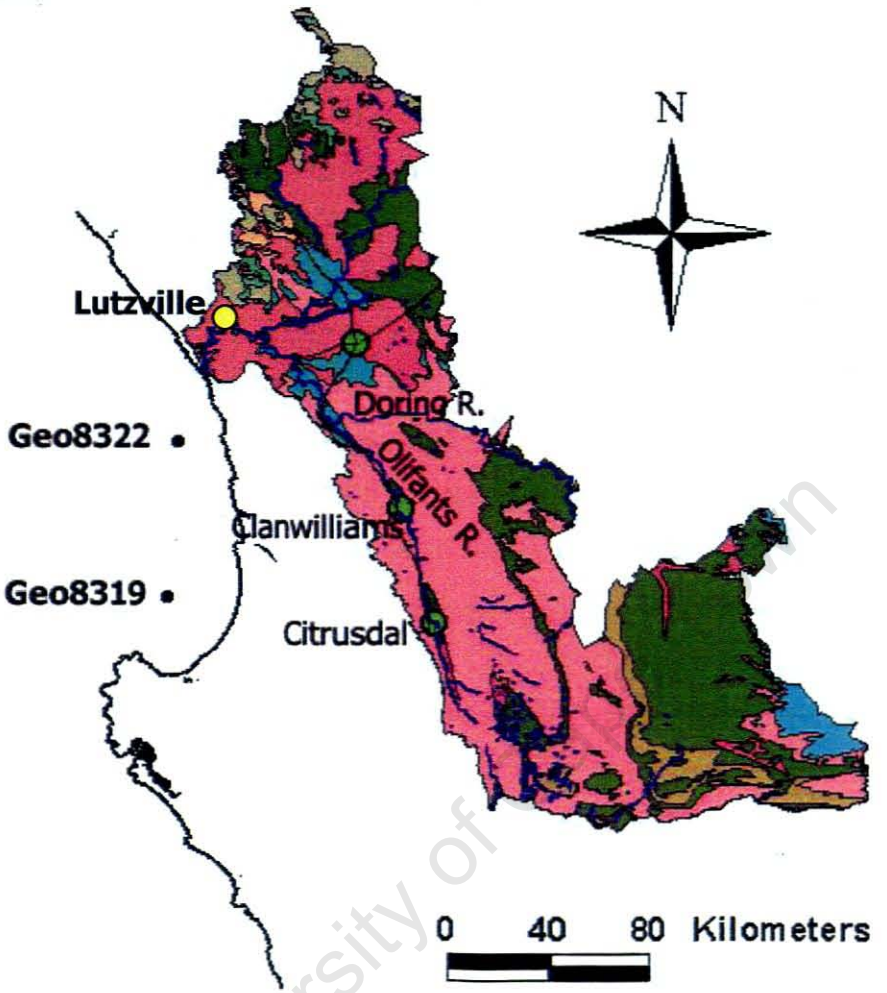

	Quartzitic Sandstone (Table Mountain Group, Cape Super Group)
	Augen Gneiss (Little Namaqualand Suite)
	Granite (Cape Granite Suite, also some Spektakel Suite)
	Tillite, Sandstone, Mudstone, Shale (Dwyka Formation, Ecca Group)
	Phylittic Shale, Greywacke, Limestone, Arenite (Malmesbury Group)
	Quartzite (Malmesbury Group)
	Schist, Limestone, Dolemite (Vanrynsdorp Formation, Malmsesbury Group)
	Alluvium, Sand, Calcrete
	Shale (Bokkeveld Group, also Karoo Sequence in east and north)
	Tillite, Shale (Ecca Group)

Figure 1.3.1.A. Geology of the Olifants River Catchment.

1.3.1.3 Climate

With the exception of the north eastern portion of the catchment, which can receive appreciable amounts of rainfall in the summer, the majority of the Olifants River catchment lies in a winter rainfall area, with a Mediterranean climate (Morant, 1984). Although small sections in the upper reaches of the Olifants receive annual rainfall of 1500 mma^{-1} and the mountains in the south west of the catchment receive on the order of 600 mma^{-1}, in general the area is arid, with an annual rainfall of less than 300 $mm{\cdot}a^{-1}$ (Langhout, 1998; Basson et al., 1998). In the eastern portion of the catchment, characterized as a semi-desert climate, the rainfall rarely exceeds 250 $mm{\cdot}a^{-1}$ (Morant, 1984). In Lutzville, 32 km from the river mouth, the average annual rainfall is 142 $mm{\cdot}a^{-1}$ (Lambrecht and Schloms, 1998). The catchment receives one of the highest sunshine durations in South Africa, increasing from south west to north with a maximum duration of 14.2 hrs in summer and 10.1 hrs in winter (Langhout, 1998). Evaporation also increases from southwest to north, with average evaporation in Lutzville being 6.8 $mm{\cdot}day^{-1}$ (Lambrechts and Schloms, 1998; Langhout, 1998). Warm temperatures prevail during the day, but drop to cool at night. The average annual temperature in Lutzville is 18.8 °C (Basson, et al, 1998).

As a result of the seasonal rainfall the rivers of the catchment have extremely variable flow. The flow of the Olifants River can be as little as one-tenth of its mean monthly flow rate or 2.5 times as great (Morant, 1984). The Doring is even more variable, ranging from one-tenth to 4.5 times it monthly flowrate (Morant, 1984). In winter, when the heavy rainfall occurs, flooding occurs in the catchment. A red-brown plume of suspended fluvial sediment, extending several hundred meters offshore, has been witnessed after heavy rains. Conversely in summer seawater penetrates as far as Ebenhaeser (Morant, 1984).

1.3.2 Berg River

The Berg River is of particular importance in the Western Cape as it is the major source of municipal and industrial water (Hall and Horgens, 1978). The river valley is 160 kilometers long with a width of 1 to 5 kilometers in the upper reaches and 10 to 20 kilometers at the coast (Fourie and Steer, 1971), with a catchment size of 4012 km^2 (Bath, 1993). The values reported by Fourie and Steer (1971) for the period of 1955-1959 are greater than those reported by Bath (1993) (Table 1.3.2.A) by as much as factor of 4 four (e.g. Vier-en-Twintig Rivers: 53 x 10^6 m^3

in Bath (1993), 204 x 10^6 m^3 in Fourie & Steer). This is in part due to a decrease in rainfall, an increase draw-off for irrigation and improved measurement techniques from 1959 to 1993 (Bath, 1993; Fourie & Steer, 1971).

Table 1.3.2.A. Flow Volumes for the Berg River and Major Tributaries (taken from Bath, 1993)

	Catchment Size (km^2)	Mean Annual Runoff (x 10^6 m^3)
Berg River (at Misverstand Weir)	4012	671
Franschoek	46	21
Banghoek	25	18
Krom	69	19
Doring	43	0.9
Kompagnies	121	16
Vis (Fish)	39	2
Klein Berg (Little Berg)	395	43
Vier-en-Twintig	183	53
Leeu	36	4
Sandspruit	152	3
Moorreesburgspruit	134	1
Matjies	676	16

(Bath, 1993)

The Berg River and its tributaries support extensive agricultural developments, and more recently industrial and urban expansion. However, up until the end of the Second World War limited irrigation from the river was practiced (Fourie and Steer, 1971). The main industrial areas along the river are Paarl, Wellington and Franschoek. The most important industries in the catchment are wineries, canneries and other food processing firms, textile milling and the manufacturing of cigarettes and processing of tobacco (Fourie and Steer, 1971). Prior to 1955 industrial waste was disposed of by lagooning, a process in which waste water or slurries are disposed of in shallow ponds in hopes that sunlight, bacterial action and oxygen will cause self purification. Considering the sandy soils and the proximity of the lagoons to the rivers considerable seepage is thought to have occurred (Fourie and Steer, 1971). The catchment contains 58 000 ha of arable land and as of 1971 another 11 000 were under irrigation (Fourie and Steer, 1971), a figure that has surely increased. Fruits, particularly wine grapes, are the most

important crop in the middle to upper reaches of the river, with grain being the most important crop below Wellington where the terrain is less mountainous.

A fledgling coastal fishing industry struggled until the mid-1900's because of poor access to the river due to the shallow waters. In 1966 the Fisheries Development Corporation of SA, Ltd. (FDC) undertook extensive dredging and harbor works in the construction of a new mouth (Figure 2.1.D.) (Van Wyk, 1983). Due to a siltation problem permanent maintenance dredging has since been required to maintain a navigable depth of 3 m (Van Wyk, 1983). The new mouth has made the river more susceptible to direct wave impact resulting in increased erosion along the southern banks of the river. The FDC (1974) estimates the near mouth bank to be receding at 4 $m{\cdot}a^{-1}$ and the low water line is receding at 6 $m{\cdot}a^{-1}$.

There are two dams on the Berg River, the Wemmershoek and Voelvlei, with capacities of 64 and 170 million m^3, respectively (Hall and Gorgens, 1978). A pumping station exists 50 km from the river mouth, where water is treated before distribution. The encroaching seawater is pushed back from the pumping station by discharging water from the Voelvlei dam (Fourie and Steer, 1971). The construction of the new mouth resulted in increased salinity upstream, requiring more dam water to push back the encroaching sea (Van Wyk, 1983).

1.3.2.1 Catchment Area Description

The Berg River rises in the Drakenstein and Franschoek mountains. The flow is predominantly northwest, reaching the sea at St. Helena Bay. The gradient of the lower reaches of the river is minimal, thus reducing the rate of flow. A tidal effect is observed in the last 80 km of the river (Fourie and Steer, 1971). The vegetation types in the catchment include: Succulent Karoo, Namaqualand Broken Veld, West Coast Strand Veld, Mountain Renosterbosveld and Mountain Fynbos (Heydorn & Tinley, 1980).

1.3.2.2 Geology

The Berg River rises in the mountainous region comprised mainly of Table Mountain Group sandstones (Hall & Gorgens, 1978). In the vicinity of Paarl a few small tributaries rise in granite hills and flow down through clay soils consisting of weathered granite material (Fourie and Steer, 1971). Downstream from Paarl the overlying Table Mountain Group sandstones are

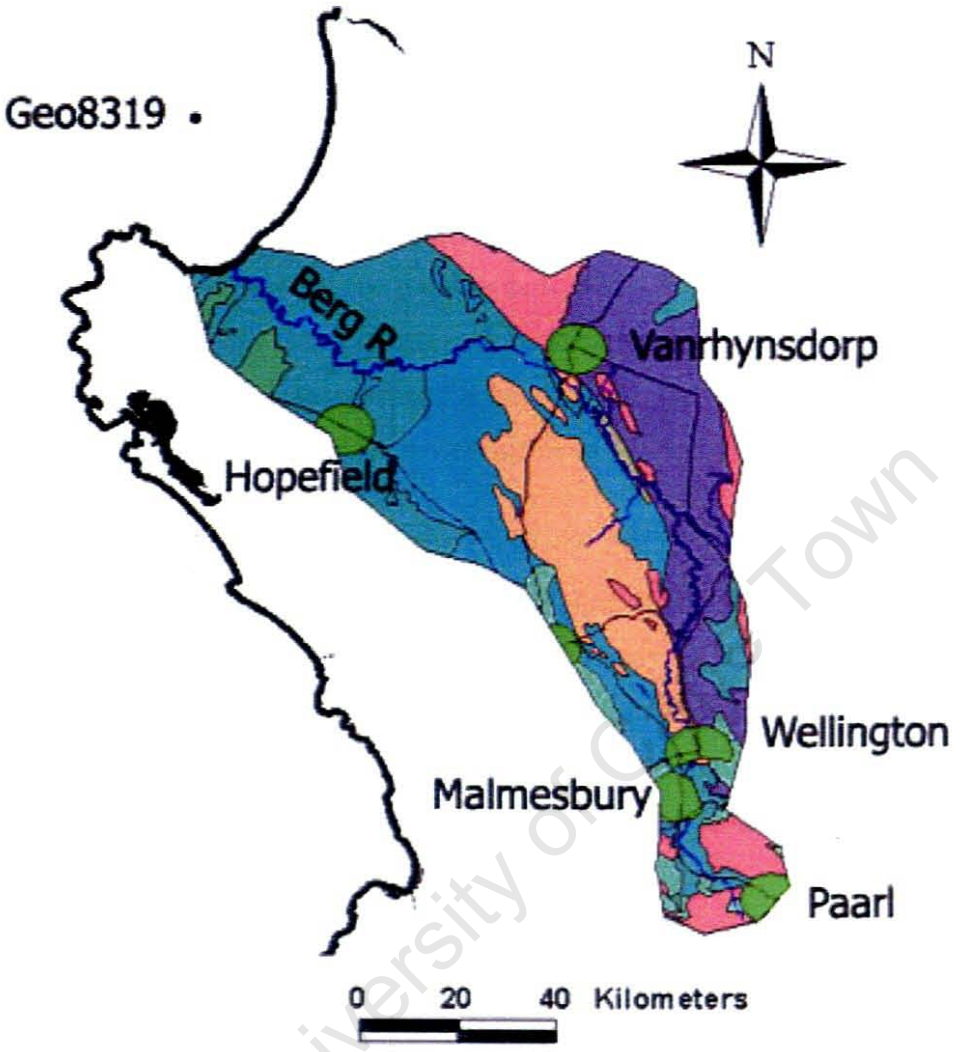

	Quartzitic Sandstone, shale (Table Mountain Group, Cape Super Group)
	Granite (Cape Granite Suite)
	Greenstone (Bridgestown Suite)
	Limestone, Sandstone, Conglomerate (Bredasdorp Formation)
	Greywacke, Shale, Limestone (Swartland Subgroup, Malmesbury Group)
	Quartzitic Sandstone, Shale, Tillite (Table Mountain Group, Cape Super Group)
	Schist, Phyllite (Swartland Subgroup, Malmesbury Group)
	Alluvium, Sand, Calcrete

Figure 1.3.2.A. Geology of the Berg River catchment. The catchment boundaries are estimated from topography and other publications.

progressively eroded away exposing a mainly Malmesbury shale bedrock (Fourie & Steer, 1971). The Malmesbury shale, which in turn produces alkaline soils, remains the underlying formation all the way to the mouth (Figure 1.3.2.A).

1.3.2.3 Climate

The whole of the Berg River basin lies in a winter rainfall area with average annual rainfall ranging from 5000 $mm{\cdot}a^{-1}$ in the mountains to 900-1200 $mm{\cdot}a^{-1}$ in the valley and dropping to 400-500 mm in the hilly plains through which the river flows for most of its length and even less as it approaches the sea (Flourie and Steer, 1971; Hall and Gorgens, 1978). Heavy winter rains make the system susceptible to periodic flooding (Flourie and Steer, 1971).

1.3.3 South African West Coast Environment & offshore Mud Belt

A strip of mud accumulation, known as the "Mud Belt", has developed off the west coast of southern Africa. The Benguela Current, which may be defined as a broad northward flow, characterizes the west coast of southwestern Africa (Shannon, 1990). However, close to the coast the subsurface flow is often southward, but current reversals are common (Shannon, 1990). The sub-surface current drags mud of the Mud Belt southward along the coast. Winds, which can reach gale force strengths capable of carrying dust 500km seaward (Heydorn & Tinley, 1980), blow surface water out to sea causing the upwelling of nutrient rich bottom waters. This nutrient source fuels the high levels of primary productivity witnessed in the near-coast surface waters on the west coast of southern Africa, supporting large fish communities (Shannon, 1990). The nutrients return to depth as sinking detrital material and decays. This decay consumes oxygen resulting in low oxygen bottom waters, especially in the semi-enclosed areas such as St. Helena Bay (Shannon, 1990).

2 Methods

2.1 Samples

The samples analyzed were collected during three sampling trips (Table 2.1.A). Samples, referred to as Geo8319-1 and Geo8322-1 individually and the mud belt cores collectively, were collected during the RV-Meteor cruise M57-1 along the western shore of South Africa from January to February 2003. Samples, both water and sediment, were collected from the Olifants Estuary, between the 12th and 14th of January 2004. These samples are referred to as OE1 through OE6 individually and as the Olifants River or Olifants River estuary cores collectively. The Berg River samples were collected on January 21st and are referred to as BR1 to BR3 individually and the Berg River or Berg River estuary cores collectively. The off-shore sediments were collected using a multi-corer, whereas the estuarine sediments were collected by hand using plastic tubes.

Table 2.1.A. Sample Site Locations: GPS Coordinates and distance to river mouth.

Core ID	Sample location	GPS Coordinates (DMS) South	GPS Coordinates (DMS) East	Distance to Mouth (m)	Image Plate # (Appendix I)
Geo8319-1	Mud Belt	32° 29' 74"	18° 04' 70"	69*	1 & 2
Ge08322-1	Mud Belt	31° 57' 22"	18° 07' 07"	105*	1 & 2
OE1	Olifants R. Estuary	31° 41' 50.4"	18° 11' 21.8"	352	3
OE2	Olifants R. Estuary	31° 42' 00.0"	18° 11' 37.8"	766	
OE3	Olifants R. Estuary	31° 33' 51.9"	18° 19' 38.2"	34 420	4 & 5
OE4	Olifants R. Estuary	31° 36' 31.8"	18° 13' 04.0"	13 494	
OE5 & OE6	Olifants R. Estuary	31° 41' 04.9"	18° 12' 04.2"	2 210	6
BR1	Berg R. Estuary	32° 46' 42.4"	18° 08' 02.3"	1 510	
BR2	Berg R. Estuary	32° 47' 20.2"	18° 08' 39.2"	3 397	
BR3	Berg R. Estuary	32° 48' 45.6"	18° 11' 43.2"	11 306	

* - Denotes water depth rather than distance to river mouth

The mud belt multi-cores (locations depicted in Figure 1.3.A) were cut into one-centimeter thick discs on board and stored in plastic petri dishes taped shut with electrical tape. The samples were refrigerated upon return to the University of Cape Town (UCT), where they remained until August of 2003, when they were processed for analysis (Figure 2.1.A).

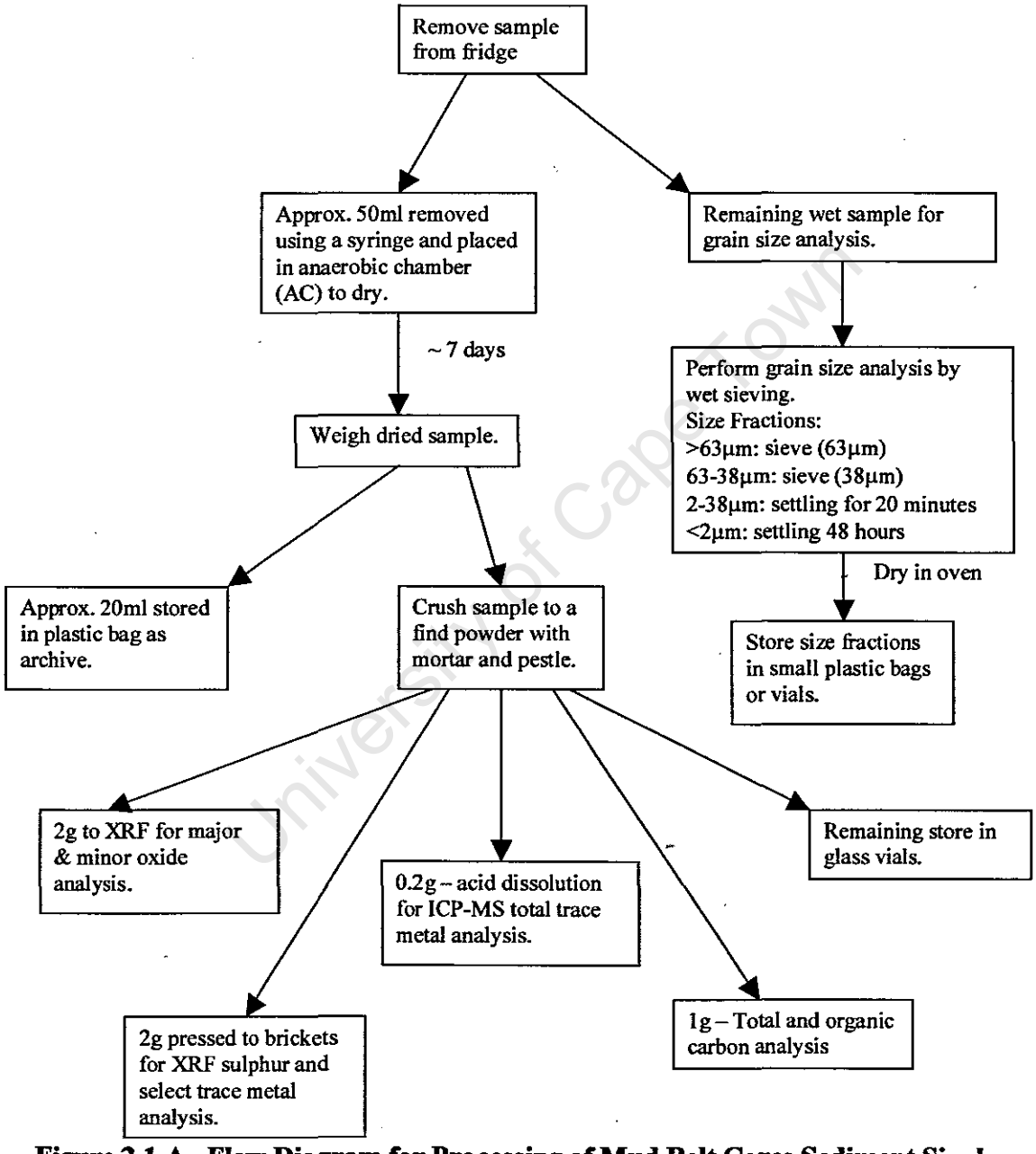

Figure 2.1.A. Flow Diagram for Processing of Mud Belt Cores Sediment Singles

Table 2.1.B gives a brief description of the Olifants and Berg river estuaries sample sites, which are shown in Figures 2.1.B and 2.1.C, respectively. The Olifants River estuary cores were

sectioned onsite and stored in individual plastic bags. The bags were put under anoxic conditions, with the exception of the sediment samples collected at site OE3, using Becton

Table 2.1.B. Site Descriptions for Olifants Estuary and Berg River Sampling Sites

Sample Site	Description
OE1	At the river mouth, 20 meters from the river bank. River bank was observed to be beach sand as was the river bed at this point.
OE2	In the off channel visible in Figure 2.1.B near the river's mouth. Approximately 150-200 meters from where the channel rejoins the river.
OE3	On the downstream side of the Lutzville bridge. The water samples were taken from the rapids near the center of the river, whereas the cores were taken a few meters from the banks where the water was calmer.
OE4	Near the town of Ebbenhauser. Of note were a group of reeds just off the river's edge. The cores were taken between the banks and the reeds. The water samples were taken on the opposite side of the reeds. Water depth increased suddenly after the reeds.
OE5	2m from the river bank about 10 meters downstream of the channel leading to the Papendorp boat launch.
OE6	In the center of the channel leading to the Papendorp boat launch, approximately 10 meters from the river.
BR1	Close to the banks separating the ocean from the Berg River, but a few hundred meters from the mouth itself, as shown in Figure 2.1.C.
BR2	Near a salt mine outside the town of Velddrift. The samples were taken 1m from the river bank which was about 30m from a dirt road. The road was not used commercially as it was part of the salt mine property.
BR3	A few kilometers upstream of the bridge leading into Velddrift.

Dickson BBL Gas Pak Plus anaerobic system envelopes. Both the water and sediment samples were kept on ice until they were transferred to a freezer. The Berg River cores were placed in a refrigerator upon return to the University of Cape Town on the evening of January 21st and sectioned the following day. The sections were placed in plastic bags and stored in the freezer. Both the Olifants River and the Berg River core sub-samples were processed in a similar manner as the mud belt cores, except that the archive portion was never defrosted and the working portion was air dried in the open rather than in an anaerobic chamber. Two sediment cores were

mM and 7 mM $NaHCO_3$ and the formic acid-bromophenol blue solution were prepared in the lab the day prior to each sampling trip. The surface water samples, as well as a set of standards were dosed with the bromophenol blue solution at each site and placed on ice. Upon return to UCT the absorbance was measured using a UV visible Aquamate Thermospectronic spectrophotometer. A set of standards were dosed and the absorbance read prior to the sampling trip. They were then placed on ice for the duration of the trip and the absorbance measured again upon return in attempt to assess any color degradation that may occur over time.

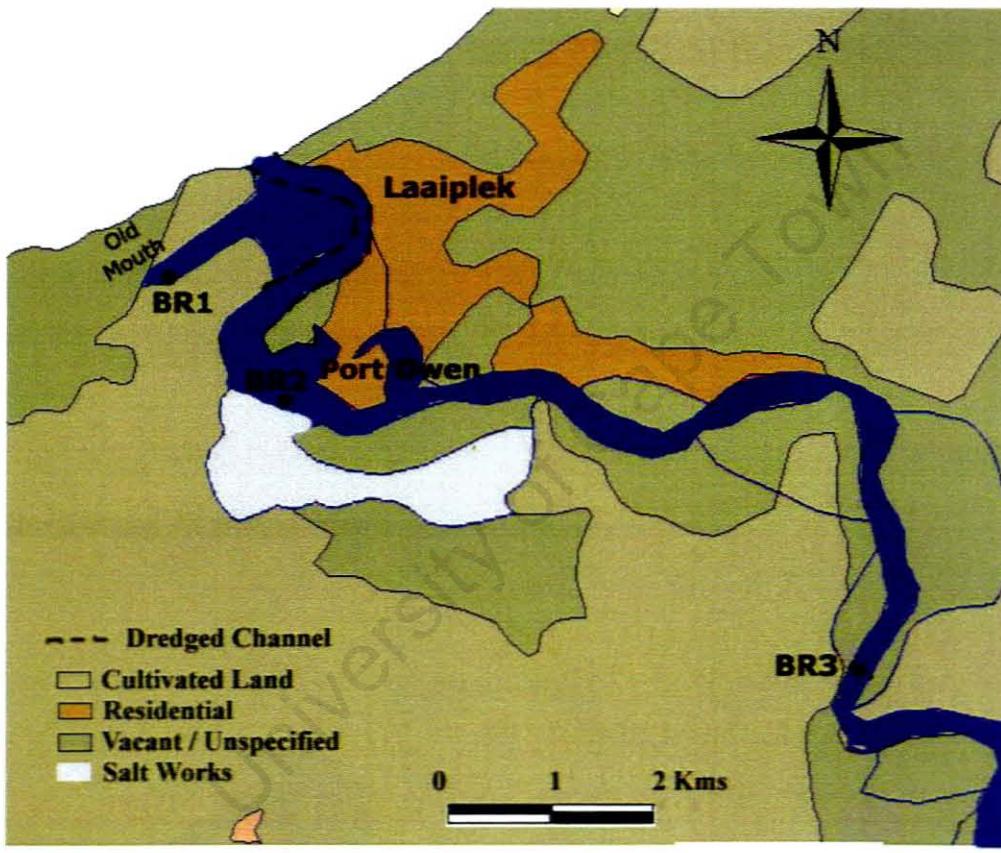

Figure 2.1.C. – Locations of Berg R. Estuary Sample Sites, the approximate boundary of the dredged channel and the location of the old mouth.

2.3 Sediment Analysis

In order to ensure that a representative sample was used in each analysis the wet sediment was stirred prior to any sub-sampling and the cone and quarter technique was used when selecting portions of the dried crushed samples for each analyses. An agate mortar and pestle was used to prevent contamination when crushing the sediments.

mM and 7 mM $NaHCO_3$ and the formic acid-bromophenol blue solution were prepared in the lab the day prior to each sampling trip. The surface water samples, as well as a set of standards were dosed with the bromophenol blue solution at each site and placed on ice. Upon return to UCT the absorbance was measured using a UV visible Aquamate Thermospectronic spectrophotometer. A set of standards were dosed and the absorbance read prior to the sampling trip. They were then placed on ice for the duration of the trip and the absorbance measured again upon return in attempt to assess any color degradation that may occur over time.

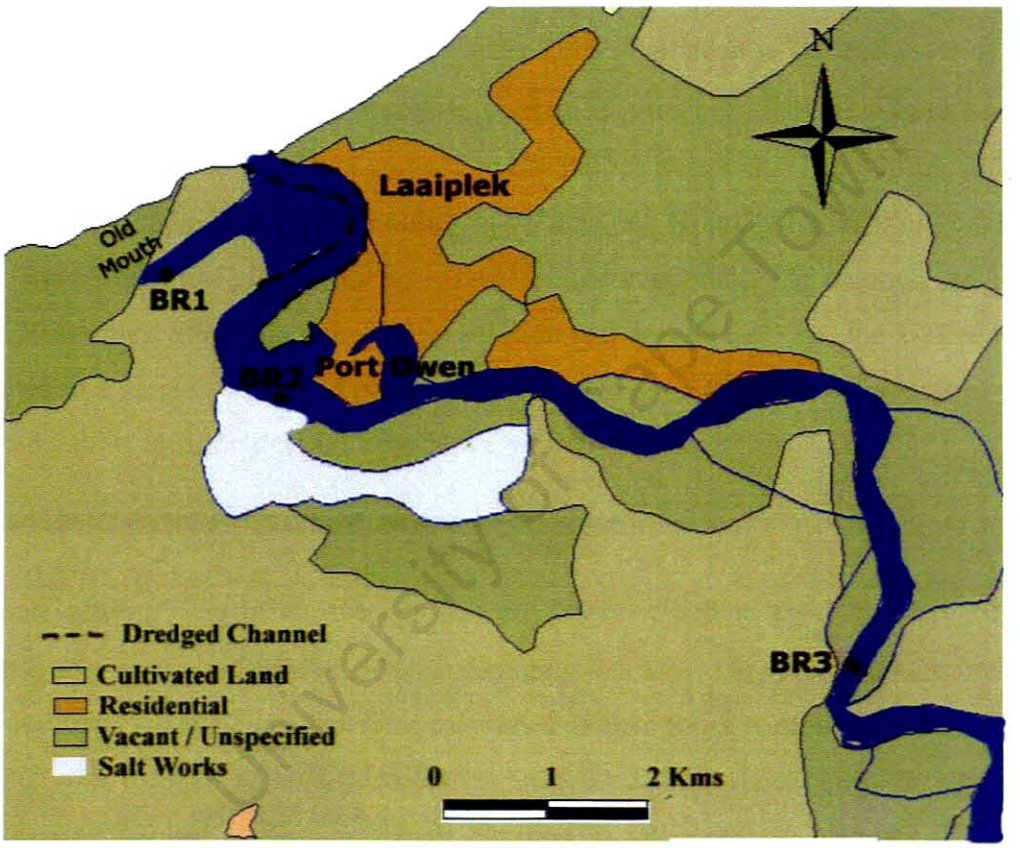

Figure 2.1.C. – Locations of Berg R. Estuary Sample Sites, the approximate boundary of the dredged channel and the location of the old mouth.

2.3 Sediment Analysis

In order to ensure that a representative sample was used in each analysis the wet sediment was stirred prior to any sub-sampling and the cone and quarter technique was used when selecting portions of the dried crushed samples for each analyses. An agate mortar and pestle was used to prevent contamination when crushing the sediments.

portions of the dried crushed samples for each analyses. An agate mortar and pestle was used to prevent contamination when crushing the sediments.

2.3.1 Grain Size

The grain size analysis procedure used for this project was designed to separate the sediment into 4 size fractions: >63 μm, 38-63 μm, 2-38 μm, and <2 μm. The wet sediment was placed in a beaker with a small amount of water, stirred and placed in a sonic bath for a few seconds to encourage particle separation. The sediment was then wet sieved through a 63 μm sieve. The >63 μm fraction was collected off the sieve and placed in an oven to dry before being weighed. The <63 μm solution was then wet sieved through a 38 μm sieve. The 38-63 μm fraction was collected off the sieve and placed in an oven to dry before weighing. The <38 μm solution was poured into one or more beakers, depending on volume, but typically two 600 mL beakers. The beaker(s) were stirred and placed in a sonic bath for a few seconds. The solution was allowed to settle for 20 minutes, after which the <2 μm solution was decanted off and the 2-38 μm fractions consolidated in a single beaker and placed in the oven to dry. It should be noted that according to the settling time equation derived from Stoke's Law (Lerman,1979):

$$t = \frac{18\eta h}{g(d_p - d_1)D^2}$$

a 20 minute settling time in an average 600 mL beaker filled to the 500 mL (~10 cm) line corresponds to a particle diameter of approximately 9.5 μm. However, Stoke's law assumes particles are ideal spheres and the time calculated is that for a particle at the surface, which results in an over estimate as most particles are suspended somewhere below the surface. Thus, 20 minutes was deemed to be a sufficient duration to settle out the majority of the fine silt fraction. In addition, a 20 minute convention is being used for the grain size analysis of the other cores collected during the Meteor cruise. Thus it is used here so as to allow direct comparison with the grain size analyses of the other cores collected on the Meteor cruise. The <2 μm solution is allowed to stand until the overlying water becomes clear, on average 7 days, after which, the water is decanted off and the beaker is placed in an oven to dry prior to weighing.

In an attempt to eliminate the scale error inherent in weighing large beakers the dried size fractions were scraped out of the beakers and weighed on wax paper. These weights were

compared with the calculated weights from the difference between weighing the empty beaker at the start and the beaker containing the dried size fractions in order to estimate the degree of the scale error.

2.3.2 Major Elements

Major elements were analyzed using X-ray fluorescent spectroscopy (XRF). The sample preparation followed the standard procedure practiced by the XRF lab in UCT's Geology Department (Willis, 1999). Approximately 1.2 g of crushed, air-dried sample were oven dried at 110 °C for eight hours in a porcelain crucible. The oven-dried samples were then placed in a furnace at 850 °C for eight hours to remove volatiles. The ignited sample (0.7 g) was added to 6 g of Sigma X-Ray flux and fused into a disk, which was then analyzed via the UCT Geology Department's XRF facility, consisting of a Philips PW1480 wavelength dispersive XRF spectrometer with a dual target Mo/Sc x-ray tube. Analytical conditions can be found in Appendix II.

2.3.3 Trace Elements

Trace elements were analyzed using Inductively coupled plasma mass spectrometry (ICP-MS). The method followed was that for complete digestion as found on the UCT website for "Bulk-rock Sample Preparation for ICP-MS Analysis (**UCT, 2003**)." The analytical standards used for the selected metals of this study were Hawaiian Basalt (BHVO-1) provided by the U.S. Geological Survey and a UCT internal sediment standard referred to as "S10." These standards, as well as a total procedural blank underwent the following preparation procedure along with each sample.

Four mL of 4:1 HF/HNO_3 was added to 50 mg of crushed, dried sample and allowed to digest for 48 hrs on a hot plate at 50-60 °C in a closed teflon container. After 48 hrs the lids were removed and the samples were left on the hot plates until all of the HF/HNO_3 evaporated.

The digested samples were then dissolved in 2 mL of concentrated HNO_3 and returned, uncovered, to the hot plates and the temperature adjusted to approximately 75 °C. Once all the HNO_3 had evaporated an additional 2 mL of HNO_3 was added and the samples returned to the

hot plate until evaporation was complete. The lids were placed back on the containers and the samples were allowed to cool to room temperature.

The digested samples were diluted with 4 mL of internal standard stock solution (10 ppb indium, rhenium, rhodium and bismuth in 5% HNO_3) and transferred to a 50 mL centrifuge tube. The containers were washed with 2 mL of internal standard stock solution, twice. The wash from each rinsing was added to the centrifuge tube. The dissolved samples were made to 50 mg by adding additional internal standard stock solution as needed.

Following, four drops of concentrated HF was added and the accurate weight recorded. The centrifuge tube lid was replaced and the tube shaken gently. The approximately 1000-times diluted sample was analyzed by the UCT Geology Department's ICP-MS facility, a Perkin Elmer, model Elan 6000 with an AS-90 auto-sampler.

2.3.4 Sulfur

Total sulfur was analyzed using XRF. A separate sub-sample from that used for major element analysis was prepared. Two drops of binder were mixed into 2g of crushed, dried sample using an agate mortar and pestle; and packed to form a loosely bound disk. The bosely bound disk is covered with approximately 7mL of boric acid and compressed with 10 tons of pressure using a hydraulic press to form the sulfur pellet for analysis. Sulfur analysis was conducted by the UCT XRF facility.

2.3.5 Total and Organic Carbon

Total and organic carbon (OC) was measured using a LECO C:H:N analyzer. The sample preparation procedure was provided by Heather Sessions of the Marine and Coastal Management (MCM), Cape Town. Samples were simply dried and crushed for total carbon analysis. To prepare the sample for organic carbon analysis the carbonate carbon was removed by adding 2 mL of 16 % hydrochloric acid to 0.3 g of crushed, dried sediment. The samples were allowed to dry in an oven at 60 °C. Once dry, the salts were removed by washing the dried sediment with ±5 mL of 1M ammonium formate. The slurry produced was filtered through 45 µm filter paper. The mud pad was scraped off the filter paper into a beaker and dried at 60°C. The dried samples were then ground with a glass rod. For both total and organic carbon analysis, approximately 5

mg of sample was accurately weighed and placed in an aluminum boat and folded into a tight packet. C:H:N analysis was conducted at the Marine & Coastal Management laboratory in Cape Town.

3 Results

3.1 Water Chemistry

No water samples were collected for trace element analysis during the Meteor cruise in which the Mud Belt cores were retrieved.

3.1.1 In-situ Multi-probe

The pH, EC, DO and temperature values of the surface waters of the estuarine sampling sites are presented in Table 3.1.A. The sample sites are listed in order of increasing distance from the river mouth for both the Olifants and Berg rivers. Samples OE2 and OE4 were taken at low tide conditions, OE1 was taken at mid-tide while the tide was coming in and OE3, OE4 and OE6 were taken during high tide. The sampling times and relevant tide times can be found in Appendix I. The pH values for the Olifants River samples range from 7.8 to 8.8, whereas those of the Berg River are between 8.2 and 8.3. The ECs range from 4.64 to 58.5 µS/cm, increasing in the direction of the sea. EC values for the two Berg River samples have a much smaller range of 52.7 to 35.5 µS/cm. The dissolved oxygen measurements range from 5.9 to 20.0 mg/L in the Olifants River estuary and from 7.2 to 10.6 mg/L in the Berg River estuary waters. Temperature readings range from 20.7 to 27.3 °C and 18.5 to 24.4 °C in the Olifants and Berg river estuaries, respectively.

3.1.2 Alkalinity

The calibration curve data for each sample location can be found in Appendix I. The "first standardization method" as described by Sarazin et al (1999) suggests the method is best when applied to samples with salinities less than 0.6 mM. A 0.7 M NaCl standard was included in the standard set of every run as a contingency for encountering alkalinities higher than 6 mM. The 7 mM absorbance was only used in the calibration curve for sampling site OE3, as the remaining sites' alkalinities all fell within the 0.5 mM to 5 mM range (Table 3.1.B). Once again the samples sites are given in order of increasing distance from river mouth. The alkalinities rise with distance from the river mouth in the Olifants River samples. The alkalinities for the Berg River samples remains relatively constant, with signs of slight decrease in the upstream direction.

Table 3.1.A: pH, EC, DO and T measurements of water samples. Collected at the water surface.

Sample Location	Dist. to mouth (m)	PH	EC (µS/cm)	DO (mg/L)	T (°C)
OE1	352	7.8	49.0	8.0	20.7
OE2	766	8.4	58.5	15.8	27.3
OE5	2 210	8.8	48.4	20.0 *	24.4
OE6	2 210	7.9	48.8	7.8	22.7
OE4 (shore side of reeds)	13 494	8.3	15.4	9.4 – 9.9	26.9
OE4 (far side of reeds)	13 494	8.3	14.9	9.5	25.7
OE3	34 420	8.1	4.6	5.9	25.5
BR1	1 510	8.2†	52.5	8.4	22.4
BR2	3 397	8.3†	52.7	10.6	18.5
BR3	11 306	8.3†	35.5†	7.2	24.4

* - A reading of 10.9 mg/L was recorded the following morning.
† - Due to multi-probe difficulties in field readings were taken in lab after samples had been frozen. (T at measurement = 15.5 °C)

Table 3.1.B Surface Water Alkalinities. Averages are reported for sites where duplicates were taken. The random error calculation is based on 3 duplicate samples and includes 2 standard deviations.

Sampling Site	Dist. to mouth	Alkalinity (mM) ± 0.05mM
OE1	352	2.95
OE2	766	3.23
OE5	2 210	2.91
OE6	2 210	2.86
OE4	13 494	4.73
OE3	34 420	5.29
BR1	1 510	2.82
BR2	3 397	2.75
BR3	11 306	2.59

3.1.3 Trace Element Analysis

The filtered and unfiltered water samples were analyzed for twenty-two elements using ICP-MS. A complete table of results can be found in Appendix I. The values measured for select elements are presented here (Table 3.1.C-D). For sites in which duplicates were taken the averages are reported. The density of the samples is approximated to be 1.01 gmL^{-1}, arrived at by averaging

the density of fresh water, 1gmL^{-1}, with that of sea water, 1.02 gmL^{-1} (Burton, 1976). Although many samples showed higher concentrations in the filtered samples than in the unfiltered samples the differences are within the random errors (Section 3.3).

Table 3.1C. Trace Element Analysis of the Olifants River estuary water samples determined by ICP-MS. Random error reported as mean plus 2 STD.

	Element Concentration (µmol/L unless otherwise specified)							
	As (±0.24)	Cd (ηmol/L) (±0.3)	Cr (ηmol/L) (±115)	Cu (±0.41)	Ni (±0.05)	Pb (ηmol/L) (±4.7)	Sr (±16.7)	Zn (±0.93)
OE1 Unfiltered	0.63	1.3	103.7	0.49	0.17	6.0	55.65	1.51
OE1 Filtered	0.60	0.7	130.8	0.51	0.14	4.2	43.53	1.51
OE2 Unfiltered	1.35	1.0	70.3	1.12	0.26	5.5	89.45	2.13
OE2 Filtered	1.33	1.4	36.0	0.83	0.29	2.3	99.38	2.46
OE5 Unfiltered	1.14	1.3	51.0	0.87	0.23	4.8	75.76	1.82
OE5 Filtered	1.14	1.2	36.8	0.88	0.22	2.4	79.09	1.90
OE6 Unfiltered	0.80	1.5	176.3	0.57	0.18	6.7	59.92	1.62
OE6 Filtered	0.87	1.3	90.4	0.69	0.19	3.2	71.55	1.37
OE4 Unfiltered	0.18	0.3	59.4	0.10	0.06	1.6	17.19	0.47
OE4 Filtered	0.11	0.3	104.2	0.12	0.06	2.9	11.71	0.69
OE3 Unfiltered	0.07	0.1	84.6	0.08	0.03	2.5	3.19	0.45
OE3 Filtered	0.11	0.2	220.5	0.18	0.04	2.1	3.88	0.32

The trace metal concentrations tend to show a maxima at sample sites OE5&OE6, decreasing in both directions from there. Lead is the only element of those presented which consistently displayed a higher concentration in the unfiltered samples compared with their filtered counterparts.

In general, the Berg River water samples have higher concentrations of Cd, Cr, Cu, and Pb than the Olifants River samples. Chromium and lead consistently show higher concetrations in the unfiltered samples compared to the filtered ones.

Table 3.1.D – Trace Element Analysis of the Berg River estuary water samples determined by ICP-MS. Random error reported as mean plus 2 STD.

	Element Concentration (µmol/L unless otherwise specified)							
	As (±0.24)	Cd (ηmol/L) (±0.3)	Cr (ηmol/L) (±115)	Cu (±0.41)	Ni (±0.05)	Pb (ηmol/L) (±4.7)	Sr (±16.7)	Zn (±0.93)
BR1 Unfiltered	1.07	3.6	801.7	1.22	0.25	23.4	71.47	5.61
BR1 Filtered	0.95	2.5	474.5	0.82	0.20	8.8	65.58	2.54
BR2 Unfiltered	1.13	1.8	78.5	0.83	0.23	3.5	72.70	1.75
BR2 Filtered	1.32	2.1	47.2	1.00	0.27	3.6	94.56	1.89
BR3 Unfiltered	0.73	2.2	134.1	0.53	0.16	8.0	54.43	1.71
BR3 Filtered	1.02	2.7	77.0	0.86	0.21	4.1	78.50	1.74

3.2 Sediment Analysis Results

3.2.1 % Water, Density, Porosity

The percent water, density and porosity averages for the cores analysed are presented in Table 3.2.A below. The complete data set can be found in Appendix I. The standard deviations are presented in parentheses. The Olifants River cores have the lowest percent waters of the three sites, corresponding with the highest average densities. The Mud Belt cores have the highest percent waters,the lowest densities, highest average porosities. The % water, density and porosity of the Berg River and the Olifants River cores vary with depth, while in the Mud Belt cores they remain relatively constant, as indicated by the differences in standard deviations.

Table 3.2.A. Average % Water, Density & Porosity for Sediment Cores

	Wt. % Water	Porosity	Density (g/cm^3)
OE2-A	24.5 (5)	0.4 (0.07)	1.68 (0.19)
OE3-B	20.1 (0.9)	0.33 (0.02)	1.67 (0.18)
OE4-A	34.8 (6.1)	0.53 (0.07)	1.54 (0.18)
OE6	28.5 (1.7)	0.44 (0.04)	1.56 (0.15)
BR1-A	35.7 (7.9)	0.48 (0.07)	1.39 (0.12)
BR2	34.3 (4.9)	0.51 (0.06)	1.51 (0.10)
BR3-B	27 (2)	0.39 (0.02)	1.47 (0.07)
Geo8313-1	54 (1.3)	0.51 (0.01)	1.03 (0.01)
Geo8322-1	64.5 (1.5)	0.57 (0.02)	0.95 (0.01)

3.2.2 Grain Size Analysis

Grain size analysis of the sediment cores showed varied grain-size distributions (Figure 3.2.A). The figure for core OE3-B has been omitted, as at no point in the sediment column is the sand fraction less than 99%. The raw data from the grain size analyses can be found in Appendix I. The Mud Belt multicore Geo8322-1 is predominantly silt, while Geo8319-1 is a muddy sand. With the exception of 2 sections of the OE4-A core and one section of the Geo8319-1 core, no section of any core has more than 25% clay. The most upstream estuarine cores of the Olifants and Berg river estuaries, OE3-B and BR3-B, respectively, have the highest sand size fractions for their respective sampling locals. The OE2-A core taken closest to the Olifants mouth also has more than 75% sand. The size fractions tend to vary with depth in most cores, however, the relation to depth differs between cores. The Mud Belt cores show a decrease in the clay fraction

Figure 3.2.A – Grain Size vs. Depth for Sediment Cores

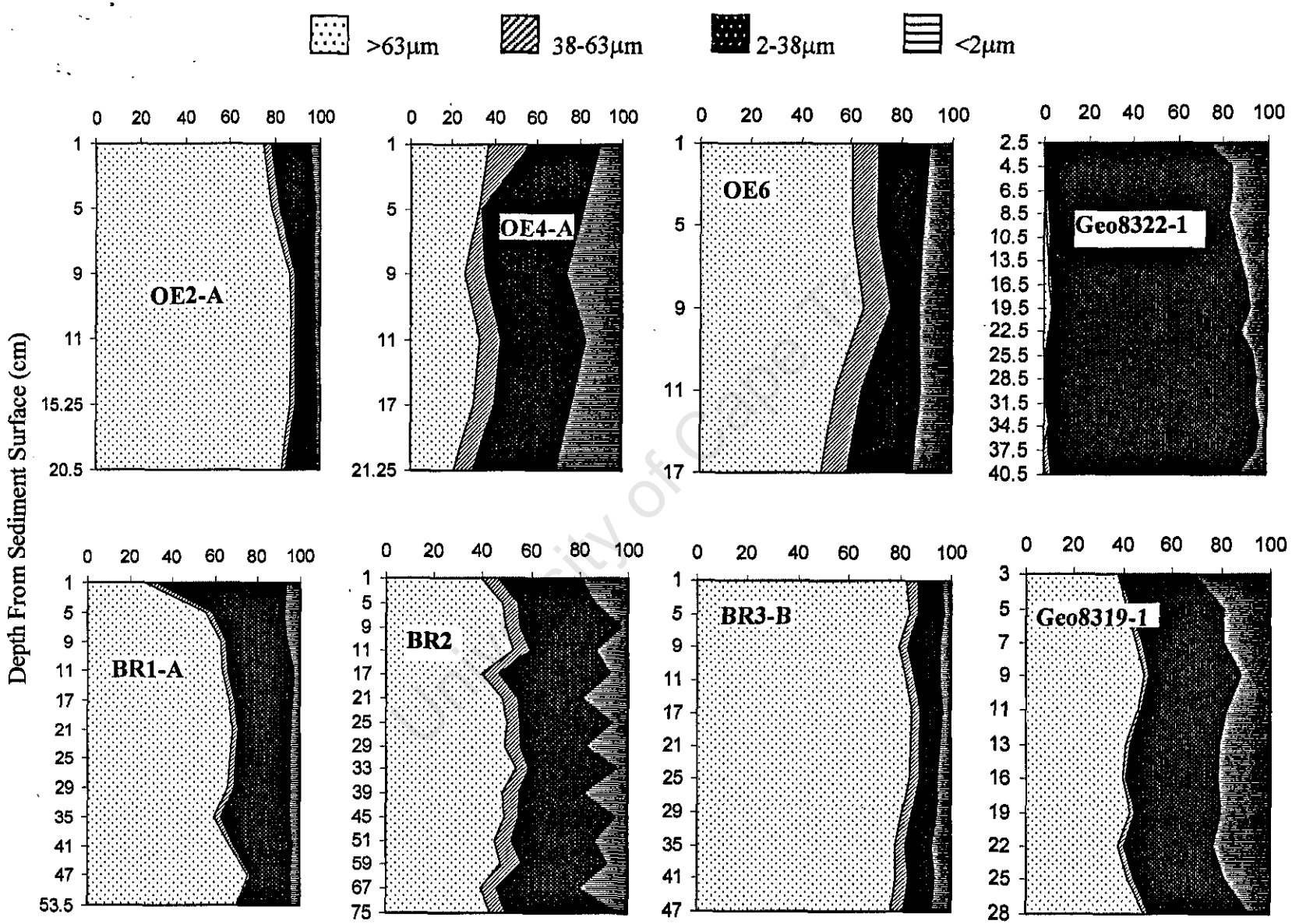

with sediment depth, whereas cores OE4-A and OE6 of the Olifants River display an increase in the clay fraction with depth. The % clay of the other Olifants River coresand the 3 Berg River cores remain relatively constant with depth, although the BR2 shows some fluctuation.

3.2.3 Major Element Analysis

Thirteen major elements were analyzed by XRF. The concentrations for select elements are presented in Tables 3.2.B-D. The sulfur results from the XRF pellets are also included here. All data presented is on a H_2O^- and LOI inclusive basis. The complete data set can be found in Appendix I. On a weight percent basis SiO_2 is the most abundant component in all the sediments analyzed, ranging roughly 40-85%. Generally Al_2O_3 is the second most abundant and Fe_2O_3 is third; the exception being the OE2-A core where the weight percent of CaO exceeds that of Al_2O_3 and Fe_2O_3. The weight percents of K_2O generally range between 1 and 2%. MgO concentrations reach 3% in one of the Mud Belt cores, but generally range from 0.1-2%. A maximum Na_2O weight percent of 4% is observed in core Geo8322, otherwise the Na_2O concentrations tend to range from 0.2-2% in the estuarine cores. The remaining components never exceed 1% by weight. On a molar basis K_2O shows the highest concentrations followed by SiO_2.

The Olifants River sediments tend to have higher concentrations of magnesium and calcium than the Berg River sediments; the means of the Olifants River sediments being 0.42 and 0.47 $mol\,kg^{-1}$ for Mg and Ca, respectively, compared with 0.12 and 0.19 $mol\,kg^{-1}$ for the Berg River sediments. The mean concentrations of the other major elements investigated appear comparable between sites. The sediments within the three sampling locations display considerable heterogeneity. For example, the sediment core mean Al_2O_3 concentrations of the Olifants River estuary range from 0.39 $mol\,kg^{-1}$ in core OE2-A to 1.33 $mol\,kg^{-1}$ in core OE4-A. In addition, fluctuations in major constituent concentrations are observed within individual sediment cores; a coefficient of variance of 97% for TiO_2 in core BR3-B being an example.

The Mud Belt cores contain more phosphorus, by roughly a factor of 2, than the estuarine sediments. The phosphorous concentrations in the Berg River and Mud Belt cores decrease with depth in the upper portion of the core before stabilizing at depth. Examination of the Olifants River cores OE3-B and OE4-A shows phosphorous concentrations begin to decrease with depth for a short depth, below which phosphorous concentrations appear to increase with depth. Cores OE2-A and OE6 show little change in P concentration throughout.

In general the Mud Belt sediments contain the highest concentrations of sulfur followed by the Berg River cores, with those of the Olifants River typically having the least. The sulfur trend in the Berg River and Mud Belt cores is an increase with depth, whereas that of the Olifants cores is to decrease with depth. Core OE6 is the exception, showing a steady increase with depth until approximately 14 cm. In cores BR1-A and Geo8322-1 the sulfur concentrations increase until a depth of approximately 30 cm, below which the concentration begins to decrease. In sediment core BR3-B the sulfur concentration remains relatively constant until approximately 30 cm, below which it displays a slight increase.

The Mud Belt cores contain more phosphorus, by roughly a factor of 2, than the estuarine sediments. The phosphorous concentrations in the Berg River and Mud Belt cores decrease with depth in the upper portion of the core before stabilizing at depth. Examination of the Olifants River cores OE3-B and OE4-A shows phosphorous concentrations begin to decrease with depth for a short depth, below which phosphorous concentrations appear to increase with depth. Cores OE2-A and OE6 show little change in P concentration throughout.

In general the Mud Belt sediments contain the highest concentrations of sulfur followed by the Berg River cores, with those of the Olifants River typically having the least. The sulfur trend in the Berg River and Mud Belt cores is an increase with depth, whereas that of the Olifants cores is to decrease with depth. Core OE6 is the exception, showing a steady increase with depth until approximately 14 cm. In cores BR1-A and Geo8322-1 the sulfur concentrations increase until a depth of approximately 30 cm, below which the concentration begins to decrease. In sediment core BR3-B the sulfur concentration remains relatively constant until approximately 30 cm, below which it displays a slight increase.

Table 3.2.B. Select Major Element Results – Olifants R.

*Oxides identified with a * are in mmol/kg, all others in mol/kg. All data is H_2O- & LOI inclusive*

Sample ID	SiO_2	Al_2O_3	Fe_2O_3	MnO*	MgO	CaO	NaO	K_2O*	P_2O_5*	S
OE2-A: 0-2 cm	12.27	0.42	0.18	6.69	0.26	1.00	0.21	70	8.6	12.5
OE2-A: 2-4 cm	12.59	0.43	0.17	7.49	0.24	0.79	0.16	69	8.4	16.8
OE2-A: 4-6 cm	12.51	0.47	0.20	6.79	0.27	0.81	0.19	94	8.8	15.3
OE2-A: 6-8 cm	13.48	0.33	0.13	5.99	0.20	0.81	0.14	60	7.7	10.0
OE2-A: 8-10 cm	13.30	0.35	0.14	6.65	0.20	0.84	0.15	67	8.4	8.7
OE2-A: 10-12 cm	13.11	0.37	0.15	6.74	0.22	0.87	0.15	65	8.8	7.7
OE2-A: 14-16.5 cm	13.46	0.34	0.13	7.17	0.20	0.79	0.14	64	8.5	5.8
OE2-A: 19-22 cm	13.12	0.39	0.16	6.88	0.23	0.76	0.14	82	8.9	8.5
OE3-B: 0-2 cm	12.46	0.88	0.30	17.59	0.42	0.46	0.22	161	6.5	0.8
OE3-B: 2-4 cm	13.13	0.76	0.29	13.07	0.42	0.42	0.20	139	6.3	0.4
OE3-B: 4-6 cm	13.02	0.71	0.28	12.68	0.42	0.39	0.18	133	5.7	0.5
OE3-B: 6-8 cm	13.39	0.71	0.26	11.98	0.38	0.36	0.17	137	5.6	0.3
OE3-B: 8-10 cm	13.58	0.62	0.24	11.23	0.37	0.34	0.16	120	5.3	0.3
OE3-B: 12-14 cm	13.62	0.66	0.25	10.74	0.36	0.33	0.17	128	5.6	0.3
OE3-B: 16-17 cm	12.61	0.86	0.32	13.91	0.48	0.48	0.22	155	6.5	0.4
OE4-A: 0-2 cm	9.99	1.47	0.39	14.89	0.68	0.48	0.33	246	12.6	12.0
OE4-A: 2-4 cm	9.76	1.44	0.41	17.80	0.69	0.38	0.28	278	12.4	14.0
OE4-A: 4-6 cm	10.43	1.41	0.39	17.42	0.69	0.42	0.27	260	11.9	9.6
OE4-A: 6-8 cm	10.21	1.46	0.40	19.38	0.69	0.44	0.29	275	12.8	6.2
OE4-A: 8-10 cm	10.39	1.43	0.39	18.29	0.69	0.44	0.28	264	12.4	6.0
OE4-A: 12-14 cm	10.36	1.43	0.39	16.89	0.69	0.44	0.26	248	12.5	8.7
OE4-A: 16-18 cm										5.0
OE4-A: 20-22.5 cm	9.90	1.46	0.42	20.89	0.73	0.43	0.23	263	13.2	4.6
OE6: 0-2 cm	12.46	0.93	0.21	6.53	0.39	0.16	0.31	177	7.7	2.7
OE6: 2-4 cm	12.45	0.95	0.23	6.54	0.39	0.17	0.27	190	8.5	4.0
OE6: 4-6 cm	12.24	0.91	0.32	8.63	0.37	0.17	0.28	154	7.8	4.1
OE6: 6-8 cm	11.96	0.89	0.33	9.67	0.36	0.16	0.30	181	7.9	3.8
OE6: 8-10 cm	12.20	0.85	0.32	8.93	0.34	0.16	0.25	173	7.9	5.7
OE6: 12-14 cm	11.69	1.00	0.36	10.02	0.42	0.17	0.29	166	8.8	7.1
OE6: 16-18 cm	12.03	1.05	0.24	6.48	0.45	0.16	0.29	204	8.3	5.0

Table 3.2.C. Select Major Element Results – Berg River Sediment Cores

*Oxides identified with a * are in mmol/kg, all others in mol/kg. All data is H_2O- & LOI inclusive*

Sample ID	SiO_2	Al_2O_3	Fe_2O_3	MnO*	MgO	CaO	NaO	K_2O*	P_2O_5*	S
BR1-A: 0-2 cm	10.05	1.21	0.30	4.65	0.00	0.52	0.04	235	21.0	4.2
BR1-A: 2-4 cm	11.46	0.95	0.22	4.23	0.03	0.42	0.04	186	15.7	5.1
BR1-A: 4-6 cm	12.07	0.85	0.20	3.94	0.04	0.40	0.03	174	14.5	7.4
BR1-A: 6-8 cm	12.91	0.71	0.16	4.41	0.04	0.37	0.03	155	12.7	5.9
BR1-A: 8-10 cm	12.09	0.81	0.18	4.13	0.01	0.34	0.05	175	13.3	4.9
BR1-A: 12-14 cm	13.04	0.74	0.16	3.39	0.02	0.33	0.03	154	11.8	7.4
BR1-A: 16-18 cm	13.31	0.67	0.15	4.07	0.04	0.32	0.05	150	11.1	7.3
BR1-A: 20-22 cm	13.25	0.67	0.14	3.95	0.04	0.29	0.03	147	9.8	10.3
BR1-A: 24-26 cm	13.12	0.71	0.15	4.21	0.06	0.31	0.07	149	9.5	11.4
BR1-A: 28-30 cm	13.19	0.75	0.16	4.19	0.02	0.29	0.03	165	12.0	6.8
BR1-A: 34-36 cm	12.31	0.88	0.19	4.05	0.03	0.32	0.04	183	11.0	12.0
BR1-A: 40-42 cm	13.04	0.79	0.17	4.08	0.02	0.28	0.04	172	10.3	9.6
BR1-A: 46-48 cm	13.24	0.71	0.15	3.81	0.03	0.28	0.05	156	9.7	7.1
BR1-A: 52-55 cm	13.61	0.70	0.15	3.86	0.01	0.29	0.01	161	9.3	7.6
BR2: 0-2 cm	11.54	1.16	0.27	4.95	0.02	0.16	0.04	236	14.7	13.2
BR2: 2-4 cm	11.10	0.92	0.33	6.63	0.27	0.14	0.23	180	13.3	10.4
BR2: 4-6 cm	11.14	0.91	0.33	6.98	0.26	0.16	0.25	183	13.6	12.1
BR2: 6-8 cm	11.25	1.00	0.36	7.29	0.28	0.16	0.23	196	13.8	12.2
BR2: 8-10 cm	11.40	0.93	0.34	7.34	0.26	0.19	0.23	185	14.2	12.2
BR2: 12-14 cm	11.68	0.92	0.33	7.37	0.26	0.14	0.24	188	12.9	13.3
BR2: 16-18 cm										13.8
BR2: 20-22 cm	11.74	1.12	0.25	5.40	0.04	0.23	0.04	221	12.1	11.9
BR2: 24-26 cm	11.81	0.92	0.32	7.70	0.26	0.12	0.22	187	11.9	15.4
BR2: 28-30 cm	11.70	0.96	0.34	7.56	0.27	0.15	0.20	192	12.3	13.2
BR2: 32-34 cm	11.37	1.00	0.35	7.11	0.29	0.14	0.21	198	11.8	12.5
BR2: 38-40 cm	11.29	0.96	0.35	7.93	0.28	0.19	0.22	196	11.9	16.8
BR2: 44-46 cm	11.54	1.13	0.25	5.31	0.03	0.15	0.02	229	12.1	17.5
BR2: 50-52 cm	11.60	0.95	0.32	6.81	0.28	0.11	0.22	191	11.0	13.7
BR2: 58-60cm	11.68	0.92	0.31	7.34	0.29	0.12	0.23	191	10.6	14.4
BR2: 66-68 cm	10.39	1.11	0.40	7.36	0.32	0.22	0.24	195	12.0	18.7
BR2: 74-76 cm	10.87	1.00	0.37	7.01	0.29	0.30	0.23	196	12.1	21.0
BR3-B: 0 - 2 cm	14.06	0.49	0.13	7.17	0.17	0.09	0.17	114	12.9	4.4
BR3-B: 2-4 cm	14.22	0.49	0.12	6.40	0.15	0.09	0.18	121	13.3	4.2
BR3-B: 4-6 cm	14.33	0.47	0.13	6.74	0.01	0.08	0.03	119	14.3	4.2
BR3-B: 6-8 cm	14.48	0.47	0.12	6.15	0.03	0.08	0.04	116	13.7	3.5
BR3-B: 8-10 cm	14.34	0.54	0.13	5.58	0.03	0.08	0.01	128	12.8	4.3
BR3-B: 12-14 cm	14.32	0.51	0.12	5.61	0.17	0.08	0.17	123	11.7	3.8
BR3-B: 16-18 cm	14.29	0.48	0.11	5.74	0.16	0.08	0.17	118	12.4	3.7
BR3-B: 20-22 cm	14.18	0.51	0.12	5.06	0.17	0.08	0.19	122	12.1	4.3
BR3-B: 24-26 cm	14.32	0.49	0.12	5.34	0.17	0.08	0.17	120	12.0	3.9
BR3-B: 28-30 cm	14.17	0.51	0.13	6.01	0.16	0.08	0.16	128	12.6	4.3
BR3-B: 34-36 cm	14.09	0.51	0.12	5.36	0.05	0.08	0.04	120	12.1	5.1
BR3-B: 40-42 cm	14.25	0.55	0.13	6.95	0.04	0.08	0.06	131	12.1	5.6
BR3-B: 46-48 cm	14.06	0.10	0.14	5.45	0.05	0.08	0.08	131	10.1	4.8
BR3-B: 50-51 cm	14.22	0.56	0.13	5.70	0.04	0.08	0.04	134	12.3	7.3

Table 3.2.D. Select Major Element Results – Mud Belt Sediment Cores

*Oxides identified with a * are in mmol/kg, all others in mol/kg. All data is H_2O- & LOI inclusive*

Sample ID	SiO_2*	Al_2O_3	Fe_2O_3	MnO*	MgO	CaO	NaO	K_2O*	P_2O_5*	S
Geo8319: 0 – 2 cm	10.35	0.86	0.20	4.59	0.43	0.25	0.41	203	28.9	18.7
Geo8319: 2 – 4 cm	9.86	0.92	0.22	4.39	0.47	0.27	0.40	221	28.8	11.5
Geo8319: 4 – 6 cm	9.84	0.93	0.22	4.49	0.48	0.27	0.45	209	29.8	12.3
Geo8319: 6 – 8 cm	10.14	0.89	0.21	4.32	0.46	0.28	0.45	198	26.2	15.3
Geo8319: 8 - 10 cm	10.27	0.86	0.20	4.45	0.43	0.30	0.43	191	21.2	11.1
Geo8319: 10 - 12 cm	10.19	0.89	0.21	4.91	0.44	0.31	0.40	201	20.3	14.6
Geo8319: 12 - 14 cm	9.81	0.95	0.22	4.63	0.49	0.32	0.44	204	18.7	13.2
Geo8319: 15 - 17 cm	9.72	0.94	0.22	4.49	0.46	0.31	0.46	205	19.0	12.7
Geo8319: 18 - 20 cm	10.00	0.92	0.22	4.41	0.48	0.29	0.42	201	17.6	15.0
Geo8319: 21 - 23 cm	9.56	0.94	0.23	4.79	0.47	0.32	0.47	208	17.6	16.8
Geo8319: 24 - 26 cm	9.99	0.93	0.23	4.89	0.48	0.25	0.40	210	16.9	13.5
Geo8319: 27 - 29 cm	10.27	0.90	0.22	5.20	0.48	0.22	0.41	206	16.5	11.4
Geo8322: 0 – 1 cm	6.57	1.19	0.35	5.16	0.72	0.62	0.65	238	30.1	11.3
Geo8322: 2 – 3 cm	6.77	1.21	0.35	5.42	0.68	0.62	0.59	248	26.5	10.6
Geo8322: 4 – 5 cm	6.66	1.21	0.35	5.29	0.70	0.63	0.60	256	22.2	13.0
Geo8322: 6 – 7 cm	6.78	1.27	0.36	5.54	0.72	0.64	0.59	265	21.0	15.0
Geo8322: 8 – 9 cm	6.83	1.22	0.35	5.36	0.68	0.62	0.58	262	21.1	20.6
Geo8322: 10 - 11 cm	6.76	1.22	0.35	5.46	0.69	0.63	0.62	249	19.4	15.8
Geo8322: 13 - 14 cm	6.80	1.24	0.35	5.57	0.67	0.68	0.55	252	18.1	8.1
Geo8322: 16 - 17 cm	6.75	1.22	0.35	5.12	0.67	0.71	0.57	249	18.6	25.0
Geo8322: 19 - 20 cm	6.54	1.22	0.36	5.40	0.71	0.72	0.59	258	17.9	21.1
Geo8322: 22 - 23 cm	6.49	1.20	0.36	5.31	0.73	0.74	0.64	241	18.1	17.4
Geo8322: 25 - 26 cm	6.80	1.18	0.36	4.92	0.72	0.66	0.60	239	18.1	27.9
Geo8322: 28 - 29 cm	6.77	1.11	0.34	4.67	0.71	0.67	0.65	224	18.1	21.1
Geo8322: 31 - 32 cm	6.96	1.15	0.36	5.33	0.72	0.53	0.63	241	18.4	27.5
Geo8322: 34 - 35 cm	6.79	1.19	0.37	5.28	0.72	0.50	0.64	250	18.5	24.4
Geo8322: 37 - 38 cm	6.71	1.15	0.35	4.95	0.72	0.57	0.63	242	17.5	17.0
Geo8322: 40 - 41 cm	6.70	1.19	0.35	5.39	0.74	0.71	0.58	241	17.9	19.1

3.2.4 Trace Element Analysis

The sediment cores were analyzed for sixteen trace elements using ICP-MS. Results of the Olifants River estuary, Berg River estuary and the off-shore Mud Belt sediment cores are presented in Tables 3.2.E, 3.2.F and 3.2.G, respectively. The complete data set can be found in Appendix I. Arsenic, cadmium, copper, lead and zinc are presented here.

The trace metal concentrations vary considerably between sample sites as well as within individual sediment columns. Although the river sediments display higher Pb concentrations than the Mud Belt sediments, the Mud Belt generally shows higher concentrations of As, Cd and Cu. Within the Mud Belt cores a background Pb concentration of approximately $0.01 - 0.03$ $mmol{\cdot}kg^{-1}$ is apparent with spikes occurring

at various depths. Core Geo8319 has nearly twice as much As as that found in Geo8322, with core means of 0.34 mmol·kg^{-1} and 0.18 mmol·kg^{-1}, respectively. Arsenic in Geo8319 shows a steady decrease with depth, whereas the arsenic concentration in Geo8322 remains fairly constant throughout.

The Berg River sediments contain more cadmium than the sediments of the Olifants River cores, with sample location means of 1.2 µmol·kg^{-1} and 7.2 µmol·kg^{-1}, respectively. The Mud Belt cores also display higher cadmium levels than the Olifants River cores, with Geo8319-1 containing even more than that witnessed in the Berg River cores. The converse appears to be true for copper with sample location means of 0.34 and 0.21 µmol·kg^{-1} for the Olifants and Berg river estuaries, respectively. However, only the Olifants River sediments OE4-A and OE6 consistently display higher copper concentrations than those found in the Berg River cores. Geo8322 has the highest average copper concentration, 0.78 µmol·kg^{-1} g, of the sampling sites. Mean sample site zinc concentrations vary from 0.69 to 2.07 µmol·kg^{-1}. Zinc does not show consistently higher concentrations in any local as compared to the others.

Table 3.2.E. – Trace element concentrations– Olifants River estuary sediment cores determined by ICP-MS (concentrations in mmol/kg unless specified otherwise)

Sample ID	As	Cd (μmol/kg)	Cu	Pb	Zn
OE2-A: 0-2 cm	0.035	2.1	0.184	0.036	0.739
OE2-A: 2-4 cm	0.034	2.2	0.172	0.037	0.723
OE2-A: 4-6 cm	0.041	1.9	0.198	0.040	0.840
OE2-A: 6-8 cm	0.036	1.4	0.124	0.028	0.580
OE2-A: 8-10 cm	0.035	1.3	0.138	0.030	0.628
OE2-A: 10-12 cm	0.032	1.3	0.144	0.033	0.676
OE2-A: 14-16.5 cm	0.023	1.4	0.145	0.032	0.584
OE2-A: 19-22 cm	0.038	1.4	0.176	0.039	0.722
OE3-B: 0-2 cm	0.042	0.4	0.225	0.050	0.926
OE3-B: 2-4 cm	0.034	0.5	0.181	0.044	0.808
OE3-B: 4-6 cm	0.031	0.3	0.170	0.042	0.772
OE3-B: 6-8 cm	0.034	0.3	0.171	0.044	0.792
OE3-B: 8-10 cm	0.031	0.3	0.163	0.040	0.693
OE3-B: 12-14 cm	0.032	0.2	0.157	0.041	0.711
OE3-B: 16-17 cm	0.040	0.4	0.197	0.048	0.863
OE4-A: 0-2 cm	0.111	1.6	0.597	0.083	2.165
OE4-A: 2-4 cm	0.120	2.0	0.690	0.096	2.104
OE4-A: 4-6 cm	0.108	1.3	0.645	0.087	1.927
OE4-A: 6-8 cm	0.108	1.1	0.647	0.090	2.157
OE4-A: 8-10 cm	0.109	1.2	0.677	0.106	2.399
OE4-A: 12-14 cm	0.120	1.5	0.593	0.087	1.851
OE4-A: 16-18 cm	0.109	1.3	0.693	0.088	1.943
OE4-A: 20-22.5 cm	0.128	1.4	0.710	0.096	2.032
OE6: 0-2 cm	0.083	1.6	0.334	0.065	1.351
OE6: 2-4 cm	0.085	1.5	0.330	0.062	1.275
OE6: 4-6 cm	0.065	1.1	0.263	0.047	0.955
OE6: 6-8 cm	0.099	1.5	0.432	0.072	1.466
OE6: 8-10 cm	0.089	1.3	0.323	0.066	1.294
OE6: 12-14 cm	0.084	1.5	0.346	0.065	1.370
OE6: 16-18 cm	0.087	1.8	0.367	0.071	1.298

Table 3.2.F. – Trace element concentrations – Berg River estuary sediment cores determined by ICP-MS (concentrations in mmol/kg unless specified otherwise)

Sample ID	As	Cd (µmol/kg)	Cu	Pb	Zn
BR1-A: 0-2 cm	0.139	15.7	0.336	0.080	1.712
BR1-A: 2-4 cm	0.103	11.6	0.250	0.068	1.345
BR1-A: 4-6 cm	0.095	9.5	0.209	0.063	1.142
BR1-A: 6-8 cm	0.077	9.0	0.199	0.055	1.114
BR1-A: 8-10 cm	0.086	9.3	0.230	0.061	1.181
BR1-A: 12-14 cm	0.071	8.5	0.205	0.054	1.026
BR1-A: 16-18 cm	0.075	8.4	0.183	0.053	1.003
BR1-A: 20-22 cm	0.071	9.2	0.182	0.053	0.979
BR1-A: 24-26 cm	0.078	8.3	0.224	0.056	0.916
BR1-A: 28-30 cm	0.079	8.0	0.220	0.056	1.011
BR1-A: 34-36 cm	0.086	10.2	0.246	0.063	1.154
BR1-A: 40-42 cm	0.078	6.0	0.215	0.059	1.049
BR1-A: 46-48 cm	0.056	4.4	0.183	0.045	0.769
BR1-A: 52-55 cm	0.062	4.1	0.209	0.056	1.011
BR2: 0-2 cm	0.123	8.4	0.303	0.159	1.802
BR2: 2-4 cm	0.089	6.4	0.238	0.065	1.405
BR2: 4-6 cm	0.113	8.2	0.285	0.081	1.698
BR2: 6-8 cm	0.111	8.0	0.296	0.082	1.702
BR2: 8-10 cm	0.103	7.7	0.273	0.072	1.565
BR2: 12-14 cm	0.099	7.7	0.258	0.067	1.600
BR2: 16-18 cm	0.109	9.2	0.305	0.083	1.774
BR2: 20-22 cm	0.094	8.1	0.301	0.081	1.620
BR2: 24-26 cm	0.080	7.3	0.229	0.072	1.491
BR2: 28-30 cm	0.081	7.6	0.269	0.077	1.583
BR2: 32-34 cm	0.087	8.6	0.251	0.075	1.464
BR2: 38-40 cm	0.097	9.4	0.255	0.076	1.458
BR2: 44-46 cm	0.094	8.9	0.287	0.077	1.425
BR2: 50-52 cm	0.074	8.5	0.217	0.058	1.052
BR2: 58-60cm	0.077	8.3	0.252	0.070	1.361
BR2: 66-68 cm	0.115	12.2	0.394	0.087	1.589
BR2: 74-76 cm	0.100	11.2	0.257	0.079	1.147
BR3-B: 0 - 2 cm	0.039	2.8	0.113	0.036	0.699
BR3-B: 2-4 cm	0.049	4.4	0.127	0.046	0.955
BR3-B: 4-6 cm	0.058	3.9	0.137	0.048	0.997
BR3-B: 6-8 cm	0.047	3.4	0.115	0.042	0.864
BR3-B: 8-10 cm	0.043	4.3	0.143	0.043	0.836
BR3-B: 12-14 cm	0.042	4.1	0.132	0.048	0.899
BR3-B: 16-18 cm	0.035	2.5	0.118	0.043	0.820
BR3-B: 20-22 cm	0.042	4.7	0.160	0.050	1.058
BR3-B: 24-26 cm	0.041	3.3	0.131	0.047	0.925
BR3-B: 28-30 cm	0.043	5.0	0.145	0.049	0.857
BR3-B: 34-36 cm	0.040	5.3	0.137	0.050	0.848
BR3-B: 40-42 cm	0.039	4.7	0.126	0.044	0.725
BR3-B: 46-48 cm	0.033	4.2	0.138	0.048	0.781
BR3-B: 50-51 cm	0.041	5.4	0.142	0.050	1.002

Table 3.2.G. – Trace element concentrations– Offshore mud belt sediment cores *determined* by ICP-MS (concentrations in mmol/kg unless specified otherwise)

Sample ID	As	Cd (µmol/kg)	Cu	Pb	Zn
Geo8319: 0 - 2 cm	0.443	8.8	0.659	0.022	0.888
Geo8319: 2 - 4 cm	0.485	11.2	0.818	0.033	1.088
Geo8319: 4 - 6 cm	0.517	8.5	0.494	0.019	0.996
Geo8319: 6 - 8 cm	0.434	9.1	0.532	0.017	0.863
Geo8319: 8 - 10 cm	0.387	5.9	0.432	0.016	0.800
Geo8319: 10 - 12 cm	0.368	8.5	0.455	0.016	0.873
Geo8319: 12 - 14 cm	0.349	8.8	0.480	0.017	0.861
Geo8319: 15 - 17 cm	0.284	10.3	0.631	0.183	0.769
Geo8319: 18 - 20 cm	0.256	13.2	0.637	0.018	0.875
Geo8319: 21 - 23 cm	0.247	9.1	0.503	0.015	0.862
Geo8319: 24 - 26 cm	0.151	13.1	0.582	0.019	0.728
Geo8319: 27 - 29 cm	0.141	14.2	0.520	0.087	0.803
Geo8322: 0 - 1 cm	0.195	1.5	0.607	0.009	1.132
Geo8322: 2 - 3 cm	0.145	1.6	0.648	0.009	1.133
Geo8322: 4 - 5 cm	0.173	3.6	1.017	0.013	1.380
Geo8322: 6 - 7 cm	0.175	2.4	0.778	0.011	1.269
Geo8322: 8 - 9 cm	0.183	1.3	0.827	0.017	1.468
Geo8322: 10 - 11 cm	0.188	1.5	0.820	0.176	1.356
Geo8322: 13 - 14 cm	0.194	1.5	0.590	0.012	1.286
Geo8322: 16 - 17 cm	0.216	1.4	0.622	0.013	1.309
Geo8322: 19 - 20 cm	0.222	1.2	0.966	0.030	1.208
Geo8322: 22 - 23 cm	0.213	1.8	0.598	0.010	1.222
Geo8322: 25 - 26 cm	0.197	1.6	0.642	0.010	1.138
Geo8322: 28 - 29 cm	0.164	2.7	0.931	0.105	1.207
Geo8322: 31 - 32 cm	0.194	1.4	0.899	0.010	1.153
Geo8322: 34 - 35 cm	0.160	3.7	0.952	0.012	1.472
Geo8322: 37 - 38 cm	0.157	2.2	0.846	0.011	1.321
Geo8322: 40 - 41 cm	0.152	2.5	0.769	0.012	1.299

3.2.5 Total & Organic Carbon

The Mud Belt cores contain significantly more organic carbon (OC) than the estuarine sediments (Table 3.2.G-I). The northern most Mud Belt core (Geo8322) contains on the order of 8%, by weight OC, whereas the southwardly core (Geo8319) contains approximately 4% OC. The % OC does not change much with depth in the offshore cores. In the estuarine sediments the weight % OC rarely exceeds 1%. The full results of the total and organic C:H:N analyses can be found in Appendix I. The OC in the estuarine sediment cores OE2-A, OE4-A, BR1-A and BR2 has a general decrease with depth, while in the remainder the wt. % OC fluctuates, but does not appear to increase or decrease with depth. The two estuarine samples taken closest to their respective rivers

mouths (OE2-A & BR1-A) are the only sediments that show a significant carbonate carbon presence. The carbonate carbon in the OE2-A sediment core exceeds the organic carbon content, whereas in BR1-A there is more organic carbon than carbonate carbon, especially in the upper portion of the sediment. On average the measured % OC in the OE3-B, OE4-A, OE6 and Geo8322 sediments exceeds the measured total carbon resulting in negative calculated carbonate C calculations.

Table 3.2.H – Olifants River Estuary Sediment Carbon Analyses

Sample ID	Total Carbon (wt%, measured)	Organic Carbon (wt%, measured)	Organic C:N ratio	Carbonate Carbon (wt%, calculated)
OE2-A: 0-2 cm	1.7	1.0	1.74	0.7
OE2-A: 2-4 cm	1.3	0.4	5.78	0.8
OE2-A: 4-6 cm	1.4	0.6	4.32	0.8
OE2-A: 6-8 cm	1.1	0.2	5.66	0.9
OE2-A: 8-10 cm	1.3	0.3	4.39	1.0
OE2-A: 10-12 cm	1.1	0.3	2.48	0.9
OE2-A: 14-16.5 cm	1.3	0.2	7.00	1.1
OE2-A: 19-22 cm	1.2	0.3	4.97	0.8
OE3-B: 0-2 cm	0.2	0.3	0.96	*n.d.*
OE3-B: 2-4 cm	0.1	0.3	1.80	*n.d.*
OE3-B: 4-6 cm	0.2	0.5	1.26	*n.d.*
OE3-B: 6-8 cm	0.1	0.3	1.63	*n.d.*
OE3-B: 8-10 cm	0.1	0.2	2.42	*n.d.*
OE3-B: 12-14 cm	0.1	0.3	2.04	*n.d.*
OE3-B: 16-17 cm	0.1	0.3	0.96	*n.d.*
OE4-A: 0-2 cm	1.1	1.2	1.83	*n.d.*
OE4-A: 2-4 cm	1.0	1.3	1.15	*n.d.*
OE4-A: 4-6 cm	0.8	0.9	1.47	*n.d.*
OE4-A: 6-8 cm	0.7	1.0	1.67	*n.d.*
OE4-A: 8-10 cm	0.7	0.9	1.41	*n.d.*
OE4-A: 12-14 cm	0.9	0.8	2.60	0.1
OE4-A: 16-18 cm	0.8	0.9	2.14	*n.d.*
OE4-A: 20-22.5 cm	0.9	1.0	2.14	*n.d.*
OE6: 0-2 cm	0.9	0.9	2.48	*n.d.*
OE6: 2-4 cm	0.8	1.1	2.37	*n.d.*
OE6: 4-6 cm	0.9	1.0	1.98	*n.d.*
OE6: 6-8 cm	0.8	0.9	1.93	*n.d.*
OE6: 8-10 cm	0.7	0.9	2.25	*n.d.*
OE6: 12-14 cm	0.9	0.8	3.38	0.1
OE6: 16-18 cm	0.8	0.9	2.75	0.0

Table 3.2.I. Berg River Estuary Sediment Carbon Analyses

Sample ID	Total Carbon (wt%, measured)	Organic Carbon (wt%, measured)	Organic C:N ratio	Carbonate Carbon (wt%, calculated)
BR1-A: 0-2 cm	2.5	1.9	3.98	0.7
BR1-A: 2-4 cm	1.7	1.2	5.79	0.5
BR1-A: 4-6 cm	2.3	1.1	5.19	1.1
BR1-A: 6-8 cm	1.4	0.8	6.46	0.6
BR1-A: 8-10 cm	1.4	1.1	3.14	0.4
BR1-A: 12-14 cm	1.2	0.8	6.24	0.4
BR1-A: 16-18 cm	1.2	0.7	5.92	0.5
BR1-A: 20-22 cm	1.1	0.7	6.42	0.4
BR1-A: 24-26 cm	1.2	0.7	5.98	0.5
BR1-A: 28-30 cm	1.2	0.7	6.43	0.5
BR1-A: 34-36 cm	1.5	0.9	6.19	0.6
BR1-A: 40-42 cm	1.2	0.7	6.56	0.5
BR1-A: 46-48 cm	1.1	0.6	6.74	0.5
BR1-A: 52-55 cm	0.9	0.5	7.47	0.4
BR2: 0-2 cm	1.4	1.8	5.64	-0.4
BR2: 2-4 cm	1.1	1.0	2.84	0.1
BR2: 4-6 cm	1.2	1.0	3.37	0.2
BR2: 6-8 cm	1.2	1.3	3.44	-0.1
BR2: 8-10 cm	1.1	1.2	3.25	-0.1
BR2: 12-14 cm	1.1	0.8	3.36	0.2
BR2: 16-18 cm	1.3	1.1	3.50	0.2
BR2: 20-22 cm	1.0	0.9	2.72	0.1
BR2: 24-26 cm	0.9	0.9	3.38	0.0
BR2: 28-30 cm	1.0	0.9	3.11	0.1
BR2: 32-34 cm	1.0	0.9	3.03	0.1
BR2: 38-40 cm	1.1	0.9	2.45	0.2
BR2: 44-46 cm	1.1	1.1	2.88	0.0
BR2: 50-52 cm	1.0	1.1	2.93	-0.1
BR2: 58-60cm	1.0	0.9	3.09	0.1
BR2: 66-68 cm	1.3	1.3	3.50	0.1
BR2: 74-76 cm	1.6	1.2	3.57	0.4
BR3-B: 0-2 cm	0.5	0.4	3.41	0.1
BR3-B: 2-4 cm	0.4	0.3	2.93	0.2
BR3-B: 4-6 cm	0.5	0.4	2.98	0.1
BR3-B: 6-8 cm	0.4	0.3	2.52	0.1
BR3-B: 8-10 cm	0.5	0.4	3.28	0.2
BR3-B: 12-14 cm	0.5	0.4	1.72	0.1
BR3-B: 16-18 cm	0.4	0.3	2.92	0.1
BR3-B: 20-22 cm	0.4	0.5	3.44	0.0
BR3-B: 24-26 cm	0.4	0.3	2.60	0.0
BR3-B: 28-30 cm	0.4	0.3	2.84	0.1
BR3-B: 34-36 cm	0.4	0.4	3.11	0.0
BR3-B: 40-42 cm	0.5	0.4	2.76	0.1
BR3-B: 46-48 cm	0.4	0.4	2.75	0.1

Table 3.2.J. Offshore Sediment Carbon Analyses

Sample ID	Total Carbon (wt%, measured)	Organic Carbon (wt%, measured)	Organic C:N ratio	Carbonate Carbon (wt%, calculated)
Geo8319-1: 0 - 2 cm	4.1	4.5	4.34	-0.4
Geo8319-1: 2 - 4 cm	4.8	5.4	4.24	-0.6
Geo8319-1: 4 - 6 cm	4.5	4.3	5.19	0.2
Geo8319-1: 6 - 8 cm	4.4	4.3	4.94	0.1
Geo8319-1: 8 - 10 cm	4.7	4.4	2.38	0.3
Geo8319-1: 10 - 12 cm	4.6	4.3	5.25	0.3
Geo8319-1: 12 - 14 cm	4.7	4.3	5.37	0.4
Geo8319-1: 15 - 17 cm	4.8	5.4	5.49	-0.6
Geo8319-1: 18 - 20 cm	4.8	4.2	5.73	0.5
Geo8319-1: 21 - 23 cm	5.0	5.3	6.02	-0.3
Geo8319-1: 24 - 26 cm	4.3	4.2	5.81	0.1
Geo8319-1: 27 - 29 cm	4.1	3.8	0.49	0.3
Geo8322-1: 0 - 1 cm	6.9	8.2	4.86	-1.3
Geo8322-1: 2 - 3 cm	7.0	8.3	4.95	-1.3
Geo8322-1: 4 - 5 cm	7.1	8.1	5.17	-1.0
Geo8322-1: 6 - 7 cm	7.4	8.1	5.02	-0.7
Geo8322-1: 8 - 9 cm	7.3	8.0	4.85	-0.8
Geo8322-1: 10 - 11 cm	7.2	8.1	5.22	-0.9
Geo8322-1: 13 - 14 cm	7.2	7.9	4.76	-0.7
Geo8322-1: 16 - 17 cm	7.1	7.9	3.48	-0.8
Geo8322-1: 19 - 20 cm	7.4	8.0	4.67	-0.7
Geo8322-1: 22 - 23 cm	7.5	8.5	4.98	-1.0
Geo8322-1: 25 - 26 cm	7.3	8.4	4.94	-1.1
Geo8322-1: 28 - 29 cm	7.4	8.7	3.67	-1.2
Geo8322-1: 31 - 32 cm	7.0	8.6	4.18	-1.6
Geo8322-1: 34 - 35 cm	7.3	8.6	4.60	-1.3
Geo8322-1: 37 - 38 cm	7.5	8.9	4.69	-1.4
Geo8322-1: 40 - 41 cm	7.1	8.6	5.15	-1.5

3.2.6 Carbon-14 Age Dating

^{14}C dating was performed on shell fragments found in the 27-29 cm and the 11-14 cm sub-samples of core Geo8319-1 and the 43 cm sub-sample of Geo8322-1.

Table 3.2.K. ^{14}C age Data for Mud Belt Cores

Sample Name	Depth	^{14}C Age	$^{14}C \pm$	Calibrated Age (yr)	1Σ (yr)	CAMS#
Geo8319-1	11-14cm	685	35	135	110 – 240	[a]
Geo8319-1	27 – 29cm	780	35	270	250 – 290	104271[b]
Geo8322-1	43cm	1260	35	655	630 – 670	104272[b]

[a] – Quadru Center Dating Laboratory, Pretoria, South Africa.
[b] – Lawrence Livermore National Laboratory, California, USA

3.3 Data Quality

The NIST-1640 standard was used during analysis of the surface water samples. The observed and certified values can be found in Appendix I. Eight duplicate surface water samples were collected from 4 sites, one filtered and one unfiltered duplicate from each of the 4 sites. However, the duplicates taken at sample site BR2 were excluded on the basis of them being considered outliers. The differences observed at BR2 were an order of magnitude greater than any of the other duplicate differences witnessed and more than two standard deviations from the mean of the differences. The reported errors for the surface water analysis is given in Table 3.3.A.

Table 3.3.A. Data Quality for Surface Water Samples (values in ηmol/L unless specified otherwise)

	Trip Blank (all values in ηmol/L)	Systematic Error (all values in ηmol/L)	Mean Absolute Error	STD of errors	Reported error (2 STD)
Mg (µmol/L)	0.9	-13.919	11503	8306	28116
Al (µmol/L)	**0.0**	-0.425	0.945	1.464	3.873
Si (µmol/L)	**0.0**	58.614	6.24	6.63	19.50
P (µmol/L)	**0.0**	-3.000	1.90	2.00	5.89
K (µmol/L)	**0.0**	0.386	1672	1131	3933
Ca (µmol/L)	**0.0**	1.278	1092	701	2493
V	**0.0**	0.000	0.355	0.425	1.205
Cr	**0.0**	0.058	0.226	0.360	0.946
Mn	**0.0**	0.030	0.059	0.056	0.171
Fe (µmol/L)	**0.0**	0.614	3.55	2.86	9.27
Co	0.0	0.000	0.002	0.002	0.006
Ni	0.0	-0.020	0.040	0.045	0.131
Cu	0.0	-0.021	0.309	0.331	0.970
Zn (µmol/L)	0.0	-0.311	1.30	2.24	5.79
As (µmol/L)	0.0	0.012	0.161	0.172	0.505
Se	0.0	-0.005	0.284	0.162	0.609
Rb	0.0	0.000	0.162	0.137	0.436
Sr (µmol/L)	0.0	0.051	12	9	29
Mo	0.0	-0.007	0.015	0.010	0.035
Cd	**0.0**	-0.006	0.001	0.001	0.003
Ba	0.0	0.047	0.015	0.009	0.033
Pb	0.0	-0.005	0.008	0.012	0.032

Trace element analysis was performed in 6 batches of 16 samples each. During 5 of the runs a BHVO-1 standard was run and during 4 of the runs the internal standard S10 was run. Eight sub-sample duplicates were analyzed for trace elements using ICP-MS. The

S10 standard was deemed most suitable for comparison with the sediment samples as S10 is a sediment itself, whereas BHVO-1 is a basalt. The reported errors for the trace element analysis is given in Table 3.3.B.

Table 3.3.B – Data Quality Data for Sediment Trace Metal Analysis (all values in µmol/L)

	Systematic Error (2 STD of mean)	Mean Error	STD of errors	Reported Error (Mean + 2 STD)
P	60.8	4.80	3.98	12.8
V	0.0368	0.134	0.078	0.290
Cr	0.301	0.074	0.051	0.176
Mn	0.924	0.431	0.388	1.206
Co	0.011	0.008	0.008	0.024
Ni	0.073	0.016	0.015	0.045
Cu	0.256	0.021	0.017	0.054
Zn	0.973	0.166	0.140	0.447
As	0.016	0.007	0.005	0.016
Se	0.008	0.003	0.003	0.009
Rb	0.072	0.104	0.078	0.261
Sr	6.04	0.148	0.111	0.369
Mo	0.006	0.001	0.000	0.001
Cd	0.003	0.000	0.001	0.001
Ba	0.296	0.280	0.264	0.808
Pb	0.069	0.005	0.003	0.011

Twenty duplicate samples were run for major element analysis using XRF. The reported error is two standard deviations from the mean error. The systematic errors were provided by the UCT XRF facility and consisted of running 18 duplicates. All of the values reported in Table 3.3.C are in mol/kg. The sulfur errors are also reported. Eighteen duplicates were run for sulfur analysis using XRF.

3.4 Calculating core averages

Calculating the average of a measured parameter (eg arsenic concentration) for each sediment core required more than simply calculating the mean of all the measurements because the resolution of analyses decreased with depth. The top 10 centimeters of each core were divided into 5 two-centimeter sub-samples, but below that every other 2 centimeters were analyzed and for deeper cores, such as BR2, the resolution weakened even further at depth. In attempt to compensate for the fact that not every centimeter of the sediment core was analyzed the values recorded were expanded to fill in the gaps.

Table 3.3.C. Data Quality for Sediment Major Element Analysis (all values in mol·kg^{-1})

	Systematic Error	Mean Error	STD of erros	Reported Error (Mean + 2 STD)
SiO2	0.012	0.170	0.147	0.463
Al2O3	0.004	0.031	0.035	0.100
TiO2	0.001	0.002	0.004	0.010
Fe2O3	0.001	0.017	0.033	0.082
MnO	0.001	0.001	0.001	0.002
MgO	0.004	0.039	0.045	0.130
CaO	0.001	0.015	0.025	0.064
Na2O	0.009	0.033	0.047	0.126
K2O	0.000	0.006	0.005	0.016
P2O5	0.002	0.000	0.000	0.001
SO3	0.001	0.004	0.007	0.019
Cr2O3	0.002	0.000	0.000	0.001
NiO	0.001	0.001	0.003	0.007
S	0.034	0.633	0.627	1.887

Thus in addition to attributing a measured parameter to the 2-centimeter sub-sample it was assumed to represent a portion of the sediment core above and below the sub-sample as well. The attributed thickness of each sub-sample is the thickness of the sub-sample (2 cm in most instances, e.g. OE3-B: 8-10 cm) plus half the distance to the bottom of the sub-sample above it and half the distance to the top of the sub-sample below it. Thus for sub-sample OE4-A: 12-14cm the thickness attributed to it is 4 cm (2 cm for the thickness of the sub-sample, plus 1 cm for half the distance to the bottom of the OE4-A: 8-10 cm sub-sample above it, plus 1 cm for half the distance to the top of the OE4-A: 16-18 cm below it). The bottom most sub-sample of each core is attributed a thickness of the sub-sample thickness, plus two times half the distance to the core above it (i.e. it assumes the measured parameter extends an equal distance below the sub-sample as above). For grain-size analysis, where every other sub-section in the top ten centimeters was analyzed the weights are found using half the distances to the next sub-sample analyzed. The measured parameter of each sub-sample is multiplied by the attributed thickness and all the products for the entire core are summed. To determine the core average for the measured parameter the sum is divided by the length of the core. This method gives proper weight to the lower resolution measurements taken down core. For this reason it is deemed to represent the core more accurately than weighting equally the recorded values when averaging.

4 Discussion

4.1 General Observations

Trace element concentrations show a clear positive correlation with fine-grained particles (Figure 4.1.A). Many researchers have witnessed a similar relationship between trace metals and fine-grained particles (e.g. Zhang et al., 2002; Haniff, 2002). The northern most Mud Belt core (Geo8322) is depleted in trace elements per fine-grained particle as compared to the other analyzed sediments. Organic carbon (OC) also shows a positive correlation with fine-grained particles. The OC content in the estuarine sediments increases mildly with % fine-particles and it is clear that more OC per fine-particle is accumulated in the Mud Belt sediments than in those of the estuaries (Figure 4.1.B). This is a reflection of high levels of primary productivity in areas of upwelling (Burton & Statham, 1990).

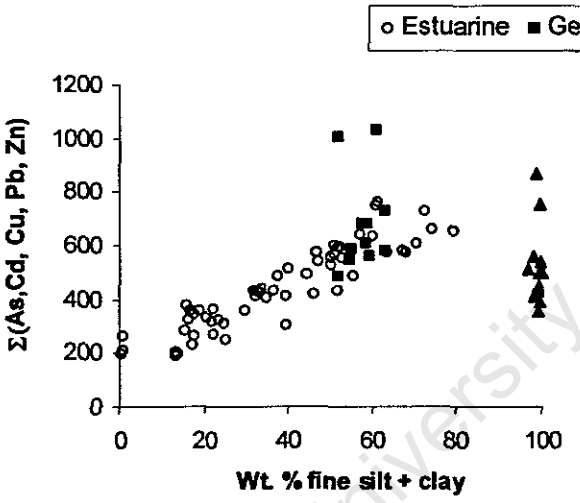

Figure 4.1.A. Σ(As, Cd, Cu, Pb, Zn) vs. Wt. % fine particles. To give each element equal weight in the summation each element is reported as a % of the mean of all the measurements for all cores for that element.

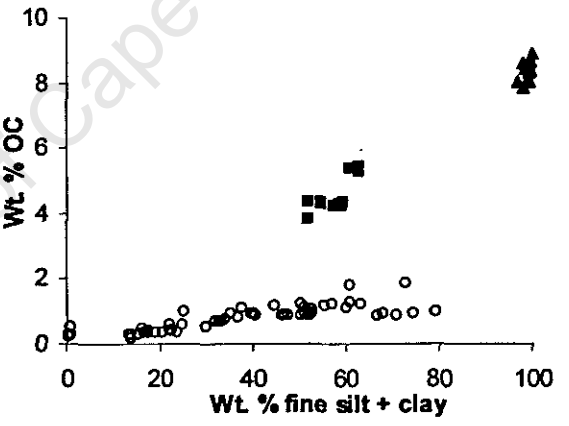

Figure 4.1.B. Organic Carbon (OC) vs. Wt. % fine particles.

4.2 Estuarine Water Chemistry

The simplified equation for salinity [Salinity(ppm) = 640 x EC(dS/m)] (Yiasoumi, 2003) was used to estimate the water salinities at time of sampling. Although the conversion equation for EC to salinity varies from region to region, the differences are not substantial, thus the above acts as a reasonable estimate. The influence of ocean water is apparent from the increase in measured

salinities toward the river mouth, with those taken closest to the mouth having salinities comparable to that of seawater. However, the time of sampling with respect to the tide affects the observed salinity in the rivers at sampling points inside the tidal prism (the distance upstream that seawater penetrates). This distance is increased in summer when river flow is low and seawater encroachment is at its maximum. The salinity witnessed at sample site OE4, near Ebenhaeser, taken near low tide was considerably less than seawater. As water samples were collected from near the surface it is difficult to state whether this is an indication that the river is able to push back the seawater entirely past Ebenhaeser or if the sample was collected from the fresh water above the salt wedge created by ocean water penetrating at depth and river water flowing at the surface (Figure 1.2.3.A). The salinity at Ebenhaeser could be expected to approach that of seawater during high tide in summer as saline waters have been recorded as far upstream as Lutzville (Morant, 1984). Thus it is expected that the water at sites OE5 and OE6, only 2 km from the mouth, had marine salinity signatures at high tide. The Berg River water samples all showed seawater salinities. The seawater is known to encroach 50 km upstream to the Berg River pumping station (Fourie & Steer, 1971). The farthest upstream sample site was only 11 km upstream (BR3) and was sampled at high tide. The lower salinity waters, i.e. stronger river influence, showed higher alkalinities as well, indicative of the effects of rock weathering on rivers.

The dissolved oxygen measurements (5.9 – 20 $mg\,L^{-1}$), combined with the shallow depth of the estuarine sampling sites, let us safely assume that oxidizing conditions prevail at the sediment water interface. The neutral to alkaline pH values recorded are consistent with Fourie & Steer (1971) who attributed them to draining of the alkaline soils of the drier regions eclipsing the drainage of the acid soils of the mountainous regions during summer. The decrease in recorded water temperatures in the upstream direction typify cold ocean water mixing with warmer river water. The high temperature witnessed at site OE2, an off-channel of the main river, suggests a high retention time for the water in the channel allowing it to be warmed by the sun.

The elemental analysis of the waters showed concentrations of the filtered samples (<45µm) often greater than the corresponding unfiltered samples. Aluminum is the only element that never displayed a higher concentration in the filtered sample than in the unfiltered sample. The

difference between the filtered and unfiltered concentrations in the instances where the filtered concentrations exceeded the unfiltered concentrations were within the reported error. Thus it is assumed that the higher concentrations witnessed in the filtered samples are a result of the trace elements being exclusively dissolved or associated with <45μm particles.

The ratio of Ca:Mg is greater in the water samples, which displayed non-marine salinities (OE3 and OE4, 0.91 and 0.35 respectively) than those which had salinities approaching that of the sea (mean of 0.18). This is consistent with the relative abundance of dissolved constituents in river vs. seawater mentioned in Section 1.2.3. However, the Ca:Mg ratio is expected to be greater than 1 if river water were dominant. Another observation that can be made is with the exception of the samples taken at site OE1, the aqueous arsenic concentrations in the Olifants River estuary follow salinity, possibly a result of Cl^- ions in seawater competing for As exchange sites (Adriano, 2003). The Sr concentration in OE2 (93 μmol/L), taken in close proximity to the Olifants River mouth, is comparable to that reported for seawater (89 μmol/L) (Fergusson, 1990). In addition, OE2 has Cd (0.98 ηmol/L) and Cu (1.12 μmol/L) concentrations comparable to those recorded in the upwelling regime of the California coast; 0.90 ηmol/L (Burton & Statham, 1990) and 1.22 μmol/L (Fergusson, 1990). The Pb concentration in the water samples collected near the river mouths (OE1, OE2, and BR) are greater than those reported for seawater (Fergusson, 1990; Burton & Statham, 1990). A negative correlation between trace element concentration and salinity is expected in systems where the river is the major source of the metal, this was not observed for any of the trace elements presented.

4.3 Sediment Analysis

An important aspect of sediment analysis, especially when comparing sediments, is choosing a method for normalizing the data that best facilitates inter-core comparison. Several methods have been proposed, some of which are described in De Groot et al. (1976). Most are based on the premise that trace elements are concentrated in the fine-grained fraction of the sediment. Some use one or more of the size fractions determined from grain size analysis as the normalization parameter. Some use Al as an indicator element for the earth's crust source (Chester & Murphy, 1990), while others rely on the assumption that Fe/Mn-oxides have the greatest capacity to host trace elements and use one or more of Fe and Mn.

Using a size fraction to normalize the data was rejected because of increased error associated with using small sample sizes in grain size analysis, as was the case in this study. Core diameters ranged from 5 to 6 cm (smaller for Mud Belt core Geo8319) were sectioned into 2 cm sub-samples (1cm for Mud Belt core Geo8322) yielding sub-sample sizes for grain size analysis with wet weights ranging from 20 to 100 grams. Data suggesting flocculation introduced debate over what size fraction or fractions to use in normalization. Core OE3-B, in particular, caused problems when attempting to normalize using the size fraction as its sand size faction exceeded 99%, producing artificially high normalized trace element concentrations.

There is greater confidence in the accuracy of the major element analysis via XRF, as compared to grain size, reflected in the random error of only 1.3% for SiO_2 (Section 3.3). There exists a strong correlation between the sand fraction and SiO_2 (Figure 4.3.A). However, the correlation breaks down at both extremes of the graph.

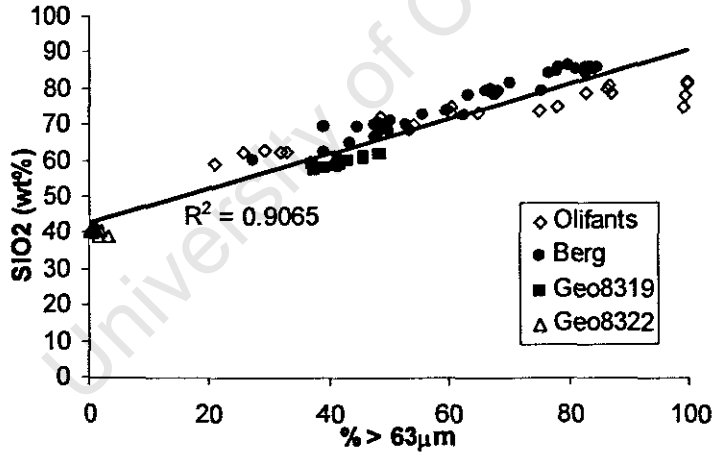

Figure 4.3.A. SiO_2 vs. % Sand for all samples (SiO_2 weight % inclusive of H_2O^- and LOI)

The three points from the OE3-B core (far right of graph, wt. % sand = 99%) do not fit the line well and SiO_2 does not show a good correlation with wt. % sand for Mud Belt core Geo8322, which is only 1% sand. Inspection of the sand size fraction of OE3-B reveals at least 10% lithic fragments, explaining the deviation from the wt. % sand vs. SiO_2 line (Figure 4.3.A). Similar deviations arise when attempting to plot Fe, Mn, Al or any combination thereof against a grain size fraction or trace element concentration. Using SiO_2 as the normalization parameter

produced what was deemed reasonable concentrations for both OE3-B and Geo8322. When comparing cores SiO_2 was used to normalize the data.

4.3.1 Statistical Analysis

Statistica™ was used to perform statistical analysis on the trace and major element analysis data in attempt to better determine what sources contribute most to the estuarine and near-shore sediments. The chemical compositions of the sediment samples were compared to values obtained from the literature for sediments found in the catchment areas. Major element data from fine-grained sediments derived from the Western Ecca Series, Bokkelveld Series, and the Malmesbury Formation from Danchin (1970), as well as data from Schloemann (1994) on soils derived from Cape granites and the Malmesbury Group, were included (Table 4.3.1.A). Rubidium and Sr were also included as those are the only trace elements that Danchin (1970), Schloemann (1994) and this study all analyzed. The identification information for the samples used from the literature can be found in Appendix III.

Discriminant analysis was performed to determine the probability of each sub-sample being in one of the predefined groups. The grouping variable utilized for discriminant analysis will be referred to as 'population' as to not be confused with 'groups' as defined in geological nomenclature. Discriminant analysis assigns an unknown to the population it is statistically most similar to of the predefined populations. It is important to recognize that the probability determined is the probability the unknown is in a particular population out of the populations provided, not the probability that it is a member of that population full stop.

The predefined populations input in Statistica™ were Ecca, Malmesbury, Bokkelveld, and Granite. The samples from Danchin (1970) and Schloemann (1994) were input as members of their respective populations as classified by the respective authors. The estuarine and offshore sediments from this study were input as unknowns. Discriminant analysis was performed on the raw data, SiO_2 normalized and Al_2O_3 normalized data. However, normalization did not alter the results significantly. Therefore, only the results from the raw data analysis are presented. Discriminant analysis produced probabilities of each core sub-sample being in one of the predefined populations, the mean probability for each core is presented in Table 4.3.1.B. It should be noted that the classification equations derived by Statistica™ for discriminant analysis

were unable to assign three of the 62 background samples input in the model to their predefined populations.

Table 4.3.1.A. – Statistica parameters for comparison of sediment samples with background materials.

Variables in Model	SiO_2^{Ψ}, $Al_2O_3^{f}$, Fe_2O_3, MgO, TiO_2, CaO, K_2O, P_2O_5, NaO_2, LOI, Rb, Sr
Tolerance	0.005
Method	Standard

f - excluded in the cases of Al normalization

Ψ - excluded in the cases of Si normalization

All of the Olifants River estuary sediments, except OE6, were determined to most likely to be members of the Ecca Group population. The easily eroded shales and tillites of the Ecca Group (Morant, 1984) form a portion of the Doring River catchment, which contributes the bulk of the Olifants River's silt load (Langhout, 1998, Morant, 1984).

Table 4.3.1.B – Population probabilities for sediment cores (using non-normalized data)

	Malmesbury	Ecca	Bokkelveld	Granite
OE2-A	0.00	1.00	0.00	0.00
OE3-B	0.02	0.98	0.00	0.00
OE4-A	0.00	1.00	0.00	0.00
OE6	0.99	0.01	0.00	0.00
BR1-A	0.00	1.00	0.00	0.00
BR2	0.67	0.33	0.00	0.00
BR3-B	0.87	0.07	0.06	0.00
Geo8319	0.00	1.00	0.00	0.00
Geo8322	0.00	1.00	0.00	0.00

Two of the three Berg River estuary sediment cores are statistically members of the Malmesbury population. The Berg River catchment overlies mainly rocks of the Malmesbury Group and the weathering resistant quartzitic sandstone of the Table Mountain Group. Sediment core BR1-A was assigned to the Ecca population, which is not likely as the Berg River does not drain any areas overlying Ecca Group formations. The Mud Belt cores also indicated to be part of the Ecca Group population. Rocks of the Ecca Group dominate the geological landscape for large portions of the areas to the north east of the Olifants and Berg River catchments (DOMEA, 1984). The tillites and shales of the Ecca Group are easily eroded (Morant, 1984) and it is probable that several rivers emptying into the Atlantic north of the Olifants River catchment derive a portion of their silt load from rocks of the Ecca Group. These sediments may be

transported southward by the subsurface current along the west coast of southern Africa (Shannon, 1990), possibly from as far north as the Orange River.

As mentioned, discriminant analysis can only determine which of the predefined groups an unknown is most probably a member of. As the catchments overly many rock types (Figure 1.3.1.B & 1.3.2.A), several possible inputs have been omitted from the analysis, due mainly to a lack of published data. In addition, chemical composition does not remain constant during weathering (Nahon, 1991), thus direct comparison is not always successful. It is probable that the estuarine and mud belt sediments were assigned to the Ecca population because the Ecca Group sediments share a characteristic of an easily eroded rock type. This is supported by inspection of the canonical scores of the groups. Although the discriminant analysis is effective at grouping the samples of the predefined populations (Figure 4.3.1.A), it is less successful in grouping the unknowns into these populations (Figure 4.3.1.B).

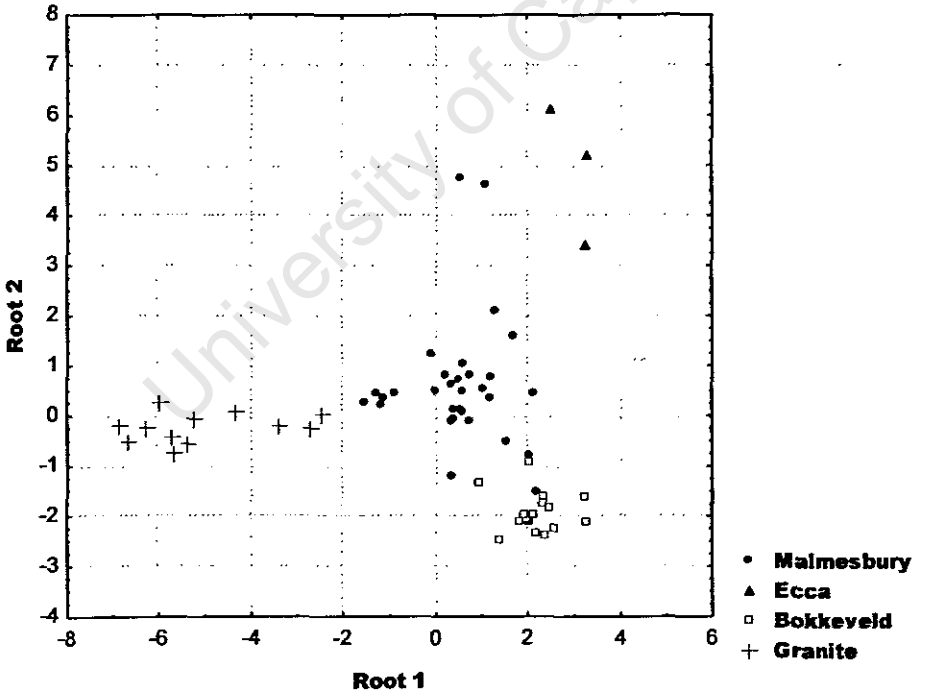

Figure 4.3.1.A – Canonical scores for the predefined samples

Attempts were made to compare the mud belt sediments with those of the estuaries using statistical analysis. Populations of "Olifants River Estuary" and "Berg River Estuary" were predefined and the estuarine sediments were input into the model as members of the their

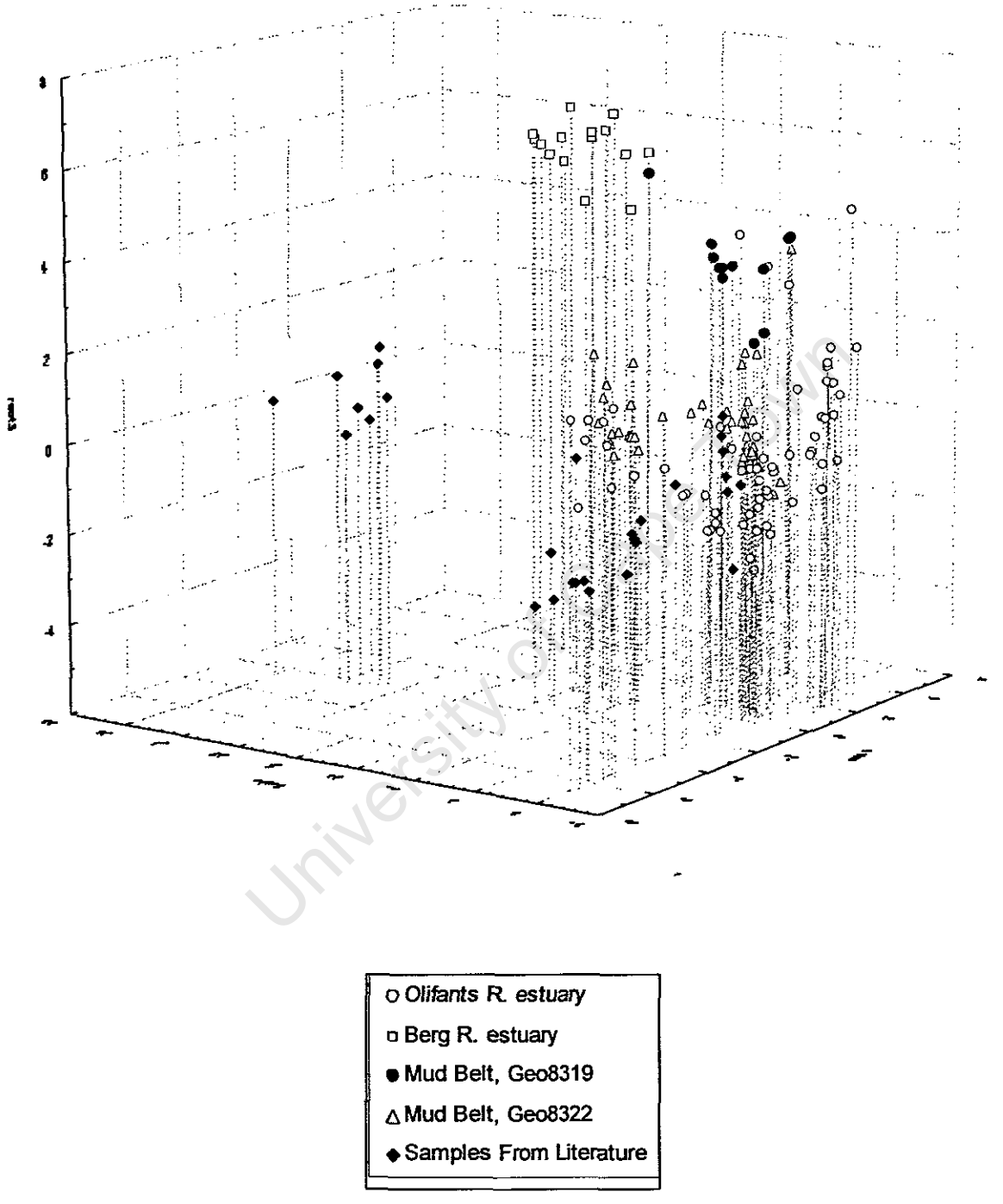

Figure 4.3.1.B. Canonical scores for sediment samples based on groups defined by samples from the literature.

respective populations, rather than as unknowns. In the modified model discriminant analysis determined the mud belt samples to be part of the Berg River estuary population. This is interesting in that in the discriminant analysis in which all the samples from this study were input as unknowns the Berg River samples were mainly assigned to the Malmesbury population, whereas those of the Olifants River and offshore mud belt samples were assigned to the Ecca population.

Discriminant analysis was performed on only the estuarine and mud belt samples using a more comprehensive list of elements (Table 4.3.1.C). Once again discriminant analysis grouped the Mud Belt sediments with the Berg River estuary population. The posterior probability that the mud belt sediments were members of the Berg Rive estuary population rather than the Olifants River estuary population was 1 for every mud belt sub sample.

Table 4.3.1.C. – Statistica™ Parameters for Discriminant analysis of sediments from this study with the offshore mud belt sediments input as unknowns.

Variables in Model	SiO_2, Al_2O_3, Fe_2O_3, MgO, TiO_2, CaO, K_2O, P_2O_5, NaO_2, MnO, SO_3, Cr_2O_3,NiO, LOI, S, Co, Ni, Cu, Zn, As, Rb, Sr, Cd, Pb
Tolerance	0.004
Method	Standard

A statistical analysis, including a more comprehensive list of trace elements, was performed using Schloemann's (1994) data on granite and Malmesbury derived soils (Table 4.3.1.D). The sediment samples from this study were input as unknowns and the model determined them all to be members of the Malmesbury population (Table 4.3.1.E) It is important to note that Schloemann used XRF for analysis of the trace element in the model and some of the data suggests poor data quality, especially for As (e.g. a 743 ppm As measurement for a granite-soil sample). However, when As was left out of the model similar results were observed. However, when the mud belt sediments are input as known populations using the same parameters as Table 4.3.1.D clear groupings become apparent, as evident by their canonical roots (Figure 4.3.1.C).

Table 4.3.1.D. – Statistica™ Parameters for discriminant analysis of sediments using data from Schloemann as the predefined groups and the samples from this study input as unknowns.

Variables in Model	SiO_2, Al_2O_3, Fe_2O_3, MgO, TiO_2, CaO, K_2O, P_2O_5, NaO_2, H_2O^-, LOI, Cu, Zn, As, Rb, Sr, Pb
Tolerance	0.005
Method	Standard

Table 4.3.1.E. Probabilities that Olifants River, Berg River and Mud Belt Sediment Samples are members of the Malmesbury Group of the Granite Group.

	Raw Data			SiO_2 normalized data with NaO_2, H_2O^-, LOI excluded from model	
	Malmesbury	Granite		Malmesbury	Granite
OE2-A	0.69	0.31		0.36	0.64
OE3-B	0.40	0.60		0.86	0.14
OE4-A	0.81	0.19		0.99	0.01
OE6	0.57	0.43		1.00	0.00
BR1-A	0.96	0.04		0.85	0.15
BR2	0.68	0.32		0.95	0.05
BR3-B	0.92	0.08		0.94	0.06
Geo8319	1.00	0.00		1.00	0.00
Geo8322	0.99	0.01		1.00	0.00

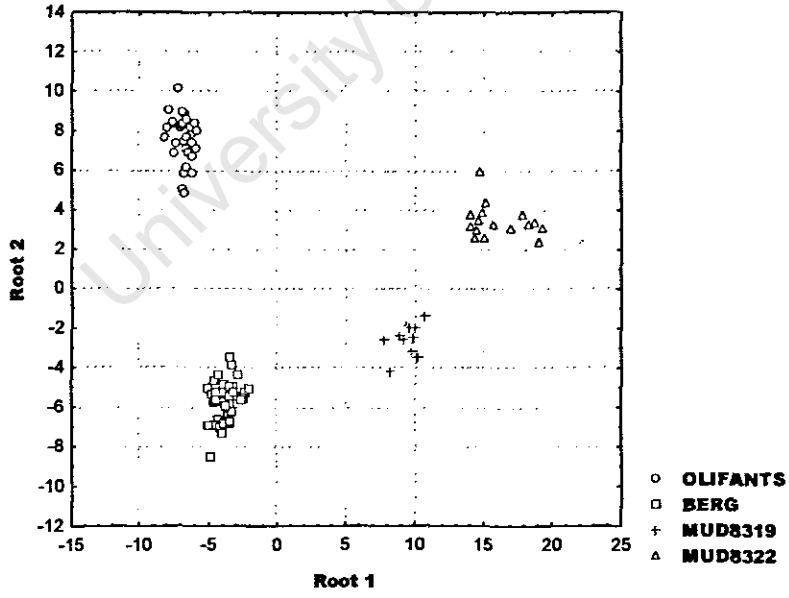

Figure 4.3.1.C. – Canonical scores for discriminant analysis of sediment samples. Populations of Olifants, Berg, Mud8319, and Mud8322 defined (no samples input as unknowns)

From the statistical analysis it can be concluded that the sediments from the Olifants River, Berg River and offshore Mud Belt are statistically different. When compared to the background data available the estuarine samples are most similar to sediments derived from the Malmesbury and Ecca groups and the mud belt sediments are most similar to the sediments from the Ecca Group. When compared to the estuarine sediments the Mud Belt sediments are statistically most similar to the sediments of the Berg River estuary, although they can statistically be clearly differentiated from both estuarine sediments as well as from each other.

4.3.2 Trace Element chemistry

Speculations on trace metal speciation were made based on concentration profiles, correlations with other sediment components, such as Fe_2O_3 and organic carbon (OC), hypothesized redox zones and a literature review of trace metal behavior. Some of the common speciations witnessed for trace elements are associations with clay particles, Fe/Me-oxides, organic matter, sulfides, and carbonates (Ackay; 2003; Tingzong et al., 1997). Correlations between the concentrations of trace elements with the concentrations of Al are often used to indicate the association of trace elements with clay minerals because of Al's role in alumino-silicates (Zhang & Liu, 2002). Thus, correlations between the trace element concentration from ICP-MS analysis and Al_2O_3 from XRF analysis can be used as indication of trace element association with clay minerals. Likewise correlations between trace element concentrations and concentrations of Fe_2O_3 or MnO, OC, S, and carbonate C from the various analyses performed can give indications of trace element association with Fe/Me-oxides, organic matter, sulfides, and carbonates, respectively. For simplicity Al_2O_3, Fe_2O_3 or MnO are sometimes referred to as Al, Fe and Mn respectively in this section. By convention correlation coefficients between 0 and 0.3 are considered no correlation, between 0.3 and 0.7 are considered weak correlations, between 0.7 and 0.99 are strong correlations and 1 is a perfect correlation.

In sediment core OE2-A Cu, Cd, Pb and Zn show strong correlations with Fe_2O_3 and Al_2O_3 (Table 4.3.2.A). This suggests that they are associated with Fe-oxides and/or clay minerals. It is difficult to differentiate, as Fe-oxides are renowned for forming coating on clay particles (Fergusson, 1990; Velde, 1992; Aston and Chester, 1973). Dissolved Cd in the pore water may be reflected by the 0.83 correlation between Cd and % water in OE2-A. This would suggest oxidizing conditions, as Cd solubility is greatest under oxidizing conditions (Tingzong et al.,

Table 4.3.2.A. Sediment Sample OE2-A: Correlation coefficients between concentrations of select sediment components.

	%38-63μm	% 2-38μm	% <2μm	Al_2O_3	Fe_2O_3	MnO	S	Cu	Zn	As	Cd	Pb	$\%H_2O$	OC %	CC %
%38-63μm		0.75	0.66	0.86	0.86	-0.41	0.94	0.74	0.76	0.50	0.90	0.45	0.87	0.82	-0.59
% 2-38μm			0.51	0.87	0.91	-0.20	0.81	0.96	0.83	0.59	0.92	0.83	0.83	0.84	-0.76
% <2μm				0.32	0.39	-0.52	0.50	0.30	0.23	0.16	0.73	-0.04	0.85	0.88	-0.48
Al_2O_3					0.99	0.42	0.80	0.95	0.97	0.49	0.81	0.87	0.74	0.68	-0.61
Fe_2O_3						0.36	0.79	0.96	0.97	0.54	0.82	0.88	0.78	0.74	-0.68
MnO							0.26	0.44	0.29	-0.38	0.43	0.51	0.14	0.03	0.20
Sulfur								0.65	0.71	0.57	0.88	0.53	0.61	0.54	-0.63
Cu									0.94	0.44	0.75	0.95	0.73	0.71	-0.68
Zn										0.62	0.67	0.90	0.66	0.65	-0.68
As											0.27	0.43	0.26	0.36	-0.75
Cd												0.59	0.83	0.75	-0.58
Pb													0.51	0.49	-0.52
% Water														0.97	-0.63
OC %															-0.70
CC %															

Table 4.3.2.B. Sediment Sample OE3-B: Correlation coefficients between concentrations of select sediment components.

	%38-63μm	% 2-38μm	% <2μm	Al_2O_3	Fe_2O_3	MnO	S	Cu	Zn	As	Cd	Pb	$\%H_2O$	OC %	CC %
%38-63μm		0.97	0.96	0.95	1.00	0.96	0.98	0.91	0.96	0.84	0.99	0.93	0.48	0.20	0.22
% 2-38μm			0.99	0.86	0.95	0.91	0.94	0.86	0.89	0.75	0.99	0.86	0.49	0.23	0.18
% <2μm				0.89	0.94	0.95	0.97	0.93	0.92	0.83	0.99	0.91	0.35	0.07	0.34
Al_2O_3					0.96	0.88	0.65	0.93	0.97	0.95	0.65	0.97	0.04	-0.18	0.49
Fe_2O_3						0.79	0.54	0.83	0.90	0.85	0.65	0.88	0.14	-0.01	0.32
MnO							0.92	0.98	0.94	0.88	0.60	0.94	0.14	-0.11	0.52
Sulfur								0.84	0.75	0.65	0.45	0.73	0.31	0.10	0.34
Cu									0.95	0.95	0.60	0.97	0.03	-0.26	0.63
Zn										0.93	0.69	0.99	0.11	-0.13	0.46
As											0.49	0.97	-0.06	-0.42	0.69
Cd												0.62	-0.23	0.04	0.24
Pb													0.05	-0.26	0.57
% Water														0.75	-0.64
OC %															-0.88
CC %															

1997). Cadmium also shows a 0.88 correlation with sulfur, suggesting the presence of CdS, the solubility of which has been shown to control the aqueous concentrations of Cd (Fergusson, 1990). Cadmium association with organic matter must also be considered, as it appears to be the main sorption material for the Cd (Fergusson, 1990). This is reflected in a 0.75 correlation coefficient for Cd and OC in OE2-A. Less significant correlations exist for As in sediment core OE2-A. Arsenic forms Fe and Ba arsenates under oxidizing conditions (Fergusson, 1990). Arsenic exhibits a 0.54 correlation with Fe and a 0.6 correlation with Ba, possibly the result of fractionation between the two arsenates. The Fe association may also be a result of Fe-oxide association. Tingzong et al. (1997) determined association with Fe and Mn oxides to be the dominant active fraction of As. Arsenic also shows weak correlations which Al_2O_3 and S, 0.49 and 0.57 respectively, which could indicate association with clay minerals or formation of sulfides.

Copper, Zn, Pb, and As show strong correlations with Al_2O_3 and Fe_2O_3, MnO, in sediment OE3-B (Table 4.3.2.B), suggesting the association with clay minerals or their associated Fe/Mn-oxide coatings. The correlations between Cd and the same major elements are weaker than that of Cu, Zn, Pb and As, but still above 0.6. Cadmium does not exhibit any other significant correlations to suggest an alternative speciation, except for a 0.7 correlation coefficient with P_2O_5, which can be an indication of bioaccumulation. However, there is no correlation with OC to support this possibility.

The correlations between the trace elements and the major oxides for sediment OE4-A are generally weaker than those for OE2-A and OE3-B (Table 4.3.2.C). The 0.79 and 0.65 correlations with MnO and Fe_2O_3, respectively, suggest a Cu association with Fe/Mn oxides. Arsenic displays a strong correlation with Fe_2O_3, which suggest association of As with Fe-oxides in sediment core OE4-A. The Cd concentration in OE4-A follows that of sulfur until below 15 centimeters (Figure 4.3.2.A). This may signify the presence of CdS and the deviation in the bottom portion of the core a result of a Cd speciation transition at depth. The 0.76 correlation between Cd and OC suggests organo-complexes to be a likely speciation of Cd. It is difficult to speculate on the speciation of Pb and Zn based on their correlation coefficients with the major soil components. Pb

Table 4.3.2.C. Sediment Sample OE4-A: Correlation coefficients between concentrations of select sediment components.

	38-63µm	2-38µm	% <2µm	Al_2O_3	Fe_2O_3	MnO	S	Cu	Zn	As	Cd	Pb	$\%H_2O$	OC %	CC %
%38-63µm		-0.93	-0.44	0.82	0.04	-0.52	0.35	-0.37	0.38	-0.01	0.77	-0.19	0.45	0.71	-0.02
% 2-38µm			0.14	-0.86	-0.18	0.29	0.00	0.07	-0.41	-0.05	-0.60	0.00	-0.09	-0.49	0.04
% <2µm				-0.03	0.60	0.98	-0.95	0.91	0.15	0.45	-0.54	0.73	-0.90	-0.51	-0.18
Al_2O_3					0.60	0.06	-0.02	0.06	0.34	0.26	0.22	-0.08	0.08	0.54	-0.20
Fe_2O_3						0.67	-0.21	0.65	-0.05	0.70	0.26	0.17	-0.15	0.32	-0.18
MnO							-0.72	0.79	0.07	0.42	-0.34	0.56	-0.71	-0.35	-0.19
Sulfur								-0.40	-0.03	0.01	0.77	-0.30	0.99	0.78	-0.17
Cu									0.19	0.26	0.03	0.63	-0.36	-0.02	-0.45
Zn										-0.28	-0.08	0.68	0.07	0.32	-0.71
As											0.51	0.17	0.04	0.15	0.38
Cd												-0.05	0.78	0.76	-0.02
Pb													-0.24	-0.06	-0.43
% Water														0.84	-0.23
OC %															-0.51
CC %															

Table 4.3.2.D. Sediment Sample OE6: Correlation coefficients between concentrations of select sediment components.

	%38-63µm	% 2-38µm	% <2µm	Al_2O_3	Fe_2O_3	MnO	S	Cu	Zn	As	Cd	Pb	$\%H_2O$	OC %	CC %
%38-63µm		-0.57	-0.34	-0.53	-0.40	-0.22	-0.26	0.25	0.57	0.60	0.17	0.44	0.54	0.34	-0.54
% 2-38µm			0.24	0.96	-0.20	-0.31	0.05	0.49	0.20	0.01	0.65	0.25	0.11	-0.73	0.83
% <2µm				0.49	0.21	0.01	0.59	0.46	0.11	0.40	0.34	0.47	-0.77	-0.35	0.00
Al_2O_3					-0.25	-0.38	0.26	0.12	0.08	-0.07	0.71	0.24	-0.14	-0.45	0.59
Fe_2O_3						0.98	0.66	0.11	0.00	0.04	-0.49	-0.08	-0.26	-0.45	0.36
MnO							0.56	0.17	0.11	0.12	-0.50	-0.03	-0.09	-0.40	0.33
Sulfur								-0.02	0.09	0.06	0.01	0.15	-0.54	-0.55	0.40
Cu									0.87	0.91	0.57	0.87	0.30	-0.21	0.13
Zn										0.92	0.66	0.91	0.44	-0.24	0.13
As											0.54	0.93	0.21	-0.05	-0.14
Cd												0.77	0.26	-0.29	0.28
Pb													0.23	-0.29	0.07
% Water														-0.23	0.28
OC %															-0.88
CC %															

displays a weak correlation with MnO (0.56) and a strong correlation with the clay size fraction, which could suggest that Pb is associated with Mn-oxides as coating of clay particles.

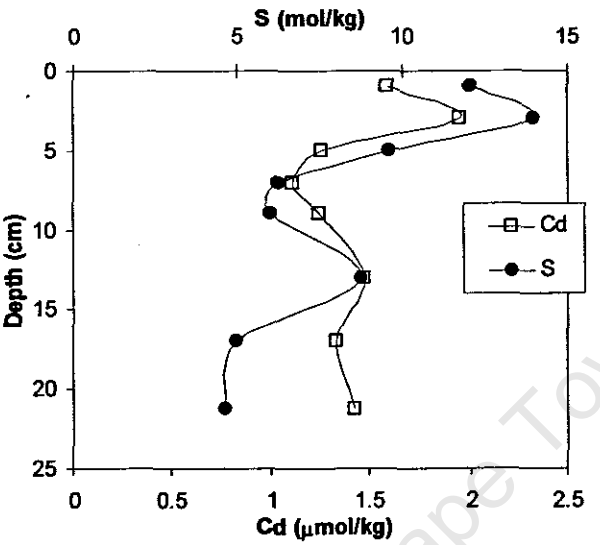

Figure 4.3.2.A. A comparison of Cd and S concentrations vs. depth – Core OE4-A

In the OE6 sediment core Cd displays strong correlations with Al_2O_3 (Table 4.3.2.D), as well as a 0.83 correlation with K, and a 0.75 correlation with MgO. This combination could be the result of Cd association with K-feldspar, a mineral component of several of the rock types found in the Olifants catchment basin (Danchin, 1970; Schloemann, 1994). This is supported by the correlation between As and the natural deposition rate as discussed in Section 4.3.3. Lead also shares a correlation with K (0.71), but not with Al_2O_3. Copper, Pb, Zn and As do not show any other correlations with other soil components that would give insight as to their chemical speciation in sediment core OE6.

All 5 trace elements focused on have strong correlations with Fe_2O_3, Al_2O_3 and to a lesser extent, MnO in the sediment samples from site BR1 (Table 4.3.2.E). In addition, many of the minor and major sediment components have strong correlations with the natural deposition rate in sediment core BR1-A (Section 4.3.3). This is a good indication that the trace elements are either associated with Fe/Mn oxides as clay particle coatings or associated with the clay particles themselves. Arsenic, Cd, Cu, Pb and Zn also show

Table 4.3.2.E. Sediment Sample BR1-A: Correlation coefficients between concentrations of select sediment components.

	%38-63μm	% 2-38μm	% <2μm	Al_2O_3	Fe_2O_3	MnO	S	Cu	Zn	As	Cd	Pb	$\%H_2O$	OC %	CC %
%38-63μm		0.88	0.59	0.83	0.84	0.61	-0.31	0.80	0.85	0.93	0.98	0.84	0.94	0.90	0.45
% 2-38μm			0.50	0.95	0.96	0.59	-0.43	0.90	0.96	0.96	0.88	0.94	0.90	0.94	0.40
% <2μm				0.62	0.64	0.50	-0.38	0.52	0.56	0.65	0.51	0.62	0.66	0.69	0.73
Al_2O_3					0.99	0.55	-0.42	0.95	0.93	0.95	0.80	0.94	0.86	0.94	0.41
Fe_2O_3						0.58	-0.47	0.92	0.94	0.96	0.83	0.94	0.89	0.97	0.43
MnO							-0.30	0.62	0.63	0.67	0.59	0.62	0.59	0.57	0.18
Sulfur								-0.33	-0.52	-0.43	-0.33	-0.37	-0.52	-0.55	-0.05
Cu									0.90	0.90	0.77	0.93	0.77	0.86	0.24
Zn										0.95	0.87	0.97	0.90	0.94	0.31
As											0.91	0.96	0.94	0.97	0.46
Cd												0.84	0.94	0.89	0.36
Pb													0.86	0.92	0.40
% Water														0.96	0.46
OC %															0.46
CC %															

Table 4.3.2.F. Sediment Sample BR2, top 20cm: Correlation coefficients between select sediment components.

	%38-63μm	% 2-38μm	% <2μm	Al_2O_3	Fe_2O_3	MnO	S	Cu	Zn	As	Cd	Pb	$\%H_2O$	OC %	CC %
%38-63μm		-0.64	0.96	0.48	-0.67	-0.59	0.32	0.23	0.59	0.57	0.23	0.56	0.57	0.27	-0.03
% 2-38μm			-0.66	0.09	0.13	-0.02	0.23	0.56	0.23	0.02	0.58	-0.06	-0.14	0.15	-0.15
% <2μm				0.66	-0.81	-0.75	0.16	0.24	0.56	0.68	0.10	0.72	0.74	0.48	-0.29
Al_2O_3					-0.75	-0.86	0.45	0.69	0.69	0.75	0.54	0.96	0.95	0.96	-0.86
Fe_2O_3						0.92	-0.40	-0.29	-0.43	-0.50	-0.32	-0.86	-0.92	-0.64	0.45
MnO							-0.18	-0.40	-0.44	-0.55	-0.27	-0.92	-0.95	-0.81	0.65
Sulfur								0.67	0.78	0.58	0.87	0.37	0.31	0.19	0.00
Cu									0.96	0.90	0.91	0.60	0.47	0.60	-0.40
Zn										0.93	0.94	0.65	0.54	0.54	-0.29
As											0.78	0.80	0.71	0.73	-0.52
Cd												0.43	0.32	0.32	-0.08
Pb													0.99	0.92	-0.74
% Water														0.88	-0.72
OC %															-0.93
CC %															

strong correlations with OC. Organic matter has also been shown to form coatings on clay minerals (Luoma, 1990). In the BR1-A sediment clay minerals, Fe/Mn-oxides and organic matter appear inter-related and the trace elements are likely partitioned between the three.

The speciations in the BR2 sediment are hard to identify from the correlation coefficients. It is hypothesized that this is the result of strongly reducing conditions prevailing down core causing trace elements and major soil components to dissociate and different behaviors of the trace elements and their former hosts under reducing conditions result in weak or no correlations. Based on this hypothesis and the proposed redox zones for sediment core BR2 (Section 4.3.5) the data from the top 20 cm of the BR2 core was looked at separately from the bottom segment. It is important to note that the separation between redox zones are not clear cut lines, but rather transition zones and that there are several redox zones with overlapping regions. The splitting of the cores attempt to separate the oxidizing zone from the heavily reducing zone. In the top 20 cm (Tables 4.3.2.F) Cu, As, Zn, and Pb all show significant correlations with Al as well as K (0.68, 0.77, 0.72, 0.97, respectively) reflecting the possible association with K-feldspar or other potassium containing clay mineral. These metals display negative correlations with Fe and Mn in the same regions, suggesting a lack of Fe/Mn coatings on the clay minerals. This is also apparent in the correlations with size fractions displayed by Al_2O_3, Fe_2O_3, and MnO. Aluminum shows a 0.66 correlation with the clay size fraction, whereas Fe and Mn show strong correlation with the sand size fraction. Arsenic and Pb exhibit strong correlations with OC in the top 20 cm and Cu and Zn display correlations of 0.60 and 0.54 with OC, respectively. As mentioned, organic material has also been shown to form coatings on clay particles (Luoma, 1990). Zinc shows a strong correlation with sulfur in the top 20 cm, but Zn sulfides typically only occur at redox potentials below −150 mV (Connell & Patrick, 1968). The presence of Zn sulfides would disprove the hypothesis that oxidizing conditions prevail above 20 cm in the BR2 sediment column. Cadmium shows a similar, although weaker, correlation with S. However, in the case of Cd the formation of CdS occurs under oxidizing conditions (Fergusson, 1990).

Table 4.3.2.G. Sediment Sample BR2, below 20cm: Correlation coefficients between select sediment components.

	%38-63μm	% 2-38μm	% <2μm	Al_2O_3	Fe_2O_3	MnO	S	Cu	Zn	As	Cd	Pb	$\%H_2O$	OC %	CC %
%38-63μm		-0.15	0.23	-0.35	0.04	0.16	0.00	-0.11	-0.41	-0.24	0.08	-0.41	0.31	0.13	-0.09
% 2-38μm			-0.83	0.00	0.18	-0.10	0.60	-0.13	-0.54	0.09	0.36	-0.06	0.04	0.53	0.16
% <2μm				0.21	0.12	0.12	-0.20	0.48	0.42	0.30	0.13	0.25	0.38	-0.01	-0.10
Al_2O_3					-0.31	-0.75	0.19	0.75	0.38	0.68	0.41	0.64	0.60	0.41	0.04
Fe_2O_3						0.78	0.45	0.21	-0.14	0.36	0.61	0.16	0.03	0.38	0.31
MnO							0.12	-0.19	-0.03	-0.10	0.07	-0.12	-0.38	-0.16	0.14
Sulfur								0.31	-0.28	0.64	0.78	0.36	0.45	0.72	0.44
Cu									0.56	0.82	0.64	0.80	0.59	0.47	0.09
Zn										0.32	-0.15	0.70	-0.15	-0.43	0.03
As											0.85	0.83	0.65	0.55	0.47
Cd												0.50	0.70	0.81	0.42
Pb													0.26	0.15	0.53
% Water														0.69	0.02
OC %															0.00
CC %															

Table 4.3.2.H. Sediment Sample BR3-B, above 12 cm: Correlation coefficients between select sediment components.

	%38-63μm	% 2-38μm	% <2μm	Al_2O_3	Fe_2O_3	MnO	S	Cu	Zn	As	Cd	Pb	$\%H_2O$	OC %	CC %
%38-63μm		-0.77	0.11	-0.42	-1.00	0.77	0.49	-1.00	-0.79	-0.60	-0.98	-0.90	0.91	0.96	-0.37
% 2-38μm			0.55	0.90	0.83	-1.00	0.18	0.83	0.21	-0.04	0.87	0.41	-0.97	-0.56	0.88
% <2μm				0.86	-0.01	-0.54	0.92	-0.02	-0.70	-0.86	0.07	-0.54	-0.32	0.39	0.88
Al_2O_3					0.53	-0.62	0.60	0.64	-0.22	-0.40	0.49	0.01	-0.32	0.06	0.72
Fe_2O_3						-0.20	0.47	0.72	-0.01	0.15	0.14	0.16	-0.38	0.61	0.05
MnO							0.20	-0.55	-0.21	0.04	-0.67	-0.35	0.83	0.17	-0.30
Sulfur								0.44	-0.18	-0.17	0.18	-0.03	0.47	0.02	0.71
Cu									0.52	0.45	0.78	0.70	-0.43	-0.09	0.49
Zn										0.93	0.71	0.97	-0.16	-0.59	0.10
As											0.45	0.87	-0.09	-0.31	-0.16
Cd												0.83	-0.32	-0.65	0.66
Pb													-0.25	-0.55	0.25
% Water														-0.26	0.23
OC %															-0.56
CC %															

In the sediment core below 20 cm (Table 4.3.2.G) correlations between Cd and S is strengthened suggesting the formation of additional CdS. Cd also shows a strong correlation with OC below 20 cm in BR2. Cadmium sulfide and Cd-organo-complexes have been shown to persist in reducing conditions (Tingzong, et al., 1997). The Cu-Al correlation also strengthens in the bottom, reducing segment of sediment core BR2, suggesting a non-exchangeable association of Cu with clay particles. Pb and As show strong correlations with OC, while Zn displays a 0.54 correlation with OC. Lead, As, and Zn are known to form stable compounds with organic matter in low pH, reducing conditions (Adriano, 2001).

Inspection of the entire length of sediment core BR3-B shows Pb, Cd, Zn and Cu have strong positive correlations with each other, but not with any of the major soil components for which data is available. Investigating the top 10 cm of sediment core BR3-B and the bottom 40 cm independently, as per the redox hypothesis of Section 4.3.5, reveals some possible associations that partially or fully dissociate when reducing conditions prevail. Cadmium shows a 0.66 correlation with carbonate carbon in the top 10 cm of the sediment column, suggesting the presence of $CdCO_3$ (Table 4.3.2.H). Copper has a strong correlation with Al_2O_3 in the top 10 cm, indicating association with clay minerals. This is supported by a 0.83 correlation with the fine silt fraction, a possible result of flocculation (Section 4.3.7). In the bottom 40 cm of the core Cu and Zn show correlations with OC (0.75 and 0.45, respectively), while As displays a strong correlation with Al_2O_3.

Correlation analysis of the entire lengths of the Mud Belt cores did not provide much insight to the speciation of the trace elements. Splitting the core into the perceived oxic and anoxic sections was less successful for core Geo8322, than for the core closest to the Berg River mouth (Geo8319). A good illustration of the benefits of this method is shown in Figure 4.3.2.B where As concentration is plotted against Al_2O_3. Two distinct populations are revealed, each with a positive correlation, but cumulatively they suggest no correlation.

Table 4.3.2.I. Sediment Sample BR3-B, below 12 cm: Correlation coefficients between select sediment components.

	%38-63μm	% 2-38μm	% <2μm	Al_2O_3	Fe_2O_3	MnO	S	Cu	Zn	As	Cd	Pb	$\%H_2O$	OC %	CC %
%38-63μm		0.62	0.88	-0.48	0.73	0.40	0.85	-0.19	-0.69	-0.46	0.38	-0.10	-0.32	0.13	0.23
% 2-38μm			0.53	-0.32	0.70	0.50	0.66	-0.03	-0.67	-0.26	0.59	0.02	-0.30	0.16	0.48
% <2μm				-0.46	0.72	0.07	0.78	0.06	-0.46	-0.26	0.55	0.30	-0.60	0.19	-0.01
Al_2O_3					-0.53	0.26	0.15	-0.02	0.34	0.72	0.19	0.03	0.40	0.04	0.06
Fe_2O_3						0.15	0.64	0.37	-0.14	-0.24	0.62	0.35	-0.57	0.34	0.20
MnO							0.28	-0.47	-0.65	-0.05	0.13	-0.60	0.36	-0.24	0.68
Sulfur								0.16	0.11	0.04	0.68	0.32	-0.50	0.27	0.34
Cu									0.68	0.47	0.60	0.80	-0.14	0.75	-0.62
Zn										0.56	0.18	0.66	-0.11	0.45	-0.51
As											0.44	0.52	0.17	0.28	-0.16
Cd												0.69	-0.33	0.64	-0.04
Pb													-0.53	0.60	-0.42
% Water														0.11	-0.23
OC %															-0.59
CC %															

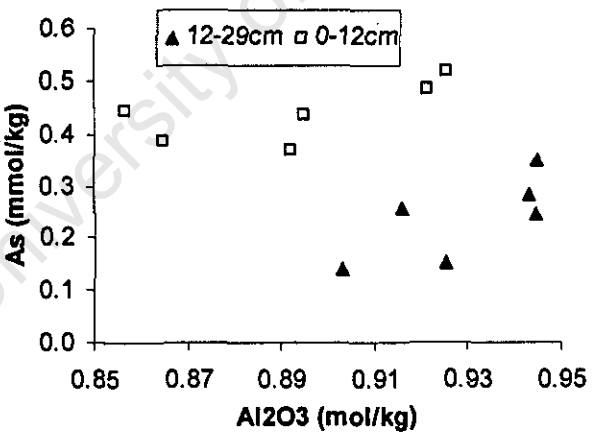

Figure 4.3.2.B. Arsenic vs. Al_2O_3 – Sediment Core Geo8319

Table 4.3.2.J. Sediment Sample Geo8319, top 12cm: Correlation coefficients between select sediment components

	%38-63μm	% 2-38μm	% <2μm	Al_2O_3	Fe_2O_3	MnO	S	Cu	Zn	As	Cd	Pb	$\%H_2O$	OC %	CC %
%38-63μm		0.23	-0.46	-0.35	-0.41	-0.63	0.27	-0.37	-0.52	0.00	-0.37	-0.46	0.22	-0.52	0.39
% 2-38μm			-0.87	-0.38	-0.42	0.28	-0.15	-0.87	-0.55	-0.19	-0.87	-0.75	0.80	-0.77	0.86
% <2μm				0.73	0.75	-0.26	-0.13	0.97	0.89	0.56	0.96	0.93	-0.46	0.89	-0.97
Al_2O_3					0.98	-0.21	-0.52	0.25	0.79	0.66	0.58	0.43	0.29	0.36	-0.14
Fe_2O_3						-0.14	-0.38	0.36	0.86	0.70	0.69	0.50	0.22	0.41	-0.26
MnO							0.29	-0.34	-0.23	-0.53	-0.18	-0.36	-0.09	-0.29	0.28
Sulfur								0.09	-0.30	-0.16	0.13	-0.18	-0.35	-0.29	-0.20
Cu									0.74	0.51	0.83	0.95	-0.53	0.90	-0.99
Zn										0.79	0.81	0.86	0.01	0.77	-0.68
As											0.53	0.60	0.41	0.39	-0.49
Cd												0.79	-0.47	0.71	-0.78
Pb													-0.35	0.96	-0.92
% Water														-0.47	0.52
OC %															-0.85
CC %															

Table 4.3.2.K. Sediment Sample Geo8319, below 12cm: Correlation coefficients between select sediment components.

	%38-63μm	% 2-38μm	% <2μm	Al_2O_3	Fe_2O_3	MnO	S	Cu	Zn	As	Cd	Pb	$\%H_2O$	OC %	CC %
%38-63μm		0.08	0.06	0.06	0.81	0.58	0.45	-0.48	-0.14	-0.49	-0.05	-0.50	0.17	0.06	-0.20
% 2-38μm			-0.84	-0.46	0.27	0.79	-0.71	-0.25	-0.43	-0.57	0.39	0.51	-0.76	-0.27	-0.16
% <2μm				0.83	0.01	-0.75	0.72	0.16	0.24	0.65	-0.72	-0.18	0.88	0.72	-0.38
Al_2O_3					0.03	-0.49	0.41	-0.20	0.12	0.73	-0.95	0.07	0.63	0.80	-0.58
Fe_2O_3						0.52	0.16	-0.04	-0.64	-0.65	0.13	0.00	0.01	0.22	-0.54
MnO							-0.38	-0.54	-0.34	-0.75	0.41	-0.09	-0.65	-0.47	0.08
Sulfur								-0.03	0.52	0.25	-0.41	-0.54	0.92	0.48	-0.16
Cu									-0.32	-0.10	0.41	0.42	0.14	0.15	-0.14
Zn										0.56	-0.37	-0.44	0.49	0.03	0.37
As											-0.81	0.02	0.51	0.47	-0.07
Cd												0.01	-0.60	-0.71	0.45
Pb													-0.23	0.40	-0.61
% Water														0.73	-0.36
OC %															-0.87
CC %															

Correlation analysis of the Geo8319 core was split below the 10-12 cm sub-sample as per the redox hypothesis of Section 4.3.5. Zinc, As, and Cd show appreciable correlations with Al_2O_3 and Fe_2O_3 above 12 centimeters, while Pb shows a weaker positive correlation with Al_2O_3 and Fe_2O_3 (Table 4.3.2.J). Zinc and Cd also show correlations with OC. Lead and Cu, which are considered to be the most strongly organically-sorbed of the divalent cations, show very strong correlations with OC (Bloom, 1981).

Below 12 cm As shows a 0.73 correlations with Al, suggesting a continued association with clay minerals (Table 4.3.2.K). This is supported by a 0.65 correlation with the <2μm fraction. The correlations, or rather lack there of, for Cu, Zn, Cd and Pb below 12 cm in sediment core Geo8319 do not give much insight as to their speciation in this region. Dividing the Geo8322 sediment core was less successful that with other cores. Anoxic conditions were thought to begin below 10 cm, however investigation of the top 10 cm did not reveal any insights into trace element speciation. In the bottom, anoxic portion of Geo8322 Cd, and to a lesser extent Cu, show correlations with OC. Considering that Geo8322 sediment contains approximately 8% OC it is likely to play a role in the speciation of many of trace elements. Arsenic displays a 0.70 correlation with carbonate C. However, the carbonate C was calculated as the difference between the measured total carbon and organic carbon. In the case of Geo8322 this value was often negative, suggesting undetectable amounts of carbonate C. Arsenic also displays a weaker correlation with Al_2O_3 below 10 cm.

Table 4.3.2.L. Sediment Sample Geo8322, above 10 cm: Correlation coefficients between select sediment components.

	%38-63μm	% 2-38μm	% <2μm	Al_2O_3	Fe_2O_3	MnO	S	Cu	Zn	As	Cd	Pb	$\%H_2O$	OC %	CC %
%38-63μm		-0.22	0.15	0.04	0.20	0.11	0.73	-0.46	0.30	0.23	-0.91	0.54	-0.17	-0.27	0.32
% 2-38μm			-1.00	0.39	-0.05	-0.12	0.49	0.79	0.73	0.89	0.57	0.53	-0.48	-0.88	0.78
% <2μm				-0.41	0.03	0.10	-0.55	-0.76	-0.76	-0.92	-0.51	-0.57	0.51	0.91	-0.82
Al_2O_3					0.77	0.91	0.39	0.21	0.27	-0.20	0.19	0.12	-0.79	-0.49	0.80
Fe_2O_3						0.71	0.06	-0.45	-0.31	-0.11	-0.28	-0.33	-0.31	-0.07	0.40
MnO							0.24	0.09	0.12	-0.57	0.08	0.00	-0.87	-0.19	0.59
Sulfur								0.38	0.85	0.33	-0.21	0.92	-0.47	-0.86	0.81
Cu									0.80	0.03	0.78	0.61	-0.53	-0.61	0.50
Zn										0.24	0.27	0.96	-0.54	-0.86	0.74
As											-0.08	0.32	0.53	-0.54	0.22
Cd												0.00	-0.30	-0.20	0.17
Pb													-0.39	-0.81	0.65
% Water														0.43	-0.70
OC %															-0.90
CC %															

Table 4.3.2.M. Sediment Sample Geo8322, below 10 cm: Correlation coefficients between select sediment components.

	%38-63μm	% 2-38μm	% <2μm	Al_2O_3	Fe_2O_3	MnO	S	Cu	Zn	As	Cd	Pb	$\%H_2O$	OC %	CC %
%38-63μm		-0.53	0.46	0.10	-0.18	0.12	-0.27	-0.13	0.24	-0.33	-0.03	-0.06	-0.77	0.14	-0.16
% 2-38μm			-0.98	-0.69	0.21	-0.66	0.56	0.47	-0.15	-0.27	0.40	-0.23	0.38	0.55	-0.47
% <2μm				0.61	-0.28	0.60	-0.58	-0.53	0.08	0.23	-0.40	0.32	-0.31	-0.51	0.42
Al_2O_3					0.20	0.77	-0.37	-0.45	0.28	0.55	-0.41	-0.09	-0.29	-0.81	0.74
Fe_2O_3						0.33	0.35	0.19	0.22	-0.01	0.29	-0.50	0.02	0.27	-0.27
MnO							-0.44	-0.16	0.27	0.28	-0.29	-0.06	-0.33	-0.50	0.30
Sulfur								0.29	-0.28	0.10	0.07	-0.22	0.47	0.27	-0.39
Cu									0.17	-0.38	0.39	0.29	0.24	0.43	-0.40
Zn										-0.44	0.59	0.15	-0.44	0.01	0.02
As											-0.77	-0.11	0.40	-0.71	0.70
Cd												-0.02	-0.10	0.62	-0.51
Pb													0.36	-0.15	0.19
% Water														0.00	0.08
OC %															-0.88
CC %															

4.3.3 Natural Deposition Rates

One method used to recognize a pollution input is to use the alkaline earth metals to estimate natural deposition rates and compare that with the deposition rate of a particular element. Shirihata et al. (1980) used Sr, Ba and Ca, weighting the concentrations they observed to give the 3 elements approximately equal weight and averaging the values to allow Sr, Ba and Ca to plot as a single point. I rather translated the sub-sample (e.g. OE6:0-2 cm) concentration of each alkaline earth metals (Sr, Ba and Ca) to a fraction of its core mean concentration. I then averaged the three fractions allowing Sr, Ba and Ca to plot as a single point. This method maintains the shape of the concentration profiles and magnitudes of the trends while ensuring equal weight is given to Sr, Ba and Ca for every point. I then plotted these points against depth, along with the concentrations of various sediment components, weighted in a similar manner as the individual alkali earth metals, for comparison. The Pearson correlation coefficient was calculated to quantify the degree to which the rate of deposition of the sediment component correlated with the natural deposition estimate. In many of the sampling locations the accumulation rate of the Al_2O_3, Fe_2O_3 and trace elements followed that of natural deposition, as indicated by their correlation coefficients (Tables 4.3.3.A). Al_2O_3 and Fe_2O_3 have been included as they are often used to represent the clay and oxide populations, respectively.

Table 4.3.3.A – Correlation coefficients between select sediment components and Sr, Ba, Ca (an estimate of natural deposition). Estuarine samples are listed in order *increasing distance from river mouth.*

	Al_2O_3	Fe_2O_3	Cu	Zn	As	Cd	Pb
OE2	0.78	0.82	0.73	0.80	0.45	0.65	0.59
OE6	-0.09	-0.15	0.74	0.95	0.91	0.60	0.88
OE4	0.15	0.19	0.30	-0.25	-0.17	-0.53	-0.10
OE3	0.99	0.94	0.95	0.97	0.96	0.68	0.98
BR1	0.91	0.93	0.87	0.96	0.96	0.89	0.95
BR2	0.49	0.15	0.58	0.25	0.53	0.68	0.37
BR3	0.50	-0.58	0.33	0.73	0.31	0.26	0.55
Geo8319	0.07	-0.38	-0.05	0.51	0.66	-0.70	-0.23
Geo8322	0.19	-0.31	-0.06	0.12	0.56	-0.25	0.18

The trace elements, as well as Al_2O_3 and Fe_2O_3, show strong positive correlations with natural deposition at sample sites, OE3 and BR1. The results of OE3 are important for the Olifants River estuary as it marks the head of the estuary and thus the river input.

Sediment core OE3-B is most likely of the cores sampled to accurately represent the deposition rates of the trace elements as the core is thought to be under oxidizing conditions throughout (Section 4.3.5), thus less likely to be subject to the metal migration in the sediment column, as discussed below. However, as pollutants are not likely to associate with large grain sized particles, which comprise over 99% of core OE3-B, it is not an ideal representative sample of the river discharge.

In the sediment core of site OE2 arsenic shows a weak correlation with the natural deposition estimate. However, inspection of the As concentration vs. depth plot (Figure 4.3.3.A) does not show an enhanced As deposition rate toward the surface, which would be expected in the case of anthropogenic impact.

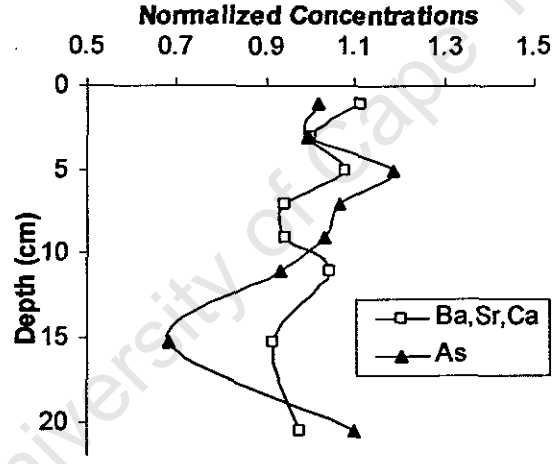

Figure 4.3.3.A. Weighted As concentration vs. an average of Ba, Sr, and Ca (an estimate of natural deposition for sediment core OE2-A

In sediment core OE6 only Al_2O_3 and Fe_2O_3 show significant deviation from the natural deposition rate. However, there is no indication of either an Fe or an Al pollutant in the river systems. With the exception of Cd, which will be discussed in detail below, none of the soil components in Table 4.3.3.A show a deviation from the natural deposition rate that would suggest anthropogenic impact for core OE4-A. The deviations witnessed are possibly the result of association with another soil component, such as organic matter, which may not be deposited at the same rate as the alkali earth metals. For example, Pb appears to be associated with organic matter in core BR3-B (Section 4.3.2). Deviations

from the estimated natural deposition rate may also be a result of grain-size effects. Strontium, Ba, and Ca have a higher frequency of correlating with the coarse silt and sand fractions than the trace elements, which tend to correlate with the clay or fine silt size fractions. The different settling velocities of the different sized particles leads to different deposition rates.

Site BR1 is of particular interest when comparing deposition rates for the Berg River because of the environment of the site. Sample site BR1, adjacent to the river mouth, resembles a salt marsh (Figure 2.1.D) and is less susceptible to the sediment redistribution mechanisms or other dynamics that result in uneven sediment distribution, such as rippling, witnessed in river beds. Thus it can be more safely assumed that the top is the most recently discharged sediment and that the sediment is relatively undisturbed. Site BR1 is in the vicinity of where the mouth of the Berg River was until 1966, which has sanded up since the construction of the new mouth (Van Wyk, 1984), suggesting an accelerated sedimentation rate in the area. Thus it could give a better insight into recent anthropogenic impact. However, the increased sedimentation rate may be a result of the increased erosion witnessed along the southern banks of the river after the construction of the new mouth (FDC, 1974). Whatever the case may be the correlations between the trace elements and the alkali earth metals are higher than any of the other cores analyzed and the grain-size distribution does not introduce the concerns raised for core OE3-B.

In the BR2 core only Pb and As give a suggestion of enrichment in the upper portion of the sediment profile (Figure 4.3.3.B). However, comparison of the measured concentrations with that of the background soils associated with the Malmesbury Group does not suggest pollution (Section 4.3.4). The deviations of the trace element concentrations from natural deposition rates witnessed in core BR3-B also do not appear to be the result of pollution.

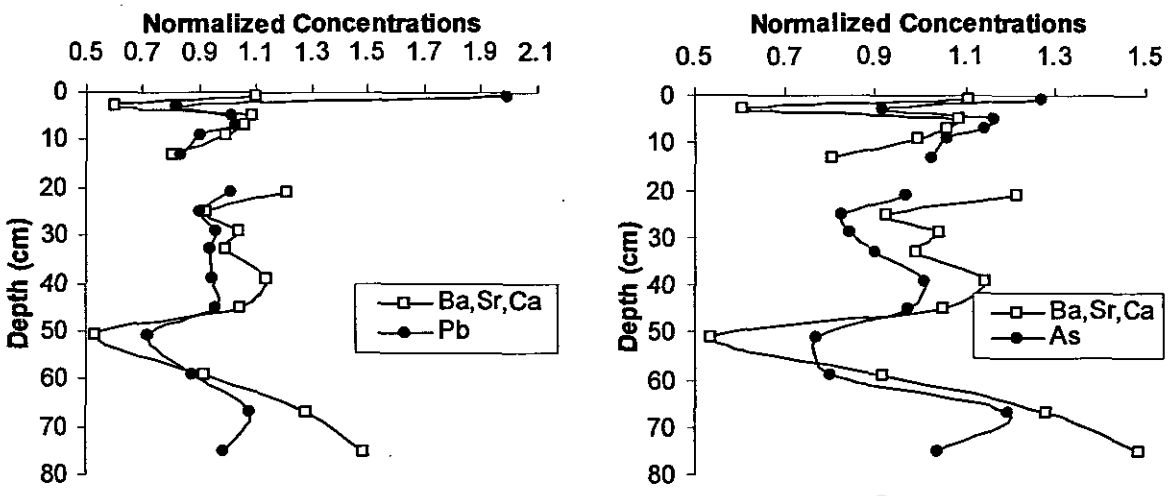

Figure 4.3.3.B - Weighted concentrations of Pb & As vs. an average of Sr, Ca, Ba (an estimate of natural deposition) for sediment core BR2

It is important to acknowledge that this comparison assumes conservative behavior of both the alkaline earth metals as well as the soil component compared to it. However, many soil components, particularly the ones focused on in this study, often exist in several different speciations throughout the sediment column and often change speciation as the sediment environment, such as redox potential, change. For example, studies of sediments in the Loch Fyne inlet, Scotland showed Mn in oxidized form to be released into the pore water under reducing conditions where it either migrated up to re-precipitate or precipitated at depth (Troup & Bricker, 1975). Several studies have recorded elevated concentrations of trace elements in the overlying waters of sediments, which they attributed to the release of those trace elements from the sediment (e.g. Martino et al., 2002). Thus elements may be deposited at natural deposition rates, but due to sediment chemistry may deviate from the plot of Sr, Ba and Ca. The strength of the above method is identifying substantially elevated concentrations in the upper part of the sediment where anthropogenic impact would influence the most.

The deposition of Pb in the Mud Belt cores show spikes in concentrations that appear to be drastic differences from natural deposition as reflected by the values in Table4.3.3.A. The Pb concentrations profiles of the Mud Belt sediments suggest a background concentration of about 2–3 $\mu mol\,kg^{-1}$, with sharp peaks occurring at various depths (Figure 4.3.3.C). Using the ^{14}C dates for the Mud Belt sediments (Section 3.2.6) and

assuming a constant deposition rate, an assumption which is supported by the dates obtained for the 11-14 cm and the 27-29 cm sub-samples of core Geo8319, the dates of the Pb peaks can be determined (Figure 4.3.3.C). The major peaks of both cores occur around 1850 and have the same magnitude, clearly indicating an occurrence of a Pb event. The likely cause of the Pb peaks is a flood event carrying large amounts of Pb rich terrestrial sediment, such as shale, out to sea. This is supported by the fact that the Pb:Al ratios of the Pb peak sub-samples are comparable to those recorded by Schloemann (1994) for Western Cape soils derived from Malmesbury Group parent material. Historical records report that in July of 1822 heavy rains washed away 3 farmers homes on the banks of the Berg River and caused "a great deal of devastation" along the Breede and Olifants rivers (DEA, 1991). In addition, what is referred to as "The Great Storm of 1822" sank several ships in the area around the same time (DEA, 1991). In 1875 the Orange River, to the north of the catchment experienced its greatest flood in history. Another theory that has been put forth is the possible use of artillery in the area by British and Dutch settlers contesting for the Cape (Rosenstein, 2004). Unfortunately, records are scarce for the region during this period and virtually non-existent for the times of the other Pb peaks.

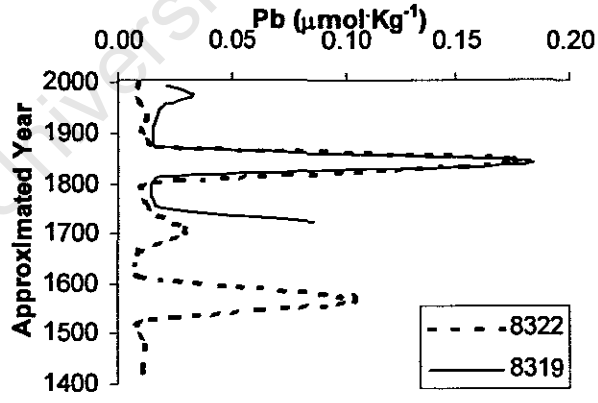

Figure 4.3.3.C. Pb concentration vs. year based on ^{14}C dating of shell fragments found in the sediments.

4.3.4 Evaluating the Pollution Possibility

Several difficulties arose when attempting to compare the estuarine sediments to the background. Firstly, estuarine sediments potentially have several inputs (Section 1.2.3.2). Secondly, few geochemical investigations have been published on the soils of the Olifants and Berg river catchments or for the near-coast sediments off the west coast of South Africa to this author's knowledge. In addition, one must be wary when comparing estuarine sediments directly to the parent rock of the catchments as elements can be either enhanced or depleted during rock weathering (Schloemann, 1994). Thirdly, there exist substantial variability between the studies that have been published (Schloemann, 1994; Danchin, 1970; Bremner, 1977), not only in the results, but also in the parameters investigated and analytical methods used. Finally, the catchments consist of several rock types with varying compositions and contributions that vary seasonally. Weighing the probabilities and likely magnitudes of all the possible inputs, soils associated with the Malmesbury Group were deemed the most applicable. However, others are also presented for comparison.

In attempt to identify a pollution presence the sediments are compared against the background using enrichment factors (EF) as defined in Burton & Stratham (1990), Zhang and Liu (2002) and others:

$$EF = [(M/Al)_{RS}] / [(M/Al)_{FR}]$$

Where $(M/Al)_{RS}$ is the ratio of the element to aluminum in the riverine sediment and $(M/Al)_{FR}$ is that for the fresh rock or soil. An EF greater than 1.5 indicates a pollution source for the element considered. Enrichment factors for the sediment cores were calculated based on four background references (Table 4.3.4.A). For elements with concentrations below detection limits the detection limit of the analytical method was used to calculate the enrichment factors; indicated by parentheses. Comparisons with the quartzitic sandstones of the Table Mountain Group (TMG) were excluded, as they are not easily weathered and are dominantly composed of quartz (SiO_2) (Morant, 1984).

When compared with Schloemann's (1994) data for soils derived from the Malmesbury Group the sediments appear to be enriched in Cd and Zn. However, it should be noted that Schloemann (1994) did not observe Cd concentrations above the detection limits of

Table 4.3.4.A. Calculated enrichment factors (EF) of the sediment cores based on 4 background references. The core averages (Section 3.5) are used to calculate EF. An EF greater then 1.5 suggests a pollution source.

	Soils associated with the Malmesbury Group[a]						Near shore sediments from the west coast of southern Africa[b]				
Core	EF_{Cu}	EF_{Zn}	EF_{As}	EF_{Cd}	EF_{Pb}		EF_{Cu}	EF_{Zn}	EF_{As}	EF_{Cd}	EF_{Pb}
OE2-A	1.5	4.8	0.4	(28.9)	0.9		0.2	0.6	*n.r.*	0.0	0.4
OE3-B	0.9	2.9	0.2	(3.2)	0.6		0.1	0.4	*n.r.*	0.0	0.3
OE4-A	1.6	3.8	0.4	(6.9)	0.6		0.2	0.5	*n.r.*	0.0	0.3
OE6	1.3	3.7	0.5	(11.4)	0.7		0.1	0.4	*n.r.*	0.0	0.3
BR1-A	1.0	3.7	0.5	(72.6)	0.8		0.1	0.4	*n.r.*	0.0	0.4
BR2	1.0	4.2	0.5	(67.8)	0.8		0.1	0.5	*n.r.*	0.0	0.4
BR3-B	1.0	5.0	0.4	(64.8)	1.0		0.1	0.6	*n.r.*	0.0	0.5
Geo8319	2.2	2.5	1.8	(80.8)	0.5		0.2	0.3	*n.r.*	0.0	0.2
Geo8322	2.4	2.9	0.8	(11.9)	0.2		0.2	0.3	*n.r.*	0.0	0.1

Table 4.3.4.A. (cont.)

	Granite Derived soils[a]						Soils derived from Coastal Sands[a]				
Core	EF_{Cu}	EF_{Zn}	EF_{As}	EF_{Cd}[c]	EF_{Pb}		EF_{Cu}	EF_{Zn}	EF_{As}	EF_{Cd}	EF_{Pb}
OE2-A	4.9	7.6	0.1	(0.9)	0.9		0.4	2.7	0.4	(1.6)	(0.5)
OE3-B	2.8	4.6	0.0	(0.1)	0.6		0.2	1.6	0.2	(0.2)	(0.3)
OE4-A	5.3	6.0	0.1	(0.2)	0.6		0.4	2.2	0.3	(0.4)	(0.4)
OE6	4.2	5.8	0.1	(0.4)	0.7		0.3	2.1	0.4	(0.6)	(0.4)
BR1-A	3.2	5.8	0.1	(2.2)	0.8		0.3	2.1	0.4	(4.0)	(0.4)
BR2	3.4	6.6	0.1	(2.1)	0.8		0.3	2.4	0.4	(3.7)	(0.5)
BR3-B	3.3	7.8	0.1	(2.0)	1.0		0.3	2.8	0.3	(3.5)	(0.6)
Geo8319	7.1	4.0	0.2	(2.5)	0.5		0.6	1.4	1.4	(4.4)	(0.3)
Geo8322	7.6	4.5	0.1	(0.4)	0.2		0.6	1.6	0.6	(0.6)	(0.1)

[a] – Schloemann (1994)
[b] – Averaged from values reported in Bremner (1977)
[c] – Cd and Al concentrations taken from Mehlomakulu (1999)
n.r. – not reported

ICP-MS for the soil samples. The Mud Belt sediments also appear to be enriched in copper. The estuarine sediments, as well as those of the mud belt appear enriched in copper and zinc as compared to granite-derived soils. However, this comparison is more

applicable to the Berg River samples as granite is more prevalent in the catchment of the Berg River (Section 1.3.2.2). When compared with soils derived from coastal sands the estuarine sediments appear to be enriched in only Zn. However, for reasons touched on in Section 4.3, the normalization parameters typically employed, such as Al, are less effective at allowing comparisons with sediments of extremely high sand content, such as those of soils derived from coastal sands, 98.7 wt. % (Schloemann, 1994). The soils derived from coastal sands analyzed by Schloemann (1990) only have 0.6 wt. % Al_2O_3, resulting in a large $(M/Al)_{FR}$ value even when the detection limit is used as the Cd concentration.

It is interesting that the combination of Cd and Zn are the two elements the estuarine sediments appear enriched in, especially when compared to the Malmesbury soils, as suggested in Section 4.3.1. In nature the bulk of Cd is found as isomorphous impurities in other minerals, such as zinc sulfides (Vlasov, 1964; Adriano, 2001). Of all the Western Cape soils analyzed, Schloemann (1994) observed the highest Zn concentrations in subsoils associated with the sediments of the Malmesbury Group.

There are several possible explanations, both anthropogenic and natural, for the enriched Cd concentrations observed. The ocean is a potential source, as high Cd concentrations are characteristic of areas of upwelling (Burton & Stratham, 1990). In the North Pacific Ocean Cd concentrations increase by a factor of 40 from the central ocean areas to the California Current upwelling regime (Bruland & Franks, 1983). However, Chester and Stoner (1974) report the Cd concentrations in near-shore surface waters of South Africa to be, although higher than most parts of the world, only on the order of 0.1 ppb. Although Cd is not known to have any biological function it has been shown to have an affinity for biogenous particulate material (Burton & Stratham, 1990). The high levels of primary productivity and large fish populations of the study area (Section 1.3.3.1) likely increase the organic matter input of Cd to the sediments. The results of Bruland (1980) and others indicate that a major transport mechanism of Cd from the euphotic zone is in soft tissues. The sediment Cd concentrations, on a quartz free basis, decreases in the upstream direction from the mouth of the Olifants River, which could signal a marine

input, but is more likely a result of the salinity gradient. In addition, correlations between Cd and OC or P_2O_5, which would indicate bioaccumulation, are not common in the sediment cores. The only sediment cores that show strong correlations between Cd and P_2O_5 are OE3 and BR1, while weak correlations exist for the top portions of BR2 and Geo8319.

Another possible input is the presence of Cd in phosphate fertilizers (Adriano, 2001). In his studies of Western Cape soils Schloemann (1994) observed the highest concentrations of extractable Cd in soils used for crop production associated with the phyllite and sandstone of the Malmesbury Group. Cadmium concentrations in phosphate fertilizers are between 7 and 170 ppm (Kabata-Pendias and Pendias, 1985). Comparing Cd concentrations to that of Sr, Ca and Ba, an estimate of natural deposition (Section 4.3.3), an elevated Cd concentration in the upper segment of the core is apparent, typical of anthropogenic impact. However, Schloemann's comparison of a cultivated versus non-cultivated Malmesbury soils did not show noticeable difference in total Cd concentrations. Although he observed higher levels of extractable Cd in the subsoil of the cultivated area, the values recorded by Schloemann are close to the detection limits of ICP-MS. A study of Cd concentrations in citrus grove soils fertilized for 36 years with a cadmium phosphate fertilizer showed Cd to be less mobile than the P carrier, with 71% of the accumulated Cd residing in the top 15 cm of the soil (Mulla, et al., 1980).

In addition to Cd applied to soils from fertilizers soils may also inherit high Cd concentrations from the parent materials. Some geology types in the catchment are known for elevated Cd levels. Soils developed from shale parent material have the highest Cd concentrations, with a mean of 7.5 ppm, while soils from sandstones and basalts have the lowest amount of Cd, with a mean concentration of 0.84 ppm (Lund et al., 1981). In addition, one cannot discount Cd partitioning within the sediment column, to be the cause of the deviation in Figure 4.3.4.A.

Cadmium enrichment appears to be characteristic of the coastal sediments of southwestern Africa. Bremner (1977) witnessed elevated cadmium concentrations in

non-cultivated sample. However, it is possible that the irrigation water that typically accompanies agriculture leached out the exchangeable Zn of the soil prior to sampling.

Unlike Cd, Zn appears to be deposited at the natural deposition rate (Figure 4.3.4.A). Although of the Western Cape soils studied by Schloemann (1994) the highest concentration of Zn were found in the subsoils associated with the Malmesbury Group, the values reported are low in comparison to other rocks and soils (Adriano, 2001). Bowen (1979) reported an average Zn concentration for world soils of 90 ppm, as compared to the 26 ppm recorded by Schloemann for soils associated with the Malmesbury Group. However, Danchin (1970) observed illite to be the dominant clay mineral in Malmesbury Group sediments and a greater Zn fixing capacity of illite over other clay minerals has been witnessed (Reddy and Perkin, 1974).

Zinc can also be found in high concentrations in the marine environment, especially in high productivity areas such as the western coast of South Africa. Zinc is an essential metal to biota (Rainbow, 1990). Several studies have shown zinc to have an affinity for organic matter (e.g. Akcay et al., 2003, and those mentioned in Adriano, 2001). Zhou et al (2003) witnessed a decrease in dissolved Zn concentrations during periods of photoplankton bloom, indicating the uptake of dissolved Zn by photoplankton. Skeletal material is thought to be a major carrier of Zn in seawater (Burton & Stratham, 1990). Some marine animals have been shown to take up zinc in a way to make it not bio-available and therefore nontoxic. One such example are barnacles, which store zinc in phosphate granules beneath the midgut and are capable of creating body concentrations of up to 150,000 μg/g (Rainbow, 1987). In addition, a low oxygen zone, often an indication of high rates of decay, is characteristic of the near shore waters off the Olifants and Berg river mouths (Shannon, 1990). The decay of metal bearing organic material would increase the metal concentrations even further.

Although the estuarine sediments appear enriched in Cu when compared to the granite-derived soils the other possible contributors have higher Cu concentrations than those observed in granites. For example, shales have average Cu concentrations of 35 ppm

(Adriano, 2001) compared to the 4.3 ppm for granite derived soils found by Schloemann (1994). Although Cu is used extensively in the farming industry as fertilizers, bactericides, and fungicides (Adriano, 2001) the enrichment factors calculated from the Malmesbury Group soils, as well as the comparisons with natural deposition rates (Section 4.3.3) do not suggest an anthropogenic impact. The Cu enrichment in the Mud Belt sediments is more pronounced. This is likely a result of the Cu bearing organic material supplementing the Cu content of the sediment. This is supported by the strong correlation between OC and Cu in the top portion of Geo8319 (Table 4.3.2.J). Copper also shows a 0.63 correlation with P_2O_5 for the same region, an indication of bioaccumulation. Copper does not show a correlation with OC in the upper portion of the Geo8322 core and only a 0.43 correlation in the bottom segment. However, the 8 % organic carbon that comprises the Geo8322 sediment surely carries with it a Cu contribution. Bloom (1981), found Cu to be the most strongly adsorbed to organic material of the divalent cations. Copper is a micronutrient and therefore taken up by marine biota (Rainbow, 1990). During weathering Cu is typically released as Cu^{2+} ions (Kabata-Pendias & Pendias, 1985), but is strongly adsorbed to OM, Fe/Mn oxides and clay minerals (Adriano, 2001) so its mobility may be limited. However, Zhang and Liu (2002) found concentrations of Cu in suspended particulate matter to decrease with increasing chlorinity. The released Cu is available to biota, as well as to dissolved or suspended organic matter which eventually are deposited in the sediment and releasing the Cu during decay..

4.3.5 Insights to Sediment Redox Zones

Although Eh measurements were not taken some chemical indicators and field observations allow speculations to be made regarding the redox zones occurring in the sediments. One such indicator is the Fe:Al ratio (Lyons et al., 2003). As Fe precipitates as iron sulfide (FeS) the ratio increases and a corresponding increase in sulfur is expected. However, if there is insufficient S available the Fe does may not precipitate, in which case the ratio decreases. Another possible indicator is the decrease in concentration of elements that typically associates with Fe/Mn oxides. As Fe/Mn oxides dissociate under reducing conditions they release the elements into solution. If the

released elements do not re-precipitate a decrease in concentration with depth is witnessed. It should be noted that the sediment samples were not washed prior to drying so pore water constituents were incorporated into the sediments upon drying, which may have hindered the ability to see the above-mentioned trend and result in over-estimates of sediment concentrations.

In most instances of this study the above-mentioned trends are not clearly defined and one is reliant on the field observations to hypothesize on redox conditions (Table 4.3.5.A).

Table 4.3.5.A. Some field observations regarding sediment redox potentials.

Sample Site	Observation
OE2	Bioturbation witnessed at the sampling site and a live shrimp was discovered at a depth of 20 centimeters in the "B" core.
OE3	Cores determined to be under oxidizing conditions throughout. No sign of FeS precipitation.
OE5 & OE6	FeS precipitation visible in 12-14cm section and below of OE5 core.
BR2	Apparent FeS precipitation starting at 16-18 cm sub-sample.
BR3	Bioturbation apparent, approximately 1cm in diameter. Anoxic zone thought to start below 20-22cm in core A and 8-10cm in core B.

For the mud belt sediments Fe:Al and S vs. depth plots suggest reducing conditions prevail below approximately 10 cm (Figure 4.3.5.A).

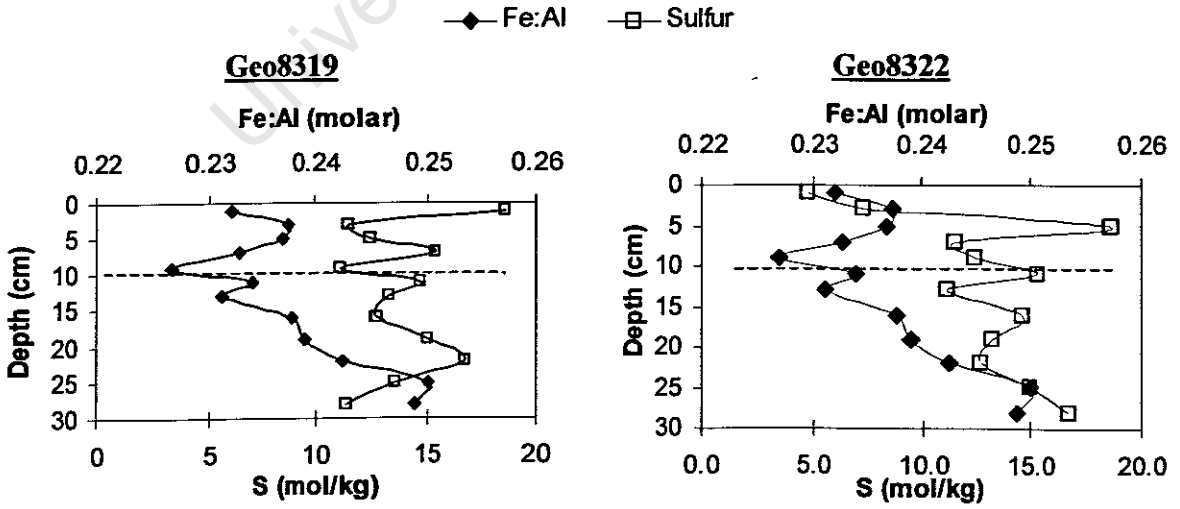

Figure 4.3.5.A – Indications of reducing environments: Fe:Al ratio and S concentration vs. depth for the mud belt cores.

The Fe:Al ratio remains relatively constant until that depth and then begins to increase. At a coinciding depth the S concentration begins to increase. This is more apparent in core Geo8322.

The profile of P_2O_5 supports the hypothesis that reducing conditions occur around 10 cm (Figure 4.3.5.B). Phosphorus is efficiently scavenged by Fe-oxides during precipitation (Standring et al., 2002). When redox potential decreases, Fe-oxides dissociate releasing the P into solution. Based on the decrease witnessed it appears that P is released fromthe Fe-oxides starting at an early depth and either migrates to below 10 cm or toward the surface where it precipitates. It is also possible that the concentration the P_2O_5 steadies at (~0.017 mol·kg^{-1}) represents a less mobile fraction of P not associated with Fe-oxides.

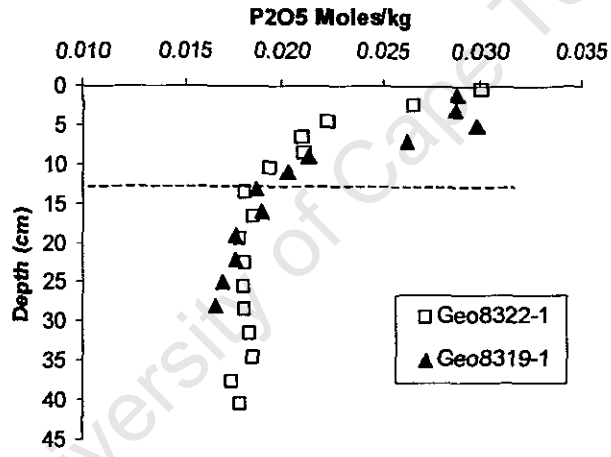

Figure 4.3.5.B. Phosphorus concentration vs. depth for the Mud Belt sediment cores.

In the BR1-A sediment core the Fe:Al ratio decreases to about 15 cm, below which it steadies (Figure 4.3.5.C). The S concentration nearly double between the surface and 15 cm and fluctuates around 9 mol·kg^{-1} below 15 cm. The decrease in Fe:Al may be the result of a redox zone in which Fe-oxides dissociate, but iron sulfides (FeS) do not yet precipitate. The dissociation of Fe-oxides is supported by the decrease in P_2O_5 with depth and the increase in S suggests the precipitation of sulfides. However, the expected increase in Fe:Al resulting from the precipitation of FeS is not witnessed.

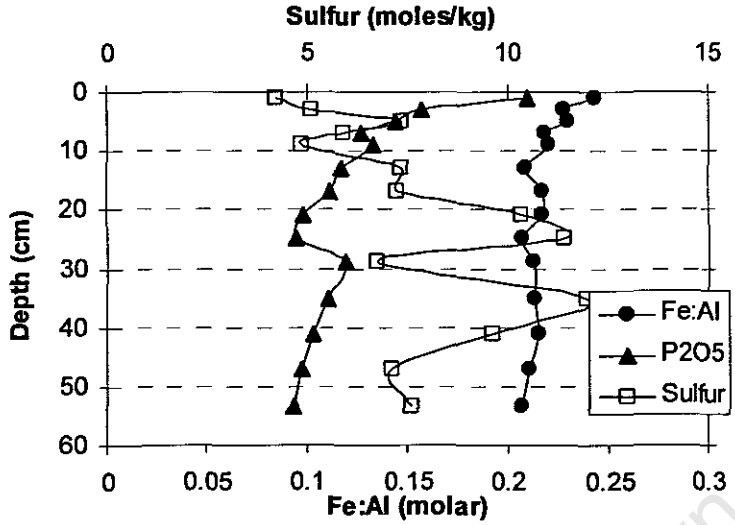

Figure 4.3.5.C. – Indications of reducing environments occurring in sediment core BR1-A. Fe:Al, S and P_2O_5 vs. Depth. For display purposes the P_2O_5 concentration (mol/kg) is multiplied by 10.

4.3.6 Estimating Active Fraction of Metals

Attempts were made to estimate the labile fraction of the selected trace elements. The method used was adopted from Zhang et al. (2002) in which the Al concentration is used to represent alumino-silicates and the amount of trace element associated with alumino-silicates is equal to a[Al], with a being a constant. Thus, the total concentration of the trace element ([M]) can be represented as:

$$[M] = a[Al] + b$$

where b represents the labile fraction, such as associating with Fe/Mn oxides, organic matter, carbonates, etc. and is thus more reactive in the estuarine environment. By plotting [M] vs. [Al] one can extrapolate the plot to [Al] = 0 and determine the labile fraction (b). To estimate the labile fraction the plot of [M] vs. [Al] must have a significant linear regression R^2 value. Zhang (2002) attributes the instances where no linear correlation is displayed to the presence of a significant labile input.

This method was designed for oxidizing conditions where the alumino-silicate associated trace elements are less likely to dissociate. For this reason the [M] vs. [Al] comparison was only applied to the top 10 cm of each core. The redox boundaries are difficult to

determine based on the information gathered. Ten cm was deemed a reasonable average depth to which oxidizing conditions still prevail (Section 4.3.5). The correlations between Cu, Zn, As, Cd, Pb and Al along with the labile fractions, as a percent of the mean concentration, are presented in Table 4.3.6.A. Negative *b* values are displayed as (0) percent labile. A minimum correlation requirement of 0.6 was defined. Correlations and the corresponding % labile estimates below this standard were omitted.

Table 4.3.6.A. Trace element correlations with Al_2O_3 for the top 10 cm of the sediment cores and estimates of the labile fraction

	Pearson correlation coefficient with Al_2O_3						% Labile based on [M] vs. [Al] plot				
	Cu	**Zn**	**As**	**Cd**	**Pb**		**Cu**	**Zn**	**As**	**Cd**	**Pb**
OLIFANTS	0.94	0.95	0.89		0.95		(0)	(0)	(0)		14.2
BERG	0.98	0.92	0.97	0.83	0.78		(0)	16.3	(0)	(0)	(0)
MUDBELT		0.86						(0)			
OE2	0.98	0.99		0.83	1.00		(0)	6.2		(0)	9.6
OE6											
OE4											
OE3	0.94	0.99	0.92	0.71	0.97		(0)	17.7	1.8	(0)	35.9
BR1	0.97	0.98	1.00	0.98	1.00		(0)	11.6	(0)	(0)	31.1
BR2	0.66	0.69	0.73		0.96		43.5	38.6	18.7		(0)
BR3	0.64						(0)				
Geo8319		0.81	0.83					(0)	(0)		
Geo8322											

Correlations between the trace elements and Al_2O_3 tend to be strong for the estuarine locations. However, inspection of the sediment cores on an individual basis shows a less clearly defined relationship; a testimony to the complexity of an estuarine environment. For the Olifants estuary the model suggests trace elements enter the estuary (OE3-B) predominantly associated with alumino-silicates, except for Pb with is 35.9% labile. Wedpohl (1974) states that lead occurs mainly in the structure of K-feldspar and mica in igneous rocks and that the loss during weathering can be as high as 40%. If a lack of correlation can be interpreted as the involvement of different particle populations (Zhang, 2002) then the middle reaches of the estuary (OE4-A & OE6) suggests a greater influence of more labile species. It is impossible to state with any certainty if the added labile fraction of the metals come from the same population as what is assumed to be associated with alumino-silicates at site OE3. A decrease in metal concentrations toward the mouth

(Table 4.3.4.B) combined with the % labile estimations at site OE2 suggest either a preferential deposition of the labile fractions in the middle reaches of the estuary or an increasing amount of the labile trace element population is brought into solution in the seaward direction and are carried out to sea.

The concentration gradient of Cd is opposite that of the other trace elements presented, showing a maximum concentration at the mouth and decreasing in the upstream direction. This may be the result of Cd having a significant marine input (as discussed in section 4.3.4) or possibly the effect of increased salinity. Cadmium forms soluble, stable chloro-complexes (Adriano, 2001). However, as discussed (Section 4.2), sea-like salinities are witnessed several kilometers upstream. Cadmium is known to go into solution as Cd^{2+} during rock weathering (Wakita & Schmitt, 1970) and has been shown to form stable complexes with chlorides, organic matter and carbonates (Adriano, 2003; Burton & Statham, 1990; Gerringa et al., 2001). Thus skepticism exists as to whether Cd can be assumed to be dominantly associated with alumino-silicates, as the model suggests. Several studies have documented the release of fluvial Cd upon entering estuarine waters (e.g. Paucot & Wollast, 1997; Bourg, 1983). The low concentrations witnessed in core OE3-B are likely due to a grain-size effect, suggesting that the SiO_2 correction is not capable of fully correcting for a 99% sand sample (Section 43). Arsenic data indicate As to be entirely in the labile fraction by the time it reaches the site OE2 suggesting the bulk of As associated with alumino-silicates, if any, entering the estuary is released or is deposited prior to reaching the mouth. The correlation witnessed between [Al] and [As] is likely a coincidence of a shared association rather than a direct one, as discussed below. Arsenic being released into solution upon estuarine mixing is possibly the result of Cl^- competing for exchange sites and is reflected in the aqueous arsenic concentrations observed (Section 4.2).

In the Berg River samples strong correlations exist between Al and the trace elements at the most seaward site (BR1-A) and weaker correlations are observed in the landward direction. As sample site BR3 is 11 kilometers from the river mouth and seawater is

Table 4.3.6.B. Avg. Concentrations of Select Trace Elements in Estuarine Sediments (Concentrations in $\mu mol \cdot kg^{-1}$ unless specified; on an SiO_2 Free basis)

	Cu	Zn	As	Cd (nmol/kg)	Pb
OE2-A	0.745	3.159	0.155	7.180	0.161
OE6	1.258	4.742	0.310	5.557	0.238
OE4-A	1.709	5.309	0.299	3.644	0.238
OE3-B	0.852	3.756	0.166	1.565	0.209
BR1-A	0.948	4.621	0.341	34.561	0.251
BR2	0.780	4.121	0.268	25.466	0.218
BR3-B	0.924	5.944	0.282	29.457	0.320

known to penetrate 50 kilometers upstream (Section 1.3.2) it can be safely assumed that considerable processes associated with estuarine mixing occur prior to the riverine constituents reaching the BR3 sampling location. Thus it is difficult to hypothesize the labile fraction entering the estuary. All that can be discussed is what is witnessed from site BR3 and downstream. Only copper shows a correlation with aluminum in the BR3 sediment core and appears to be primarily associated with alumino-silicates. In studies of sediments of the Amazon and Yukon rivers copper was found to be predominantly held in lattice positions (Gibbs, 1973). In addition, with the possible exception of Pb, Cu is the most strongly adsorbed of the transition metals on Fe and Al oxides (Adriano, 2003). The bonding strength of Cu makes the suggested 43.5% labile fraction for sediment core BR2 difficult to explain. However, Cu is also very strongly bound to organic materials, in fact Reimer and Toth (1970) ranked the sorption of copper on sedimentary materials in the following order: humic acid > montmorillonite > illite > kaolinite. Dissolved organics have been shown to flocculate with clays and hydrous ferric oxides during estuarine mixing; one study attributing 25% of the humic materials present in the sediment to this process (Swanson et al, 1972). This may also explain the labile fractions suggested for As, Zn and Pb as they are also known to associate with humic materials. In addition, the flocculation of trace element bearing organic matter with clays in the estuary zone between site BR3 and the mouth would explain the correlations between Al_2O_3 not witnessed in BR3-B. Considering the elevated levels of organic material in the coastal waters of the study area, this process may also explain the higher concentrations witnessed in cores BR1-A and BR2 compared to that of BR3-B.

A correlation with Al_2O_3 exists for Zn and As for Mud Belt core Geo8319, with corresponding zero labile fractions. However, the *b* values of the linear regression lines would indicate a labile fraction of –182 and –157% for Zn and As, respectively. This impossibility combined with the proposed Zn and As associations discussed in Section 4.3.2, lead to the interpretation that the values reported in Table 4.3.6.A are a result of a shared correlation between Fe/Mn oxides and Zn, As and Al_2O_3.

It is important to recognize several drawbacks of this application. Firstly, it assumes that a correlation between Al and the trace element is a result of association between not only the two, but also Al as part of alumino-silicates. In fact it is quite likely that they share a correlation with a controlling factor. Using Fe/Mn oxides as an example, Fe and Mn oxides regularly form coating on clay particles (Fergusson, 1990; Velde, 1992; Aston and Chester, 1973). So even if the trace element is associated entirely with Fe/Mn oxides in this model the association will be attributed to alumni-silicates resulting in an under-estimation of the labile fraction. Secondly, it assumes that [Al] accurately represents the clay particles. Thirdly, one must be wary in applying it to estuarine sediments where anoxic conditions, capable of mobilizing trace elements associated with silicates, often prevail even at depths shallower than 10 cm.

4.3.7 Indications of Estuarine Dynamics

The large proportion of sand size particles in cores OE2-A, OE3-B and BR3-B (Figure 3.2.A) indicate a dynamic environment with mean vertical mixing velocities typically greater than the settling velocities of a fine silt or clay sized particles (Section 1.2.3.2). The mouth of an estuary is typically high energy as a result of the wave action. Although the sample location OE2 was in an off channel protected from direct impact of waves its close proximity to the mouth makes it the most susceptible to changing water directions with the waxing and waning of the tides. The changing water movement associated with the tides causes re-suspension of sediments, especially the lighter fine-grained particles, leaving the larger particles behind (Schubel, 1971). In addition, there could be an input from seawater carrying coastal sands. This is consistent with Heydorn & Tinley (1980) who concluded from aerial photographs that the coast around the Olifants River mouth

was eroding. An atmospheric input of wind blown sand also exists, especially during the summer months when the wind direction is predominantly from the north-east. The high Ca:Mg ratios (4.2 to 5.7) witnessed for sediment core OE2-A supports the possibility of a marine input. The Ca:Mg ratio for soils derived from coastal sands reported by Schloemann (1994) is 3.3 and that for near shore sediments near Walvis Bay, Namibia, reported by Bremner (1977) is 16.1. Danchin (1970) and Schloemann (1994) reported Ca:Mg ratios for soils derived from rocks of the Malmesbury group of 0.34 and 0.26, respectively. However, it is more probable that the observed Ca:Mg ratios are a result of abundant Ca^{2+} ions in seawater substituting for Mg^{2+} in bonding sites.

Of particular interest regarding estuarine dynamics is the frequency with which Fe_2O_3, MgO, MnO and Al_2O_3 correlate more strongly with the fine and coarse silt sized fractions as opposed to the clay fraction (Tables 4.3.2.A-M). This is best explained by being a result of aggregation leading to higher concentrations of Fe/Mn oxides and organic material coatings in the silt size particles than in the clays (Luoma, 1990). Aggregation is characteristic of estuarine environments where high ionic strength seawater decreases the double layer of clay particles, reducing their repulsive forces. The probability of flocculation is increased by the concentration of suspended particles in estuarine environments (Section 1.2.3.1). The regularity of correlation between the oxides and the silt size particles suggests a good deal of mixing which is likely the result of the circulation pattern discussed in Section 1.2.3.1. In such a flow pattern the vertical mixing velocity of the tidal prism is lowest where the underlying seawater penetration nears zero. In this zone smaller particles are able to settle out. The small grain-size (>60 % fine silt and clay) of core OE4-A suggests Ebenhaeser is in the vicinity where the sub-surface seawater penetration ceases. This would agree with Morant (1984) who suggested the tidal prism likely extends to Ebenhaeser.

4.3.8 Estuary as a Filter

Comparing the chemical compositions of the estuarine sediments to those of the offshore sediments reveals how well the estuaries trap the trace elements. The analysis of this section assumes the Olifants and the Berg Rivers are the dominant inputs to the sediments

of sample sites Geo98319 and Geo9322. The validity of this assumption has been discussed in previous sections.

Plotting the weight % of fine material (fine silt & clay) versus the metal concentrations shows the Mud Belt cores to be deficient in Zn and Pb (Figure 4.3.8.A-B). A similar relationship is witnessed when Zn and Pb are plotted against Al_2O_3. The estuarine sediments show a clear relationship between Zn, Pb and the weight % of fine material. Based on this relationship the Mud Belt cores are expected to contain more Zn and Pb for the amount of fine material in the sediments. This would suggest that either the Zn and Pb are preferentially retained in the respective estuaries, or that the trace elements have been released into solution. Considering the much higher organic matter content in the Mud Belt sediments and that Pb and Zn both have a high affinities for organic matter (Bloom, 1981) one expects higher Zn and Pb concentrations in the offshore sediments. The absence of higher Zn and Pb concentrations in light of this is a testament to the estuaries ability to retain Zn and Pb. However, just as biota can take up metals and deposit them in sediments as part of decaying matter, they are also capable of releasing particulate associated metals into solution (Rainbow, 1990). In the Mud Belt cores Zn and Pb only appear to be correlated with organic matter in the top 12 cm of core Geo8319 (Tables 4.3.2.J-K). In addition, in both Mud Belt cores OC has a strong correlation with

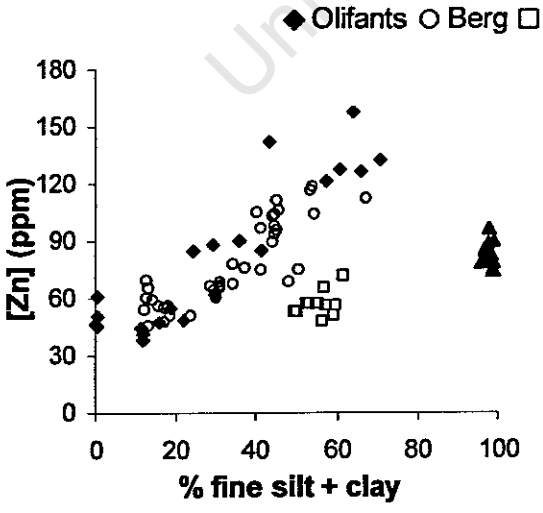

Figure 4.3.8.A – Zn vs. % Fine Material

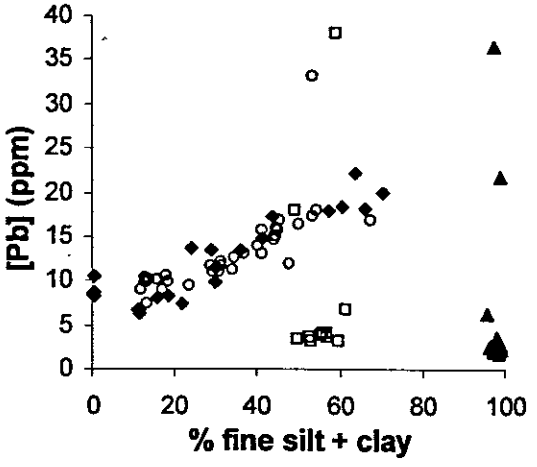

Figure 4.3.8.B – Pb vs. % Fine Material

either the clay or fine silt fraction (Tables 4.3.2.J-M). This suggests that in the offshore environment in the vicinity of the Berg River mouth Pb and Zn are being taken up and deposited by organic matter and yet the concentrations per fine material remains lower than in the estuarine sediments.

As related to fine particles Cu levels in the Mud Belt sediments are comparable to those in the estuarine sediments (Figure 4.3.8.C). However, when Cu is plotted against Al_2O_3 the Mud Belt cores appear to be enriched in Cu (Figure 4.3.8.D.). As Cu does not show a correlation with Al_2O_3 in the mud belt sediments (Tables 4.3.1.J-M) this enrichment is likely the result of Cu associating with a sediment component other than clay minerals. Fe_2O_3 shows strong correlations with Al_2O_3 in the upper portion of the Geo8319 sediment and a weak correlation in the upper portion of Geo8322 (MnO has a 0.69

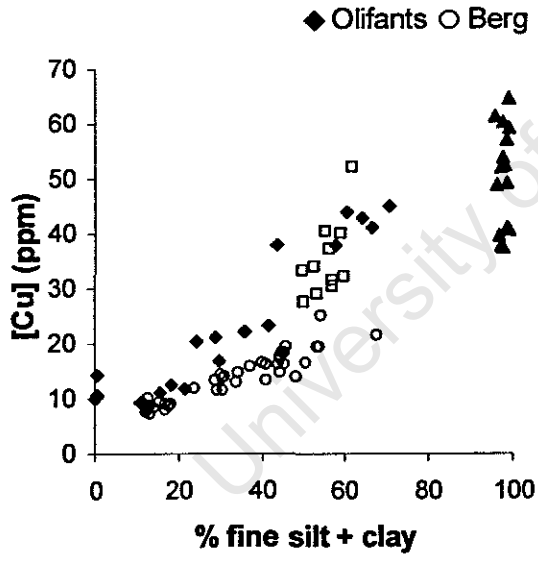

Figure 4.3.8.C – Cu vs. % Fine Material

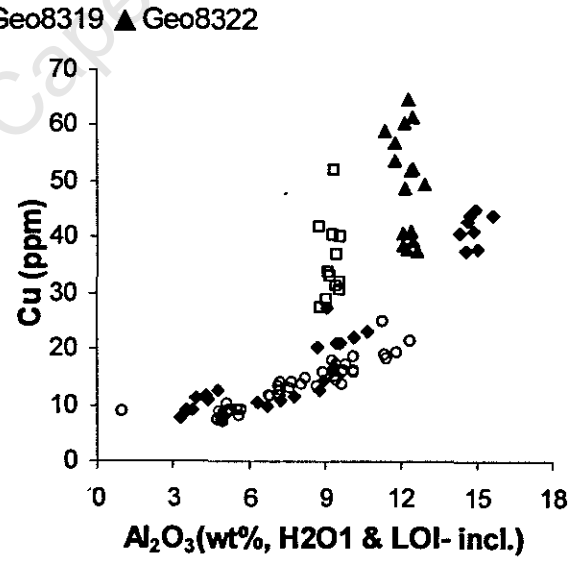

Figure 4.3.8.D – Cu vs. Al_2O_3

correlation with Al_2O_3). Thus it is not likely that Cu is associating with Fe/Mn oxides. Copper-organic matter association is the likely candidate as copper is the most strongly adsorbed to humic acid of the divalent cations (Bloom, 1981). Copper shows a strong correlation with organic carbon in the top 12 cm of Geo8319 and a 0.43 correlation in the bottom portion of Geo8322 (Tables 4.3.2.J-M). Although these values are by no means

conclusive, they are the strongest correlations Cu exhibits with the major soil components in the Mud Belt cores.

Plotting Cd vs. % fine material separates the Olifants River estuary and the northern Mud Belt (Geo8322) sediments from the southerly mud belt site (Geo8319) and the Berg River estuary sediments (Figure 4.3.8.E). Geo8322 and the Olifants River estuary sediments have similar Cd:% fine material ratios, whereas the Berg River estuary and Geo8319 have a similar Cd:% fine material ratio. The Cd:% fine material ratio of the Berg River and 8319 sediment being greater than their northern counterparts. This is also apparent in the higher Cd concentrations witnessed in the Geo8319 and the Berg River estuary sediments. Comparing Cd with Al_2O_3 shows similar trends. These results suggest there is more Cd entering the Berg River system and being deposited in the estuarine sediments, as well as the mud belt in proximity to the river mouth.

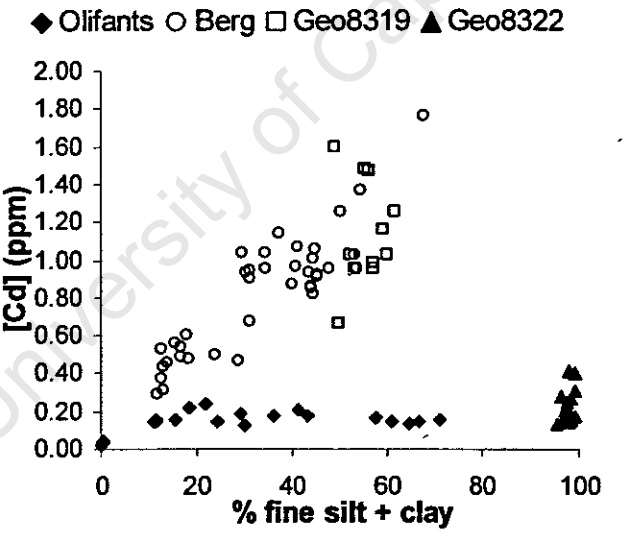

Figure 4.3.8.E – Cd vs. % Fine Material

Arsenic appears to be enriched in the Mud Belt sediment, Geo8319, but not in the northerly one (Figure 4.3.8.F). The plot of As vs. Al_2O_3 resembles that of As vs., % fine material. The elevated concentrations in the Mud Belt sediments suggest that the estuaries are not effective at trapping As. This is supported by the trend witnessed of increasing aqueous As concentrations in the direction of the river mouths.

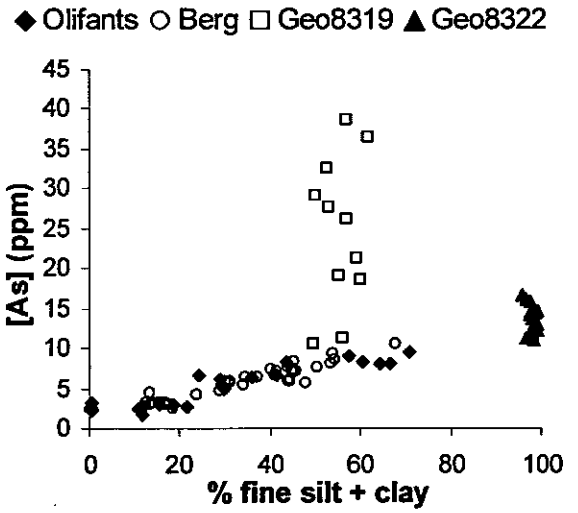

Figure 4.3.8.F – As vs. % Fine Material

5 Conclusions

With the exception of the predominantly fine silt mud belt core, Geo8322, trace elements show strong positive correlations with fine-sized particles. Percent organic matter also shows a positive correlation with fine-grained sediments, with the mud belt cores accumulating more OM per fine-particle than the estuarine sediments as a result of the high levels of primary productivity in upwelling regime. The trace elements appear to associate predominantly with clay minerals (alumino-silicates), Fe/Mn oxides, and organic matter. These soil components often showed positive correlations with each other making it difficult to differentiate speciation. Trace element correlations with S and carbonate carbon were also witnessed. Cadmium and As are the trace elements that most frequently displayed correlations with S or carbonate C. C:H:N analysis indicate only the sediment cores from sites OE2, BR1 and to a lesser extent, BR2 and BR3 have a significant carbonate fraction. Analysis of the correlation coefficients between trace and major elements, suggest that the trace elements change speciation within the sediment column. However, comparison of trace element concentrations with that of Al in the perceived oxic portion of the sediments does not often suggest a significant labile fraction.

Comparison with estimates of natural deposition rates and compositions of soils occurring in the catchments did not suggest an anthropogenic pollution input. From the data available the estuarine and Mud Belt sediments are enriched in Cd, Cu and Zn in comparison to the background soils. The estuaries appear to effectively trap Zn and Pb, with sediments displaying higher Zn and Pb concentrations per fine-grained particle than those witnessed in the Mud Belt sediments. The Cu levels per fine-grained particle in the estuarine and offshore sediments are comparable to each other. However, the Cu concentration associated with clay minerals and/or Fe/Mn oxide coatings appear to be supplemented by another speciation in the Mud Belt sediments, most likely as organo-complexes. The Olifants River estuary and Mud Belt core (Geo8322) taken closest to its mouth have similar Cu per fine-sized particle concentration, which are lower than those of Berg River estuary sediments and the Geo8319 Mud Belt sediment taken closest to the

Berg River mouth. The Geo8319 sediment is enriched in As compared to the other sediments studied.

This investigation has shed some light on the trace element accumulation, distribution and speciation in the near-shore environment of the Berg and Olifants rivers, but much is yet to be known, particularly with regard to background concentrations. A more comprehensive investigation of the geochemistry of the soils and parent materials in the catchments are necessary to better determine if the input of metals to the river estuaries and the offshore mud belt are predominantly natural or anthropogenic. In addition, analytical methods of determining speciation, such as sequential extraction, should be performed to better evaluate the potential mobility of the trace elements. The Olifants and Berg rivers are important sources of water for the farming community, as well as for municipal use in the Western Cape. Based on this investigation of the estuarine waters and sediments the rivers appear to be in good health in regards to trace element concentrations.

6 Bibliography

Ackay, H., Oguz., A., Karapire, C., 2003. Study of Heavy Metal Pollution and Speciation in Buyak Menderes and Gediz River Sediments. *Water Research*, Vol. 37, pp.813-822.

Adriano, D.C., 2001. Trace Elements in Terrestrial Environments. Springer-Verlag.

Aston, S.R., and Chester, R., 1973. The Influence of Suspended Particles on the Precipitation of Iron in Natural Waters. *Estuarine Coastal Marine Science*, Vol. 1, pp.225-231.

Basson, M.S., Theron, T.P., Little, P.R., Luger, M., 1998. Olifants/Doring River Basin Study, Main Report. Report # PE000/00/0198, Department of Water Affairs and Forestry, South Africa.

Bath, A.J., 1993. Western Cape Systems Analysis: Water Quality, Vol. 2 Data for Berg River Basin. Report # PG000/00/2891. Department of Water Affairs and Forestry, South Afirca

Baut-Mènard, P.E., 1984. Fluxes of Metals Through the Atmosphere and Oceans. In: Nriagau, J.O., Ed. Changing Metal Cycles and Human Health. Dahlem Konferenzen: Springer-Verlag; pp.43-69.

Bloom, P.R., 1981. Metal-Organic Interactions in Soils. In: Chemistry in the Soil Environment. Dowdy, R.H., Ryan, J.A., Volk, V.V. and Baker, D.E., eds. ASA Special Publication 40. American Society of Agronomy, USA.

Bourg, A.C.M., 1983. Role of Fresh Water/Sea Water Mixing on Trace Metal Adsoption Phenomena. In: Trace Metals in Seawater. Wong, C.S., Burton, J.D., Boyle, E.A., Bruland, K.W., Goldberg, E.D., Eds. Plenum, New York, pp. 195-208.

Bowen, H.J.M., 1979. Environmental Chemistry of the Elements. Academic Press, New York.

Bradford, W.L., 1972. A study on the Chemical Behavior of Zinc in Chesapeake Bay Water using Anodic Stripping Voltametry. Chesapeake Bay Institute, John Hopkins University, Technical Report 76. Reference 72-7. Baltimore, USA.

Brady, N.C. & Weil, R.R., 1999. *The Nature and Properties of Soils*, 12th ed. Prentic Hall Publishers, USA.

Bremner, J.M., 1977. Sediments on the Continental Margin Off South West Africa Between Latitudes 17° and 25°S. Doctor of Philosophy Thesis, University of Cape Town, South Africa.

Bruland, K.W. and Franks, R.P., 1983. Mn, Ni, Cu, Zn and Cd in the western North Atlantic. In: Trace Metals in Sea Water, Wong, C.S, Boyle, E., Bruland, K.W., Burton, J.D., and Goldberg, E.D., Eds. Plenum Press, New York, p.395.

Bruland, K.W., 1980. Oceanographic Distribution of Cadmium, Zinc, Nickel and Copper in the North Pacific. *Earth Planet. Sci. Lett.*, Vol. 47, 176.

Bulpin, 1980. Discovering Southern Africa. 2nd Edition. Bulpin Publications, Cape Town, South Africa.

Burton, J.D., 1976. Basic Properties and Processes in Estuarine Chemistry. In: Estuarine Chemistry. Burton, J.D., Liss, P.S., Eds. Academic Press, London.

Burton, J.D., Statham, P.J, 1990. Trace Metals in Seawater. In: Heavy Metals in the Marine Environment. Furness, R.W., Rainbow, P.S., Eds. CRC Press Inc., United States. pp.5-26.

Chester, R. and Murphy, K.J.T., 1990. Metals in the Marine Atmosphere. In: Heavy Metals in the Marine Environment. Furness, R.W., Rainbow, P.S., Eds. CRC Press Inc., United States. pp.27-49.

Chester, R. and Stoner, J.H., 1974. The Distribution of Zinc, Nickel, Manganese, Cadmium Copper and Iron in some surface waters from the world ocean. *Marine Chemistry,* Vol. 2, pp.17-32.

Connell, W.E. and Patrick, W.H. Jr, 1968. Sulfate Reduction in Soil: Effects of Redox Potential and pH. *Science, Vol. 159, pp.86-87.*

Coward, B.D., 1981. A review of the Geology of the Cape West-Coast. Stellenbosch, CSIR Report T/SEA 8115. 70pp.

Danchin, R.V., 1970. Aspects of The Geochemistry of Some Selected South African Fine Grained Sediments. Doctor of Philosophy Thesis, University of Cape Town, South Africa.

Davies, B.E., 1980. In: Applied Soil Trace Elements, Davies, B.E., Ed. Wiley & Sons.

De Groot, A.J., Salomons, W., Allersma, E., 1976. Processes Affecting Heavy Metals in Estuarine Sediments. In: Estuarine Chemistry, Burton, J.D. and Liss, P.S., Eds. Academic Press, London.

Department of Environmental Affairs (DEA), 1991. Caelum – A History of Notable Weather Events in South Africa 1500-1990. Weather Burea, Department of Environmental Affairs.

Department of Mineral and Energy Affairs, 1984. Geological Map of the Republic of South Africa, Transkei, Bophuthatswana, Venda and Ciskei and of the Kingdoms of Lesotho and Swaziland. The Government Printers, Cape Town.

Department of Water Affairs, 1964. Monthly Flow Records of Gauging Stations Up to September 1960. *Hydrographic Survey Publication* No. 8. Vol. I. 464 pp., South Africa

Dyer, K.R., 1979. Estuaries and Estuarine Sedimentation. In: Estuarine Hydrography and Sedimentation, Dyer, K.R., Ed., Cambridge University Press, pp. 1-18.

Eagle, G.A. and Barlett, P.D., 1984. Preliminary Chemical Study of Four Cape Estuaries. CSIR Report T/SEA 8307. 23pp. Stellenbosch, South Africa.

Fergusson, J.E., 1990. The Heavy Elements: Chemistry, Environmental Impact and Health Effect Pergamon Press, Oxford OX3 OBW, England.

Fisheries Development Corporation of SA Ltd. (FDC), 1974. Berg River Erosion. Report No. F22-2. South Africa.

Förstner, U. 1982. Chemical Forms of Metal Enrichment in Recent Sediments. In: Amstutz, G., et al., eds., Ore Genesis, New York, Springer-Verlag, p.191-199.

Fourie, J.M., Steer, A.G. 1971. Water Quality Survey of the Berg River for the Period 1963 to 1970. National Insitute for Water Research, South Africa.

Fergusson, J.E., 1990. The Heavy elements: Chemistry, Environmental Impact and Health Effects. Pergamon Press, UK.

Gerringa, L.J.A., de Baar, H.J.W., Notling, R.F., Paucot, H., 2001. The Influence of Salinity on the Solubility of Zn and Cd sulphides in the Scheldt Estuary. *Journal of Sea Research*, Vol. 46, pp.201-211.

Gibbs, R.J., 1973. Mechanisms of Trace Metal Transport in Rivers. *Science*, Vol. 180, pp. 71-73.

Hall, G.C. and Gorgens, A.H.M., 1978. Studies of Mineralization in South African Rivers. South African National Scientific Programmes Report No. 26. March 1978. CSIR

Haniff, N., 2002. Trace Metal Accumulation in Urban Sediments, Black River, Western Cape, South Africa. MSc. Thesis, University of Cape Town, South Africa.

Heydorn, A.E.F., Tinley, K.L., 1980. Part I Synopsis of the Cape Coast. Natural Features, Dynamics & Utilization. CSIR, South Africa.

Jenkins, D.A. & Wyn Jones, R.G., 1980. Trace Elements in Rocks, Soils, Plants, and Animals. In: Applied Soil Trace Elements, Davies, B.E., Ed. Wiley & Sons.

Kabata-Pendias, A. and Pendias, H., 1985. Trace Elements in Soils and Plants. CRC Press, Florida, USA.

Langhout, C., 1998. Olifants/Doring River Basin Study, Physical characteristics and Land use. Report # PE000/00/0298. Department of Water Affairs and Forestry, South Africa. (need full ref)

Lambrechts, J.J.N., Schloms, B.H.A., 1998. Olifants/Doring River Basin Study, Soil and Irrigation Potential Investigation. Report # PE000/00/0498. Department of Water Affairs and Forestry, South Africa.

Lerman, A., 1979. Geochemical Processes. Water and Sediment Environments. Wiley Publishers, New York.

Luoma, S.N., 1990. Processes Affecting Metal Concentrations in Estuarine and Coastal Marine Sediments. In: Heavy Metals in the Marine Environment. Furness, R.W., and Rainbow, P.S., Eds. CRC Press, pp. 51-66.

Lund, L.J., Betty, E.E., Page, A.L., and Elliot, R.A., 1981. Occurance of Naturally High Cd Levels in Soils & Its Accumulation by Vegetation. *Journal of Environmental Quality*, Vol. 10(4), pp. 551-6.

Lyons, T.W., Werne, J.P., Hollander, D.J., Murray, R.W., 2003. Contrasting Sulfur Geochemistry and Fe/Al and Mo/Al ratios across the last oxic-to-anoxic Transition in the Cariaco Basin, Venezuela. *Chemical Geology*, Vol. 195, Issue 1-4, pp.131-157.

Martino, M., Turner, A., Nimmo, M., Millward, G.E., 2002. Resuspension, Reactivity and Recyling of trace Metals in the Mersey Estuary, UK. *Marine Chemistry*, Vol. 77, pp.171-186.

McBride, Murray B. (1994). *Environmental Chemistry of Soils.* Oxford University Press, New York.

Mulla, D.J., Page, A.L., and Ganje, T.J., 1980. Cd Accumulation & Bioavailability in Soils From Long-Term Phosphorous Fertilization. *Journal of Environmental Quality*, Vol. 9, pp. 408-412.

Morales-Alamo, R., Haven, D.S., 1966. Aspects of Biodeposition by Oysters and Other Invertebrate Filter Feedsers, *Limnology and Oceanography*, 11(1966) 487-498.

Morant, P.D., 1984. Estuaries of the Cape. Part II: Synopses of Available Information on Individual Systems. Report No. 26 Olifants (CW 10). CSIR Research Report 425. Stellenbosch, SA. July 1984.

Nahon D.B., 1991. Introduction to the Petrology of Soils and Chemical Weathering. John Wiley & Sons, Inc., New York.

Paucot, H. & Wollast, R., 1997. Transport and Transformation of Trace Metals in the Scheldt Estuary. *Marine Chemistry*, Vol. 58(1-2), pp. 229-244.

Pritchard, D.W. and Carter, H.H., 1971. Estuarine Circulation Patterns. In: The Estuarine Environment: Estuaries and Estuarine Sedimentation. American Geological Institute, Washington D.C., USA. pp. IV – 1 to 17.

Rainbow, P.S., 1987. Heavy Metals in Barnacles. In: Barnacle Biology, Southward, A.J., Ed. A.A. Balkema, Rotterdam, p.405.

Reddy, M.R., and Perkin, H.F., 1974. *Soil Science Society Am Proc.*, Vol. 38, pp.229-231.

Reimer, D.N. & Toth, S.J., 1970. Adsoption of copper by clay Minerals, Humic Acid and Bottom Muds. *Journal of American Water Works Association*, Vol. 62, pp. pp.195-197.

Rosenstein, D., 2004. Personal communication.

Salomons, W. and Förstner, U. 1984. *Metals in the Hydrosphere*. Springer-Verlag, Berlin.

Sarazin, G., Michard, G., Prevot, F. 1999. A Rapid and Accurate Spectroscopic Method For Alkalinity Measurements in Sea Water Samples. *Water Research*, 33, 290-294.

Schloemann, H., 1994. The Geochemistry of some Common Western Cape Soils. Doctor of Philosophy Thesis, University of Cape Town, South Africa.

Schubel, J.R., 1971. Sources of Sediments to Estuaries. In: The Estuarine Environment: Estuaries and Estuarine Sedimentation. American Geological Institute, Washington D.C., USA. pp. V – 1 to 19.

Schubel, J.R. and Carter, H.H., 1984. The Estuary as a Filter for Fine-Grained Suspended Sediment. In: The Estuary as a Filter. Kennedy, Victor S., Ed. Academic Press, pp. 81-106.

Schubel, J.R. and Kennedy, V.S., 1984. The Estuary as a Filter: An Introduction. In: Estuaries as a Filter. Kennedy, V.S., Ed. Academic Press, pp. 1-14.

Shacklette, H.T., 1985. Foreward. In: Trace Elements in Soils and Plants, Kabata-Pendias, A. and Pendias, H. CRC Press, Florida, USA.

Shannon, Dr. L.V., 1990. The Benguela Current System. In: Marine Science and Technology in South Africa. Herbst, J.F., Ed. Foundation for Research Development, pp. 17-19.

Shirahata, H., Elia, R.W., Patterson, C.C., 1980. Chronological Variations in Concentrations and Isotopes Compositions of Anthropogenic Atmosphereic Lead in Sediments of a Remote Subapline Pond. *Geochimica et Cosmochimica Acta*, Vol. 44, pp. 149-162.

Short, F.T. & Short, C.A., 1984. The Seagrass Filter: Purification of Estuarine and Coastal Waters. In: The Estuary as a Filter. Kennedy, V.S., ed. Academic Press, Florida.

Strandring, W.J.F., Oughton, D.H., Salbu, B., 2002. Remobilisation of ^{109}Cd, ^{65}Zn, and ^{54}Mn from freshwater-labelled river sediments when mixed with seawater. *Environment International*, Vol. 28, pp.185-195.

Swanson, V.E., Love, A.H., and Frost, I.C., 1972. Geochemistry and Diagenesis of Tidal-Marsh Sediment, Northeastern Gulf of Mexico. *Bulletin of U.S. Geological Survey*, Vol. 1360, pp.83

Thomas, R.L., 1972. The Distribution of Mercury in the Surficial Sediments of Lake Huron. *Canadian Journal of Earth Science*, Vol. 10, pp.194-204.

Thompson, D.R., 1990. Metal Levals in Marine Vertebrates. In: Heavy Metals in the Marine Environment. Furness, R.W. And Rainbow, P.S., eds. pp. 143-182.

Tingzong, G., DeLaune, r.D., Patrick, W.H. Jr., 1997. The Influence of Sediment Redox Chemistry on Chemically Active Forms of Arsenic, Cadmium, and Zinc in Estuarine Sediments. *Environmenl International*, Vol. 23, No. 3, pp.305-316.

Troup, B.N. & Bricker, O.P., 1975. Processes Affecting the Transport From Continents to Oceans. In: Marine Chemistry in the Coastal Environment, Church, T.M., Ed. American Chemical Society. pp. 133-

Van Wyk, A.C., 1983. Effects of Dredging on the Berg River Estuary. MSc. Thesis, Univeristy of Cape Town, South Africa.

Velde, B., 1992. Introduction to Clay Minerals. Chapman & Hall, London.

Vlasov, K.A., 1964. Geochemistry and Mineralogy of Rare Elements and Genetic Types of Their Deposits, Section 12: Cadmium Minerals Israel Prg. For Sci. Transl., Jerusalem, Vol. II, p.945.

Wakita, H. and Schmitt, R.A., 1970. Cadmium. In: Handbook of Geochemistry, Ed: Wedepohl, K.H., Vol. II-3, pp.48-B-1 to 48-O-1.

Wark, J.W. and Keller F.J., 1963. Preliminary Study of Sediment Sources and Transport in the Potomac River Basin. Interstate Comm. on Potomac River Basin Tech. Bull. 1963-11, 28 p.

Wedepohl, K.H., Ed. (1974): Hand-book of Geochemistry. Vol. II-4, Springer-Verlage, Berlin, Heidelberg, New York.

Willis, J.P., 1999. Instrumental Parameters and Data Quality For Routine Major and Trace Element Determinations By WDXRFS. Information Circulation, University of Cape Town, South Africa.

Wolman, MG 1967: A cycle of Sedimentation and erosion in Urban River Channels. Geografisca Annalar, 49, Ser. A, 385-395.

Yen, T.F., 1977. Chemical Aspects of Marine Sediments. In: Chemistry of Marine Sediments. Yen, T.F., ed., Ann Arbor Science Publishers, Inc., USA, pp. 1-38.

Yiasoumi, B., 2003. Section 5 of Farm Water Quality and Treatment, Agfact AC.2. NSW Agriculture. www.agric.nsw.gov.au.

Zhang, J. and Liu, C.L., 2002. *Riverine Composition and Estuarine Geochemistry of Particulate Metals in China-Weathering Features, Anthropogenic Impact and Chemical Fluxes.* Estuarine, Coastal and Shelf Science, Vol. 54, pp. 1051-1070.

Zhang, C., Wang, L., Li, G., Dong, S., Yang, J., Wang, X., 2002b. Grain Size Effect on Multi-Element Concentrations in Sediments From the Intertidal Flats of Bohai Bay, China. *Applied Geochemistry*, Vol. 17, pp. 59-68.

Zhou, J.L., Liu, Y.P., Abrahams, P.W., 2003. Trace Metal Behavior in the Conwy stuary, North Wales. *Chemosphere*, Vol. 51, pp.429-440.

Zirino, A. and Yamamoto, S., 1972. a pH-dependent Model for the Chemical Speciation of Copper, Zinc, Cadmium, and Lead in Seawater. *Limnol. Oceanography*, Vol. 17, pp. 661-671.

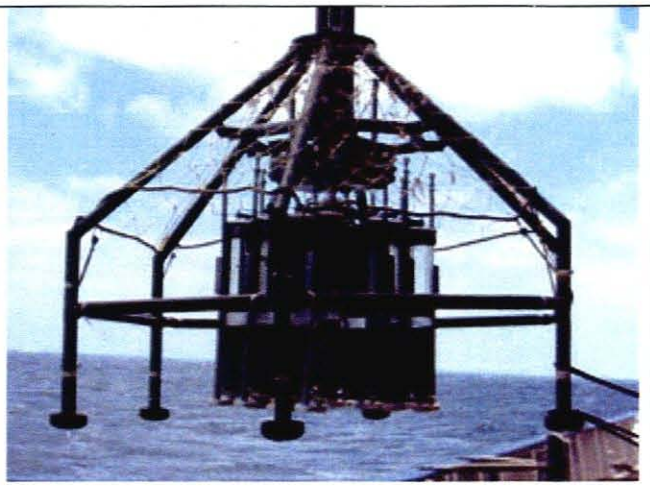

Plate 1. Retrieval of the multi-corer aboard the Meteor Cruise M57-1.

Plate 2. Sectioning of a multi-corer sediment core.

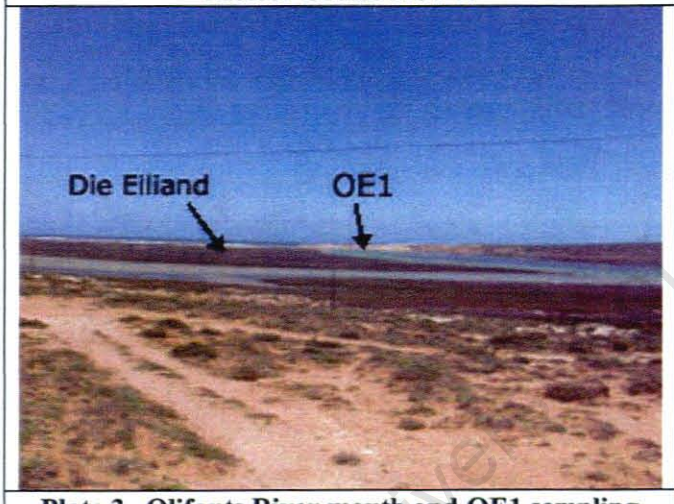

Plate 3. Olifants River mouth and OE1 sampling point.

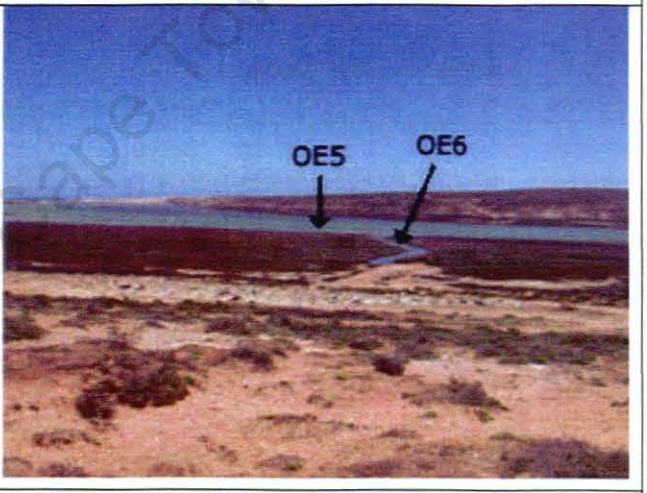

Plate 4. Small channel near viswater where sample OE6 was collected. OE5 collected in main river.

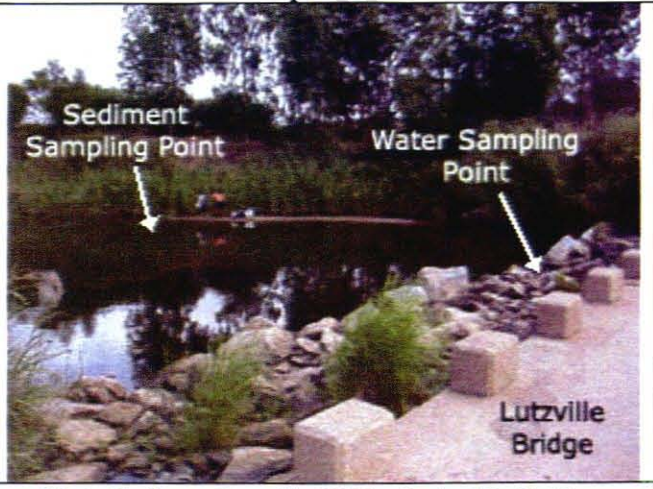

Plate 5. Sampling site OE3 – Lutzville Bridge.

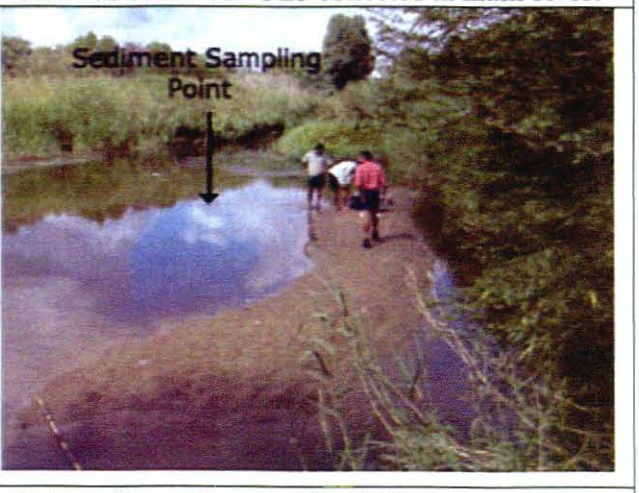

Plate 6. Sampling point for OE3 sediment cores.

Table I.A. Sampling times and Tide Data for Olifants and Berg River Samples

Sample ID	Sampling Time	Time of Low Tide	Time of High Tide
OE1	3pm 13/1/04	1:09pm	6:22pm
OE2	1pm 13/1/04	1:09pm	6:22pm
OE5	4:30pm 14/1/04	2:08pm	5:09pm
OE6	10:30am 15/1/04	~3pm	8:30am
OE4	12:30pm 14/1/04	2:08pm	7:40am
OE3	8am 14/1/04	2:08pm	7:40am
BR1	10:20am 21/1/04	9:09 am	3:14pm
BR2	2pm 21/1/04	9:09 am	3:14pm
BR3	3pm 21/1/04	9:09 am	3:14pm

Table I.B. Spectrophotometer Readings and Calibration Curve Corelation Coefficients for Surface Water Alkalinity Measurements

	Spectrophotometer Readings (Å)										
NaCl (mM)	OE1	OE2	OE3	OE4	OE5	OE6	BR1	BR2	BR3	Calibration Run	Calibration After Trip
0.5	0.315		0.364	0.31	0.316		0.295	0.304	0.299	0.285	0.283
1	0.365		0.37	0.358	0.361		0.34	0.342	0.405	0.334	0.327
2	0.49		0.483	0.482	0.481		0.403	0.423	0.43	0.42	0.412
3	0.621		0.619	0.617	0.618		0.556	0.519	0.527	0.517	0.515
4	0.757		0.741	0.731	0.723		0.633	0.641	0.655	0.645	0.646
5	0.879		0.909	0.906	0.902		0.778	0.784	0.804	0.812	0.783
7	1.284		1.245	0.964	1.22		1.11	1.131	1.065	1.161	1.172
Sample	0.614	0.65	0.95	0.858	0.59	0.586	0.512	0.463	0.506	0.276	0.261
Duplicate					0.593		0.509	0.496	0.502		
R^{2*}	0.9994		0.9927	0.9987	0.9979		0.9909	0.9998	0.9732	0.9996	0.9995

* - Second degree polynomial fit, as per Sarazin (1999)

Table I.C. Trace Metal Results of Water Samples for Olifants and Berg Rivers

	Concentrations in ppb											
	Mg	Al	Si	P	K	Ca	V	Cr	Mn	Fe	Co	Ni
NIST-1640	6157	63.5	3084	88.0	979	6994	*n.d.*	35.6	120	*n.d.*	20.3	28.6
certified	5819	52.0	4730	-	994	7045	12.99	38.6	121.5	34.3	20.28	27.4
TRIP BLANK	22.8	*n.d.*	*n.d.*	*n.d.*	*n.d.*	*n.d.*	*n.d.*	*n.d.*	*n.d.*	*n.d.*	0.017	0.12
OE1 Unfiltered	1014975	89.6	754	95.3	246817	179806	13.2	5.34	19.1	664	0.56	9.95
OE1 Filtered	824045	3.91	483	167	207473	162534	21.5	6.73	12.2	625	0.43	7.86
OE2 Unfiltered	1715040	103	978	173	414462	286200	83.7	3.62	21.0	1505	0.90	15.3
OE2 Filtered	2030902	13.6	954	222	513733	363602	46.3	1.85	18.7	1270	0.97	17.0
OE3 Unfiltered	27998	48.0	543	84.8	3982	25198	24.2	4.35	136	102	0.29	1.79
OE3 Filtered	37746	4.05	1219	370	5363	34883	34.6	11.4	94.6	298	0.26	2.08
OE4 Unfiltered	225142	52.0	714	36.0	49756	70731	24.8	3.06	44.8	228	0.29	3.27
OE4 Filtered	167687	10.0	492	238	39708	63506	8.65	5.36	7.72	138	0.19	3.27
OE5 Unfiltered 1	1357813	165	743	88.3	343186	271324	78.2	2.74	15.3	1286	0.92	13.3
OE5 Filtered 1	1774081	9.53	560	94.8	429012	322283	53.7	2.22	9.62	1215	0.86	13.8
OE5 Unfiltered 2	1485819	127	780	154	367703	262444	76.8	2.51	17.1	1277	0.92	13.5
OE5 Filtered 2	1399552	11.0	568	76.1	348040	245065	57.6	1.57	10.7	905	0.70	11.5
OE6 Unfiltered	1108811	156	857	51.9	270859	190681	30.8	9.08	52.9	969	0.82	10.4
OE6 Filtered	1394465	9.08	599	97.5	323787	236040	24.7	4.65	56.6	846	0.82	11.3
BR1 Unfiltered 1	1652932	230	1430	109	404734	276118	74.3	63.7	18.9	1528	0.90	17.8
BR1 Filtered 1	1520441	34.7	1076	84.9	381862	258913	66.4	43.4	13.8	989	0.72	14.6
BR1 Unfiltered 2	1047507	114	934	114	276817	202223	77.2	18.9	11.5	1114	0.61	10.7
BR1 Filtered 2	1014269	5.03	672	158	253162	190497	11.1	5.44	8.70	621	0.44	8.88
BR2 Unfiltered 1	1276281	32.0	730	50.0	325344	223218	69.7	3.15	3.62	921	0.62	12.3
BR2 Filtered 1	1901004	14.1	928	130	458151	331735	60.7	2.56	3.90	1236	0.73	15.5
BR2 Unfiltered 2	1557006	35.7	959	106	382344	264931	89.96	4.94	4.09	1170	0.72	13.9
BR2 Filtered 2	1986664	7.94	1027	109	493481	357061	57.5	2.31	4.26	1295	0.87	15.5
BR3 Unfiltered 1	1070760	57.7	1259	183	246373	174780	32.2	4.00	33.3	807	0.53	9.24
BR3 Filtered 1	1426707	9.9	1621	106	336006	242316	46.7	4.69	24.9	871	0.63	11.5
BR3 Unfiltered 2	957095	53.2	1190	380	227722	165868	79.0	9.81	25.6	855	0.55	9.75

n.d. – Not Detected

Table I.C. Trace Metal Results of Water Samples for Olifants and Berg Rivers

	Concentrations in ppb											
	Mg	Al	Si	P	K	Ca	V	Cr	Mn	Fe	Co	Ni
NIST-1640	6157	63.5	3084	88.0	979	6994	*n.d.*	35.6	120	*n.d.*	20.3	28.6
certified	5819	52.0	4730	-	994	7045	12.99	38.6	121.5	34.3	20.28	27.4
TRIP BLANK	22.8	*n.d.*	*n.d.*	*n.d.*	*n.d.*	*n.d.*	*n.d.*	*n.d.*	*n.d.*	*n.d.*	0.017	0.12
OE1 Unfiltered	1014975	89.6	754	95.3	246817	179806	13.2	5.34	19.1	664	0.56	9.95
OE1 Filtered	824045	3.91	483	167	207473	162534	21.5	6.73	12.2	625	0.43	7.86
OE2 Unfiltered	1715040	103	978	173	414462	286200	83.7	3.62	21.0	1505	0.90	15.3
OE2 Filtered	2030902	13.6	954	222	513733	363602	46.3	1.85	18.7	1270	0.97	17.0
OE3 Unfiltered	27998	48.0	543	84.8	3982	25198	24.2	4.35	136	102	0.29	1.79
OE3 Filtered	37746	4.05	1219	370	5363	34883	34.6	11.4	94.6	298	0.26	2.08
OE4 Unfiltered	225142	52.0	714	36.0	49756	70731	24.8	3.06	44.8	228	0.29	3.27
OE4 Filtered	167687	10.0	492	238	39708	63506	8.65	5.36	7.72	138	0.19	3.27
OE5 Unfiltered 1	1357813	165	743	88.3	343186	271324	78.2	2.74	15.3	1286	0.92	13.3
OE5 Filtered 1	1774081	9.53	560	94.8	429012	322283	53.7	2.22	9.62	1215	0.86	13.8
OE5 Unfiltered 2	1485819	127	780	154	367703	262444	76.8	2.51	17.1	1277	0.92	13.5
OE5 Filtered 2	1399552	11.0	568	76.1	348040	245065	57.6	1.57	10.7	905	0.70	11.5
OE6 Unfiltered	1108811	156	857	51.9	270859	190681	30.8	9.08	52.9	969	0.82	10.4
OE6 Filtered	1394465	9.08	599	97.5	323787	236040	24.7	4.65	56.6	846	0.82	11.3
BR1 Unfiltered 1	1652932	230	1430	109	404734	276118	74.3	63.7	18.9	1528	0.90	17.8
BR1 Filtered 1	1520441	34.7	1076	84.9	381862	258913	66.4	43.4	13.8	989	0.72	14.6
BR1 Unfiltered 2	1047507	114	934	114	276817	202223	77.2	18.9	11.5	1114	0.61	10.7
BR1 Filtered 2	1014269	5.03	672	158	253162	190497	11.1	5.44	8.70	621	0.44	8.88
BR2 Unfiltered 1	1276281	32.0	730	50.0	325344	223218	69.7	3.15	3.62	921	0.62	12.3
BR2 Filtered 1	1901004	14.1	928	130	458151	331735	60.7	2.56	3.90	1236	0.73	15.5
BR2 Unfiltered 2	1557006	35.7	959	106	382344	264931	89.96	4.94	4.09	1170	0.72	13.9
BR2 Filtered 2	1986664	7.94	1027	109	493481	357061	57.5	2.31	4.26	1295	0.87	15.5
BR3 Unfiltered 1	1070760	57.7	1259	183	246373	174780	32.2	4.00	33.3	807	0.53	9.24
BR3 Filtered 1	1426707	9.9	1621	106	336006	242316	46.7	4.69	24.9	871	0.63	11.5
BR3 Unfiltered 2	957095	53.2	1190	380	227722	165868	79.0	9.81	25.6	855	0.55	9.75

n.d. – Not Detected

Table I.C. (cont.)

	Cu	Zn	As	Se	Rb	Sr	Mo	Cd	Ba	Pb	Cu
NIST-1640	86.5	73.5	25.7	22.4	1.96	120	47.4	23.5	142	28.9	86.5
Certified	85.2	53.2	26.67	21.96	2.00	124.2	46.75	22.79	148.0	27.89	85.2
TRIP BLANK	0.18	0.65	0.97	1.96	0.019	0.18	0.021	*n.d.*	0.32	0.20	0.18
OE1 Unfiltered	30.8	97.6	46.5	126	60.5	4828	7.07	0.14	17.4	1.24	30.8
OE1 Filtered	31.8	97.7	44.6	93.9	47.4	3776	5.73	0.076	12.9	0.85	31.8
OE2 Unfiltered	70.4	138	99.9	147	99.8	7760	8.90	0.11	14.2	1.12	70.4
OE2 Filtered	52.2	159	98.7	204	117	8622	10.9	0.15	15.7	0.47	52.2
OE3 Unfiltered	5.00	29.0	5.09	2.60	0.88	277	1.11	0.012	18.3	0.51	5.00
OE3 Filtered	11.3	21.0	7.97	5.09	1.04	336	1.35	0.025	19.4	0.43	11.3
OE4 Unfiltered	6.18	30.6	13.4	23.0	11.8	1491	3.59	0.031	37.1	0.34	6.18
OE4 Filtered	7.52	44.5	8.37	21.2	9.41	1016	2.88	0.037	28.6	0.59	7.52
OE5 Unfiltered 1	54.6	115	85.6	149	87.7	6407	10.1	0.14	21.7	0.75	54.6
OE5 Filtered 1	65.6	149	88.9	164	95.2	7468	11.9	0.15	22.5	0.72	65.6
OE5 Unfiltered 2	54.6	120	83.9	140	88.4	6737	9.67	0.15	22.8	1.23	54.6
OE5 Filtered 2	44.7	97.0	79.5	138	84.7	6254	9.94	0.12	20.8	0.27	44.7
OE6 Unfiltered	36.1	105	59.1	130	65.8	5199	7.75	0.16	16.7	1.38	36.1
OE6 Filtered	43.4	88.5	64.6	153	77.3	6207	9.60	0.15	18.9	0.66	43.4
BR1 Unfiltered 1	107	580	90.1	155	93.0	7324	9.18	0.58	13.4	8.42	107
BR1 Filtered 1	71.6	218	89.6	152	89.4	6694	9.46	0.37	11.8	3.23	71.6
BR1 Unfiltered 2	46.9	146	69.4	114	64.7	5077	7.14	0.23	10.4	1.18	46.9
BR1 Filtered 2	31.9	111	51.4	113	55.2	4685	6.28	0.19	7.71	0.37	31.9
BR2 Unfiltered 1	44.1	105	76.5	145	76.2	5815	7.99	0.19	8.07	0.73	44.1
BR2 Filtered 1	60.8	117	97.3	162	97.4	7777	10.7	0.23	8.68	1.10	60.8
BR2 Unfiltered 2	60.6	121	91.8	152	89.2	6798	9.45	0.21	9.92	0.72	60.6
BR2 Filtered 2	64.5	128	98.4	179	109	8630	12.1	0.23	9.00	0.38	64.5
BR3 Unfiltered 1	31.8	91.2	50.6	121	60.8	4943	6.56	0.24	21.4	1.91	31.8
BR3 Filtered 1	48.3	108	75.0	142	80.6	6651	8.50	0.29	24.6	0.50	48.3
BR3 Unfiltered 2	35.1	130	58.3	97.4	54.9	4501	5.96	0.24	18.7	1.38	35.1
BR3 Filtered 2	59.3	118	76.5	157	86.0	6968	9.17	0.31	26.7	1.16	59.3

Appendix I

Table I.D. Olifants R. Sediment Cores Grains Size, % Water, Porosity & Density Results

Sample ID	% Sand (>63μm)	% Coarse Silt (38-63μm)	% Fine Silt (2-38μm)	% Clay (<2μm)	% Water	Porosity	Density (kg/m3)
OE2-A: 0-2 cm	74.8	3.5	16.9	4.8	34.8	0.55	1584
OE2-A: 2-4 cm					25.7	0.42	1649
OE2-A: 4-6 cm	77.8	3.7	15.9	2.5	28.5	0.40	1404
OE2-A: 6-8 cm					20.7	0.39	1902
OE2-A: 8-10 cm	86.2	2.3	8.6	2.9	21.0	0.31	1483
OE2-A: 10-12 cm	86.9	2.2	8.8	2.1	22.2	0.42	1898
OE2-A: 14-16.5 cm	86.6	2.0	9.4	2.0	21.6	0.39	1818
OE2-A: 19-22 cm	82.7	1.8	13.7	1.7	21.5	0.36	1693
OE3-B: 0-2 cm	99.1	0.3	0.3	0.3	20.3	0.35	1717
OE3-B: 2-4 cm					19.0	0.30	1618
OE3-B: 4-6 cm	99.3	0.2	0.2	0.2	21.7	0.35	1638
OE3-B: 6-8 cm					20.2	0.33	1646
OE3-B: 8-10 cm	99.6	0.1	0.1	0.2	19.5	0.34	1742
OE3-B: 12-14 cm	99.7	0.1	0.1	0.1	19.9	0.33	1673
OE3-B: 16-17 cm					20.0	0.33	1663
OE4-A: 0-2 cm	36.9	19.7	33.0	10.5	42.5	0.56	1340
OE4-A: 2-4 cm					44.8	0.64	1449
OE4-A: 4-6 cm	32.0	1.8	47.7	18.5	36.5	0.54	1496
OE4-A: 6-8 cm					30.9	0.56	1841
OE4-A: 8-10 cm	25.8	10.0	38.0	26.2	31.6	0.49	1579
OE4-A: 12-14 cm	33.0	9.7	40.0	17.3	34.4	0.50	1469
OE4-A: 16-18 cm	29.3	10.2	36.3	24.2	28.3	0.46	1640
OE4-A: 20-22.5 cm	20.7	8.6	39.1	31.6	29.2	0.44	1525
OE6: 0-2 cm	60.2	10.9	19.7	9.3	31.9	0.47	1502
OE6: 2-4 cm					27.1	0.42	1562
OE6: 4-6 cm	60.4	9.9	18.1	11.6	27.5	0.41	1505
OE6: 6-8 cm					29.6	0.51	1753
OE6: 8-10 cm	64.9	10.9	10.7	13.5	27.5	0.41	1514
OE6: 12-14 cm	54.0	10.1	23.1	12.8	28.3	0.43	1543
OE6: 16-18 cm	48.4	10.1	25.3	16.1	27.5	0.43	1565

Table I.E. Berg R. Sediment Cores Grains Size, % Water, Porosity & Density Results

Sample ID	% Sand (>63μm)	% Coarse Silt (38-63μm)	% Fine Silt (2-38μm)	% Clay (<2μm)	% Water	Porosity	Density (kg/m3)
BR1-A: 0-2 cm	27.2	5.1	60.8	6.9	54.7	0.61	1124
BR1-A: 2-4 cm					45.8	0.56	1227
BR1-A: 4-6 cm	55.6	3.1	33.4	7.8	41.6	0.51	1232
BR1-A: 6-8 cm					36.8	0.47	1295
BR1-A: 8-10 cm	62.5	2.8	28.4	6.3	40.5	0.51	1274
BR1-A: 12-14 cm	63.2	2.5	31.1	3.2	33.8	0.48	1435
BR1-A: 16-18 cm	66.6	2.4	27.5	3.6	33.0	0.45	1383
BR1-A: 20-22 cm	68.1	2.5	25.1	4.3	32.9	0.49	1517
BR1-A: 24-26 cm	67.2	2.5	25.5	4.8	32.2	0.49	1531
BR1-A: 28-30 cm	66.1	2.8	25.9	5.2	32.0	0.49	1530
BR1-A: 34-36 cm	59.7	3.1	31.9	5.2	35.7	0.54	1534
BR1-A: 40-42 cm	67.4	1.6	27.4	3.6	30.8	0.45	1478
BR1-A: 46-48 cm	75.2	1.2	18.8	4.8	27.4	0.41	1518
BR1-A: 52-55 cm	70.1	1.1	24.2	4.6	23.0	0.30	1315
BR2: 0-2 cm	39.0	7.2	33.7	20.0	50.7	0.68	1350
BR2: 2-4 cm					35.3	0.53	1519
BR2: 4-6 cm	47.7	6.9	31.5	13.8	36.4	0.56	1564
BR2: 6-8 cm					35.9	0.45	1275
BR2: 8-10 cm	49.9	5.9	41.1	3.0	35.4	0.48	1357
BR2: 12-14 cm	52.8	7.0	27.0	13.2	35.4	0.49	1410
BR2: 16-18 cm	40.0	6.6	46.0	7.3	36.3	0.44	1219
BR2: 20-22 cm	48.2	6.2	26.5	19.0	33.3	0.48	1469
BR2: 24-26 cm	50.1	5.4	38.0	6.5	29.3	0.44	1530
BR2: 28-30 cm	49.3	6.3	26.7	17.7	28.5	0.47	1670
BR2: 32-34 cm	53.6	5.4	36.5	4.6	29.3	0.45	1541
BR2: 38-40 cm	48.1	6.8	26.4	18.7	32.4	0.58	1800
BR2: 44-46 cm	49.3	5.9	39.6	5.1	32.6	0.47	1446
BR2: 50-52 cm	44.8	7.3	34.0	13.9	32.9	0.55	1694
BR2: 58-60cm	47.6	8.4	35.1	8.9	31.3	0.57	1839
BR2: 66-68 cm	39.2	6.4	34.2	20.2	35.0	0.54	1551
BR2: 74-76 cm	43.3	6.4	45.5	4.8	32.5	0.50	1558
BR3-B: 0 - 2 cm	82.6	4.1	9.4	3.8	30.5	0.42	1390
BR3-B: 2-4 cm					30.1	0.41	1378
BR3-B: 4-6 cm	83.4	3.4	10.3	2.9	29.0	0.43	1502
BR3-B: 6-8 cm					27.8	0.40	1435
BR3-B: 8-10 cm	79.7	3.3	12.7	4.3	27.5	0.40	1457
BR3-B: 12-14 cm	82.7	3.4	9.5	4.4	26.4	0.36	1387
BR3-B: 16-18 cm	84.8	3.1	8.5	3.6	26.6	0.40	1516
BR3-B: 20-22 cm	84.2	3.2	8.1	4.5	27.2	0.37	1372
BR3-B: 24-26 cm	83.6	3.7	6.9	5.7	26.1	0.37	1439
BR3-B: 28-30 cm	81.1	3.4	10.1	5.4	25.7	0.38	1488
BR3-B: 34-36 cm	77.7	4.4	9.9	7.9	25.0	0.40	1630
BR3-B: 40-42 cm	78.0	5.0	10.4	6.5	27.7	0.38	1379
BR3-B: 46-48 cm	76.5	5.0	10.6	7.8	24.4	0.37	1514
BR3-B: 50-51 cm					24.0	0.40	1672

Table I.F. Mud Belt Sediment Cores Grains Size, % Water, Porosity & Density Results

Sample ID	% Sand (>63μm)	% Coarse Silt (38-63μm)	% Fine Silt (2-38μm)	% Clay (<2μm)	% Water	Porosity	Density (kg/m3)
Geo8319-1: 0 - 2 cm					53.6	0.49	1008
Geo8319-1: 2 - 4 cm	37.3	1.2	29.9	31.6	53.2	0.50	1036
Geo8319-1: 4 - 6 cm	41.7	1.5	38.0	18.8	55.6	0.53	1032
Geo8319-1: 6 - 8 cm	45.5	2.0	33.1	19.4	53.6	0.51	1038
Geo8319-1: 8 - 10 cm	48.3	1.7	38.0	12.0	54.3	0.51	1035
Geo8319-1: 10 - 12 cm	45.8	1.1	35.3	17.8	53.6	0.51	1039
Geo8319-1: 12 - 14 cm	40.9	2.0	36.1	21.0	53.7	0.51	1040
Geo8319-1: 15 - 17 cm	39.2	1.8	37.6	21.4	54.3	0.51	1034
Geo8319-1: 18 - 20 cm	42.9	1.9	35.0	20.3	55.1	0.51	1016
Geo8319-1: 21 - 23 cm	37.4	2.7	36.4	23.5	56.4	0.52	1015
Geo8319-1: 24 - 26 cm	41.4	2.5	36.8	19.3	53.2	0.51	1045
Geo8319-1: 27 - 29 cm	48.4	2.2	40.4	8.9	51.4	0.49	1043
Geo8322-1: 0 - 1 cm					67.6	0.60	962
Geo8322-1: 2 - 3 cm	0.7	0.8	70.5	28.0	65.1	0.59	978
Geo8322-1: 4 - 5 cm	0.6	0.4	83.0	16.0	65.1	0.58	965
Geo8322-1: 6 - 7 cm	0.8	0.7	82.5	16.0	64.3	0.57	955
Geo8322-1: 8 - 9 cm	0.8	1.2	80.3	17.6	64.8	0.58	969
Geo8322-1: 10 - 11 cm	1.3	1.3	82.9	14.5	64.7	0.57	954
Geo8322-1: 13 - 14 cm	1.8	0.7	85.9	11.6	62.4	0.55	962
Geo8322-1: 16 - 17 cm	1.9	1.6	87.1	9.4	63.6	0.56	953
Geo8322-1: 19 - 20 cm	3.4	0.9	88.1	7.6	64.8	0.57	949
Geo8322-1: 22 - 23 cm	1.8	0.9	85.5	11.9	65.3	0.55	921
Geo8322-1: 25 - 26 cm	0.5	0.4	93.0	6.1	65.3	0.57	943
Geo8322-1: 28 - 29 cm	0.4	0.4	94.2	5.0	66.1	0.58	945
Geo8322-1: 31 - 32 cm	1.0	0.5	93.2	5.3	65.3	0.57	944
Geo8322-1: 34 - 35 cm	2.0	0.3	94.5	3.3	64.3	0.56	939
Geo8322-1: 37 - 38 cm	0.1	2.2	92.7	5.0	62.0	0.54	944
Geo8322-1: 40 - 41 cm	0.7	2.9	83.2	13.2	61.4	0.53	946

Table I.G. XRF Results – Olifants R. Cores (all results in weight %)

Sample ID	SiO2	Al2O3	TiO2	Fe2O3	MnO	MgO	CaO	Na2O	K2O	P2O5	SO3	Cr2O3	NiO	H2O-	LOI	Sum	Sulfur
OE2-A: 0-2 cm	73.7	4.3	0.38	2.85	0.047	1.03	5.59	1.28	0.66	0.121	0.529	0.026	0.008	0.60	8.01	99.17	4.02
OE2-A: 2-4 cm	75.7	4.4	0.38	2.77	0.053	0.96	4.45	1.00	0.65	0.119	0.429	0.023	0.009	0.93	7.44	99.22	5.39
OE2-A: 4-6 cm	75.2	4.8	0.40	3.12	0.048	1.07	4.55	1.19	0.89	0.125	0.595	0.019	0.006	0.97	6.34	99.31	4.92
OE2-A: 6-8 cm	81.0	3.3	0.32	2.05	0.042	0.82	4.53	0.88	0.57	0.110	0.273	0.019	0.008	0.40	5.14	99.44	3.19
OE2-A: 8-10 cm	79.9	3.5	0.35	2.22	0.047	0.82	4.71	0.91	0.63	0.119	0.334	0.017	0.006	0.37	5.28	99.24	2.79
OE2-A: 10-12 cm	78.8	3.8	0.36	2.35	0.048	0.87	4.88	0.95	0.61	0.125	0.291	0.019	0.005	0.37	5.76	99.17	2.46
OE2-A: 14-16.5 cm	80.9	3.5	0.33	2.13	0.051	0.82	4.42	0.89	0.60	0.121	0.189	0.016	0.008	0.33	5.40	99.67	1.85
OE2-A: 19-22 cm	78.8	4.0	0.34	2.56	0.049	0.91	4.29	0.87	0.77	0.127	0.306	0.023	0.006	0.48	5.60	99.14	2.71
OE3-B: 0-2 cm	74.9	8.9	0.45	4.87	0.125	1.70	2.56	1.37	1.52	0.092	0.046	0.035	0.010	0.12	2.38	99.09	0.25
OE3-B: 2-4 cm	78.9	7.8	0.41	4.56	0.093	1.71	2.34	1.22	1.31	0.089	0.028	0.037	0.008	0.10	1.23	99.79	0.13
OE3-B: 4-6 cm	78.3	7.2	0.42	4.46	0.090	1.70	2.17	1.13	1.25	0.081	0.022	0.036	0.007	-0.01	2.18	99.01	0.15
OE3-B: 6-8 cm	80.4	7.2	0.40	4.22	0.085	1.52	2.03	1.08	1.29	0.079	0.032	0.033	0.006	0.08	1.10	99.64	0.10
OE3-B: 8-10 cm	81.6	6.3	0.35	3.88	0.080	1.50	1.89	1.02	1.13	0.075	0.024	0.032	0.011	0.00	1.64	99.59	0.11
OE3-B: 12-14 cm	81.8	6.7	0.38	3.92	0.076	1.44	1.86	1.08	1.21	0.079	0.021	0.035	0.009	0.06	0.96	99.68	0.09
OE3-B: 16-17 cm	75.7	8.8	0.44	5.11	0.099	1.92	2.70	1.37	1.46	0.093	0.027	0.039	0.012	0.07	1.27	99.10	0.12
OE4-A: 0-2 cm	60.0	15.0	0.77	6.29	0.106	2.76	2.67	2.07	2.32	0.179	0.063	0.028	0.006	2.03	6.18	100.53	3.85
OE4-A: 2-4 cm	58.6	14.7	0.71	6.49	0.126	2.79	2.11	1.75	2.62	0.175	0.151	0.024	0.008	2.40	6.69	99.39	4.48
OE4-A: 4-6 cm	62.6	14.3	0.72	6.18	0.124	2.78	2.38	1.70	2.45	0.169	0.090	0.027	0.008	1.30	5.81	100.71	3.08
OE4-A: 6-8 cm	61.3	14.9	0.75	6.42	0.137	2.78	2.49	1.77	2.59	0.181	0.063	0.028	0.008	1.23	5.92	100.56	1.99
OE4-A: 8-10 cm	62.4	14.6	0.74	6.17	0.130	2.77	2.45	1.72	2.49	0.176	0.071	0.027	0.007	1.03	5.66	100.45	1.92
OE4-A: 12-14 cm	62.3	14.5	0.72	6.19	0.120	2.76	2.49	1.61	2.33	0.177	0.053	0.027	0.008	0.91	6.24	100.46	2.79
OE4-A: 16-18 cm	63.1	15.6	0.81	6.78	0.157	0.01	2.95	0.31	2.53	0.183	0.038	0.030	0.007	1.08	5.92	99.49	1.60
OE4-A: 20-22.5 cm	59.5	14.9	0.72	6.73	0.148	2.93	2.41	1.45	2.48	0.188	0.056	0.028	0.006	1.56	6.99	100.12	1.47
OE6: 0-2 cm	74.8	9.5	0.62	3.30	0.046	1.59	0.92	1.90	1.67	0.109	0.015	0.017	0.007	0.56	4.94	100.03	0.86
OE6: 2-4 cm	74.8	9.6	0.65	3.62	0.046	1.56	0.97	1.70	1.79	0.121	0.024	0.018	0.006	0.47	4.86	100.30	1.28
OE6: 4-6 cm	73.5	9.3	0.84	5.06	0.061	1.50	0.94	1.71	1.45	0.111	0.084	0.024	0.012	0.44	4.73	99.77	1.32
OE6: 6-8 cm	71.9	9.0	0.87	5.34	0.069	1.46	0.91	1.83	1.70	0.112	0.120	0.028	0.009	0.51	5.50	99.39	1.23
OE6: 8-10 cm	73.3	8.7	0.86	5.04	0.063	1.37	0.90	1.56	1.63	0.113	0.124	0.027	0.009	1.01	4.39	99.08	1.83
OE6: 12-14 cm	70.3	10.2	0.88	5.79	0.071	1.68	0.94	1.79	1.56	0.125	0.130	0.025	0.009	1.22	5.25	99.89	2.27
OE6: 16-18 cm	72.3	10.7	0.65	3.90	0.046	1.83	0.87	1.79	1.92	0.118	0.022	0.016	0.006	1.12	5.16	100.47	1.60

Table I.H. XRF Results – Berg R. Cores (all results in weight %)

Sample ID	SiO2	Al2O3	TiO2	Fe2O3	MnO	MgO	CaO	Na2O	K2O	P2O5	SO3	Cr2O3	NiO	H2O-	LOI	Sum	Sulfur
BR1-A: 0-2 cm	60.4	12.4	0.58	4.72	0.033	0.01	2.91	0.22	2.22	0.298	0.170	0.026	0.004	3.98	11.73	99.64	1.35
BR1-A: 2-4 cm	68.9	9.7	0.52	3.46	0.030	0.12	2.33	0.27	1.75	0.223	0.133	0.024	0.006	2.90	8.84	99.12	1.64
BR1-A: 4-6 cm	72.6	8.7	0.49	3.12	0.028	0.14	2.23	0.18	1.64	0.205	0.095	0.022	0.010	1.99	7.89	99.28	2.37
BR1-A: 6-8 cm	77.6	7.3	0.46	2.48	0.031	0.18	2.05	0.21	1.46	0.180	0.088	0.020	0.004	1.62	6.36	99.98	1.89
BR1-A: 8-10 cm	72.7	8.2	0.47	2.85	0.029	0.03	1.89	0.28	1.65	0.189	0.081	0.022	0.008	2.16	8.98	99.56	1.56
BR1-A: 12-14 cm	78.4	7.6	0.49	2.48	0.024	0.09	1.86	0.21	1.45	0.167	0.083	0.017	0.014	1.51	6.17	100.52	2.37
BR1-A: 16-18 cm	80.0	6.9	0.48	2.34	0.029	0.17	1.80	0.31	1.41	0.158	0.049	0.019	0.007	1.17	5.81	100.60	2.33
BR1-A: 20-22 cm	79.6	6.8	0.43	2.31	0.028	0.18	1.61	0.19	1.38	0.139	0.088	0.016	0.007	1.02	5.64	99.43	3.31
BR1-A: 24-26 cm	78.8	7.3	0.44	2.35	0.030	0.22	1.71	0.41	1.40	0.134	0.097	0.021	0.004	0.89	5.79	99.61	3.66
BR1-A: 28-30 cm	79.3	7.7	0.51	2.55	0.030	0.08	1.65	0.19	1.55	0.170	0.062	0.020	0.007	1.33	5.82	100.92	2.17
BR1-A: 34-36 cm	74.0	8.9	0.49	2.99	0.029	0.12	1.81	0.24	1.72	0.157	0.156	0.020	0.006	1.47	7.68	99.84	3.85
BR1-A: 40-42 cm	78.4	8.0	0.50	2.72	0.029	0.08	1.58	0.23	1.62	0.147	0.091	0.031	0.010	1.04	5.64	100.17	3.07
BR1-A: 46-48 cm	79.6	7.2	0.44	2.38	0.027	0.14	1.56	0.29	1.47	0.138	0.079	0.014	0.006	0.99	5.94	100.26	2.29
BR1-A: 52-55 cm	81.8	7.1	0.44	2.32	0.027	0.05	1.62	0.08	1.51	0.132	0.066	0.017	0.006	0.81	4.69	100.71	2.45
BR2: 0-2 cm	69.3	11.8	0.84	4.24	0.035	0.06	0.92	0.26	2.22	0.209	0.066	0.024	0.008	1.67	8.25	99.97	4.22
BR2: 2-4 cm	66.7	9.4	1.08	5.25	0.047	1.09	0.76	1.43	1.70	0.188	0.297	0.028	0.011	4.86	6.32	99.09	3.34
BR2: 4-6 cm	66.9	9.3	1.08	5.27	0.050	1.05	0.92	1.54	1.72	0.194	0.324	0.032	0.008	4.73	6.85	99.97	3.88
BR2: 6-8 cm	67.6	10.2	1.12	5.73	0.052	1.13	0.88	1.41	1.85	0.196	0.471	0.032	0.009	2.58	6.71	99.94	3.90
BR2: 8-10 cm	68.5	9.5	1.13	5.42	0.052	1.04	1.07	1.44	1.75	0.202	0.541	0.030	0.009	2.17	6.40	99.22	3.92
BR2: 12-14 cm	70.2	9.4	1.18	5.19	0.052	1.03	0.79	1.48	1.77	0.184	0.320	0.028	0.006	1.93	6.28	99.77	4.26
BR2: 16-18 cm																	4.43
BR2: 20-22 cm	70.5	11.4	0.82	3.93	0.038	0.17	1.30	0.25	2.09	0.172	0.084	0.022	0.004	1.69	6.76	99.25	3.83
BR2: 24-26 cm	71.0	9.4	1.20	5.12	0.055	1.03	0.69	1.35	1.76	0.169	0.287	0.029	0.011	1.47	5.85	99.40	4.93
BR2: 28-30 cm	70.3	9.8	1.22	5.37	0.054	1.08	0.87	1.23	1.81	0.175	0.389	0.031	0.007	1.41	6.12	99.93	4.24
BR2: 32-34 cm	68.4	10.1	1.08	5.56	0.050	1.16	0.76	1.32	1.87	0.168	0.316	0.029	0.010	1.62	6.65	99.09	4.01
BR2: 38-40 cm	67.9	9.8	1.09	5.60	0.056	1.12	1.08	1.34	1.84	0.169	0.501	0.053	0.012	2.30	6.91	99.71	5.38
BR2: 44-46 cm	69.4	11.5	0.76	4.05	0.038	0.13	0.84	0.15	2.16	0.172	0.063	0.021	0.004	2.56	7.27	99.06	5.62
BR2: 50-52 cm	69.7	9.7	0.94	5.18	0.048	1.13	0.59	1.35	1.80	0.157	0.242	0.026	0.008	2.19	6.64	99.69	4.38
BR2: 58-60cm	70.2	9.3	0.97	5.01	0.052	1.19	0.69	1.41	1.80	0.151	0.256	0.030	0.009	2.12	6.49	99.68	4.61
BR2: 66-68 cm	62.4	11.3	1.02	6.36	0.052	1.28	1.26	1.50	1.83	0.171	0.426	0.032	0.009	3.05	8.37	99.05	5.99
BR2: 74-76 cm	65.3	10.2	1.06	5.90	0.050	1.16	1.70	1.44	1.84	0.172	0.873	0.034	0.011	1.88	7.70	99.35	6.73
BR3-B: 0-2 cm	84.5	5.0	1.04	2.00	0.051	0.68	0.48	1.03	1.07	0.183	0.017	0.021	0.007	0.55	3.02	99.60	1.40
BR3-B: 2-4 cm	85.4	5.0	0.99	1.89	0.045	0.59	0.50	1.10	1.14	0.189	0.015	0.023	0.001	0.56	2.89	100.37	1.36
BR3-B: 4-6 cm	86.1	4.8	1.07	2.10	0.048	0.03	0.46	0.21	1.12	0.203	0.017	0.018	0.001	0.43	3.95	100.64	1.34
BR3-B: 6-8 cm	87.0	4.8	1.08	1.92	0.044	0.14	0.46	0.23	1.09	0.195	0.017	0.015	0.003	0.40	2.60	99.93	1.13
BR3-B: 8-10 cm	86.2	5.5	1.03	2.13	0.040	0.11	0.45	0.09	1.21	0.182	0.011	0.021	0.004	0.42	3.09	100.45	1.39
BR3-B: 12-14 cm	86.0	5.2	1.02	1.87	0.040	0.68	0.46	1.06	1.16	0.166	0.010	0.016	0.002	0.38	2.63	100.72	1.23
BR3-B: 16-18 cm	85.8	4.9	0.97	1.78	0.041	0.63	0.45	1.06	1.12	0.177	0.012	0.043	0.009	0.48	2.52	100.04	1.18
BR3-B: 20-22 cm	85.2	5.2	1.04	1.93	0.036	0.68	0.46	1.15	1.15	0.172	0.011	0.027	0.009	0.37	2.66	100.08	1.37

Table I.H. (cont)

Sample ID	SiO2	Al2O3	TiO2	Fe2O3	MnO	MgO	CaO	Na2O	K2O	P2O5	SO3	Cr2O3	NiO	H2O-	LOI	Sum	Sulfur
BR3-B: 24-26 cm	86.1	5.0	1.01	1.85	0.038	0.70	0.45	1.05	1.13	0.171	0.011	0.020	0.003	0.34	2.54	100.37	1.25
BR3-B: 28-30 cm	85.2	5.2	1.03	2.01	0.043	0.63	0.46	1.00	1.21	0.178	0.010	0.019	0.005	0.38	2.73	100.10	1.38
BR3-B: 34-36 cm	84.7	5.2	0.98	1.94	0.038	0.20	0.44	0.27	1.13	0.172	0.010	0.014	0.004	0.42	4.53	100.01	1.65
BR3-B: 40-42 cm	85.6	5.6	1.00	2.01	0.049	0.18	0.45	0.36	1.24	0.171	0.014	0.030	0.056	0.38	2.94	100.12	1.79
BR3-B: 46-48 cm	84.5	1.0	5.98	2.20	0.039	0.20	0.42	0.48	1.24	0.144	0.010	0.020	0.003	0.44	2.97	99.66	1.53
BR3-B: 50-51 cm	85.5	5.7	0.96	2.10	0.040	0.18	0.45	0.27	1.26	0.175	0.013	0.021	0.005	0.82	2.95	100.40	2.35

Table I.I. XRF Results – Mud Belt Cores (all results in weight %)

Sample ID	SiO2	Al2O3	TiO2	Fe2O3	MnO	MgO	CaO	Na2O	K2O	P2O5	SO3	Cr2O3	NiO	H2O-	LOI	Sum	Sulfur
Geo8319: 0 - 2 cm	62.21	8.74	0.48	3.18	0.03	1.74	1.43	2.55	1.91	0.41	0.12	0.02	0.01	3.51	12.82	99.16	5.99
Geo8319: 2 - 4 cm	59.26	9.40	0.49	3.49	0.03	1.90	1.51	2.48	2.08	0.41	0.10	0.04	0.01	3.94	14.04	99.18	3.67
Geo8319: 4 - 6 cm	59.15	9.44	0.50	3.50	0.03	1.95	1.52	2.77	1.97	0.42	0.10	0.02	0.01	3.69	14.49	99.58	3.96
Geo8319: 6 - 8 cm	60.93	9.13	0.49	3.33	0.03	1.86	1.55	2.78	1.87	0.37	0.11	0.02	0.01	3.50	13.60	99.58	4.91
Geo8319: 8 - 10 cm	61.72	8.82	0.48	3.13	0.03	1.75	1.66	2.70	1.80	0.30	0.12	0.02	0.01	3.36	13.35	99.24	3.56
Geo8319: 10 - 12 cm	61.23	9.09	0.49	3.33	0.03	1.77	1.73	2.46	1.89	0.29	0.14	0.02	0.01	3.59	13.41	99.49	4.68
Geo8319: 12 - 14 cm	58.94	9.64	0.49	3.49	0.03	1.97	1.81	2.72	1.92	0.27	0.15	0.09	0.04	3.69	14.11	99.36	4.22
Geo8319: 15 - 17 cm	58.39	9.62	0.50	3.58	0.03	1.86	1.74	2.85	1.93	0.27	0.16	0.03	0.01	4.01	14.24	99.22	4.07
Geo8319: 18 - 20 cm	60.08	9.34	0.50	3.50	0.03	1.94	1.62	2.62	1.90	0.25	0.17	0.02	0.01	3.99	13.67	99.64	4.80
Geo8319: 21 - 23 cm	57.44	9.63	0.49	3.66	0.03	1.90	1.82	2.90	1.96	0.25	0.18	0.02	0.01	4.08	14.79	99.17	5.37
Geo8319: 24 - 26 cm	60.06	9.43	0.50	3.69	0.03	1.92	1.41	2.50	1.98	0.24	0.12	0.02	0.01	3.87	13.43	99.20	4.32
Geo8319: 27 - 29 cm	61.70	9.21	0.52	3.59	0.04	1.92	1.21	2.54	1.94	0.23	0.12	0.03	0.01	3.63	12.41	99.08	3.65
Geo8322: 0 - 1 cm	39.49	12.10	0.52	5.62	0.04	2.91	3.47	4.05	2.24	0.43	0.27	0.03	0.01	5.98	21.91	99.05	3.61
Geo8322: 2 - 3 cm	40.68	12.36	0.53	5.64	0.04	2.74	3.46	3.66	2.33	0.38	0.28	0.03	0.01	6.11	21.11	99.36	3.40
Geo8322: 4 - 5 cm	40.01	12.33	0.53	5.55	0.04	2.81	3.52	3.71	2.41	0.31	0.28	0.03	0.01	6.43	21.13	99.09	4.18
Geo8322: 6 - 7 cm	40.71	12.93	0.54	5.72	0.04	2.90	3.59	3.65	2.50	0.30	0.32	0.03	0.01	6.44	20.26	99.95	4.80
Geo8322: 8 - 9 cm	41.05	12.45	0.53	5.61	0.04	2.73	3.50	3.57	2.47	0.30	0.32	0.03	0.01	6.49	20.26	99.37	6.60
Geo8322: 10 - 11 cm	40.63	12.41	0.54	5.55	0.04	2.77	3.53	3.82	2.35	0.28	0.36	0.03	0.01	6.43	20.29	99.01	5.08
Geo8322: 13 - 14 cm	40.83	12.60	0.54	5.55	0.04	2.70	3.84	3.42	2.38	0.26	0.32	0.03	0.01	6.56	19.94	99.01	2.59
Geo8322: 16 - 17 cm	40.55	12.43	0.52	5.53	0.04	2.72	4.00	3.54	2.35	0.26	0.35	0.03	0.01	6.37	20.77	99.47	8.02
Geo8322: 19 - 20 cm	39.30	12.49	0.54	5.68	0.04	2.88	4.04	3.67	2.43	0.25	0.40	0.03	0.01	5.73	22.04	99.53	6.77
Geo8322: 22 - 23 cm	38.99	12.26	0.52	5.70	0.04	2.93	4.13	3.99	2.27	0.26	0.41	0.03	0.01	5.91	22.40	99.84	5.59
Geo8322: 25 - 26 cm	40.84	12.06	0.52	5.68	0.03	2.90	3.73	3.71	2.25	0.26	0.36	0.03	0.01	6.67	20.52	99.57	8.95
Geo8322: 28 - 29 cm	40.70	11.36	0.50	5.43	0.03	2.86	3.76	4.02	2.11	0.26	0.40	0.03	0.01	6.83	20.97	99.28	6.75
Geo8322: 31 - 32 cm	41.81	11.76	0.52	5.68	0.04	2.90	2.99	3.91	2.27	0.26	0.35	0.03	0.01	7.16	20.13	99.82	8.81
Geo8322: 34 - 35 cm	40.83	12.16	0.53	5.84	0.04	2.91	2.79	3.95	2.36	0.26	0.38	0.03	0.01	7.12	20.01	99.22	7.82
Geo8322: 37 - 38 cm	40.30	11.76	0.51	5.61	0.04	2.88	3.18	3.88	2.28	0.25	0.39	0.03	0.01	6.52	21.61	99.25	5.44
Geo8322: 40 - 41 cm	40.25	12.15	0.53	5.65	0.04	2.99	3.97	3.60	2.27	0.25	0.36	0.03	0.01	5.76	22.01	99.88	6.12

Table I.J. ICP-MS Results – Olifants River Cores (all results in ppm)

Sample ID	P	V	Cr	Mn	Co	Ni	Cu	Zn	As	Se	Rb	Sr	Mo	Cd	Ba	Pb
OE2-A: 0-2 cm	551.6	34.5	30.5	147.2	4.2	10.0	11.7	48.3	2.6	0.9	37.1	234.6	1.5	0.2	133.4	7.4
OE2-A: 2-4 cm	708.7	33.4	31.6	148.1	4.4	10.1	11.0	47.3	2.5	0.2	37.1	214.9	2.1	0.2	132.9	7.6
OE2-A: 4-6 cm	527.4	34.5	29.9	150.5	4.6	10.6	12.6	54.9	3.0	0.3	40.9	240.1	1.8	0.2	145.0	8.2
OE2-A: 6-8 cm	532.7	21.0	24.3	141.2	3.3	7.6	7.9	37.9	2.7	0.3	28.1	210.4	1.0	0.2	111.1	5.9
OE2-A: 8-10 cm	521.1	28.3	28.0	134.8	3.6	7.9	8.7	41.0	2.6	0.2	28.4	200.4	0.7	0.1	113.1	6.3
OE2-A: 10-12 cm	623.6	25.4	29.3	138.7	3.9	9.0	9.2	44.2	2.4	0.4	32.1	234.5	0.6	0.1	126.0	6.8
OE2-A: 14-16.5 cm	582.9	27.2	25.6	133.6	3.5	8.1	9.2	38.2	1.7	0.4	29.9	198.9	0.4	0.2	110.6	6.6
OE2-A: 19-22 cm	575.7	29.6	28.5	135.5	4.0	9.4	11.2	47.2	2.8	0.3	38.8	202.0	0.6	0.2	136.8	8.1
OE3-B: 0-2 cm	403.7	62.3	85.3	614.9	10.6	21.1	14.3	60.5	3.2	0.6	64.9	114.3	0.3	0.0	370.6	10.4
OE3-B: 2-4 cm	344.9	57.4	95.7	384.6	9.5	19.8	11.5	52.8	2.6	0.4	53.5	94.7	0.2	0.1	310.8	9.1
OE3-B: 4-6 cm	323.6	56.6	95.4	372.1	9.2	19.0	10.8	50.5	2.3	0.4	49.6	83.5	0.3	0.0	267.5	8.8
OE3-B: 6-8 cm	321.3	60.7	81.8	343.3	9.0	17.8	10.9	51.8	2.6	0.5	52.5	87.0	0.2	0.0	306.0	9.1
OE3-B: 8-10 cm	297.0	54.4	87.3	323.2	8.3	17.0	10.4	45.3	2.3	0.6	46.1	75.5	0.2	0.0	269.3	8.4
OE3-B: 12-14 cm	283.6	50.9	78.5	298.4	7.9	16.5	10.0	46.5	2.4	0.1	46.9	74.6	0.2	0.0	259.0	8.4
OE3-B: 16-17 cm	378.7	60.9	104.2	434.7	10.2	21.7	12.5	56.4	3.0	0.4	58.7	107.2	0.3	0.0	344.9	9.9
OE4-A: 0-2 cm	665.7	104.7	83.4	693.7	16.0	30.9	37.9	141.5	8.3	0.8	71.8	117.9	1.3	0.2	347.7	17.3
OE4-A: 2-4 cm	683.8	105.4	81.4	915.0	17.7	32.9	43.8	137.5	9.0	1.1	103.0	126.8	1.3	0.2	377.3	19.8
OE4-A: 4-6 cm	696.5	104.4	81.4	864.9	16.5	30.8	41.0	126.0	8.1	0.2	96.3	125.3	0.8	0.1	373.0	18.0
OE4-A: 6-8 cm	723.6	110.7	83.5	984.2	17.2	32.8	41.1	141.0	8.1	0.2	98.4	128.4	0.9	0.1	384.1	18.7
OE4-A: 8-10 cm	700.6	106.5	83.5	946.5	16.7	31.7	43.0	156.8	8.2	0.5	92.2	125.7	0.9	0.1	378.7	22.0

Table I.K. ICP-MS Results –Berg River Cores

Sample ID	P	V	Cr	Mn	Co	Ni	Cu	Zn	As	Se	Rb	Sr	Mo	Cd	Ba	Pb
BR1-A: 0-2 cm	846.7	66.8	72.8	120.9	6.4	23.7	21.3	111.9	10.4	1.3	101.3	115.2	0.8	1.8	246.5	16.7
BR1-A: 2-4 cm	812.2	54.6	58.7	98.7	5.2	18.4	15.9	87.9	7.7	0.2	84.1	97.5	0.7	1.3	217.5	14.0
BR1-A: 4-6 cm	844.8	48.8	52.2	91.8	4.6	16.3	13.3	74.7	7.1	0.9	77.9	94.0	0.5	1.1	195.4	13.0
BR1-A: 6-8 cm	751.0	44.2	45.8	93.2	4.0	13.9	12.7	72.8	5.8	0.5	69.1	88.9	0.5	1.0	179.0	11.5
BR1-A: 8-10 cm	918.3	50.0	51.9	111.3	4.6	16.1	14.6	77.2	6.5	0.5	77.5	86.9	0.6	1.0	191.8	12.6
BR1-A: 12-14 cm	801.6	42.1	43.9	97.2	3.9	13.4	13.0	67.1	5.3	0.5	66.6	81.3	0.5	1.0	175.5	11.2
BR1-A: 16-18 cm	778.6	41.7	43.4	95.9	3.8	13.0	11.6	65.6	5.6	0.8	65.1	75.8	0.7	0.9	166.0	11.0
BR1-A: 20-22 cm	345.0	35.6	35.7	71.3	3.3	11.5	11.5	64.0	5.3	0.3	63.1	69.3	0.9	1.0	175.3	11.1
BR1-A: 24-26 cm	410.1	38.8	38.5	80.1	3.8	12.7	14.2	59.9	5.8	0.5	66.4	77.1	1.1	0.9	187.1	11.5
BR1-A: 28-30 cm	470.0	42.7	41.9	91.4	3.9	13.6	14.0	66.1	5.9	0.5	69.5	75.4	0.9	0.9	190.4	11.7
BR1-A: 34-36 cm	504.7	49.9	50.0	94.4	4.6	15.6	15.7	75.4	6.5	0.5	76.8	80.1	1.8	1.1	206.6	13.0
BR1-A: 40-42 cm	480.5	47.3	44.9	103.0	4.4	14.5	13.7	68.6	5.8	0.1	73.4	71.8	1.0	0.7	191.3	12.1
BR1-A: 46-48 cm	399.6	34.1	32.3	70.4	3.2	10.3	11.6	50.3	4.2	0.7	58.9	62.0	0.8	0.5	146.3	9.4
BR1-A: 52-55 cm	485.4	42.8	39.3	84.5	3.9	12.7	13.3	66.1	4.6	0.8	69.9	71.8	0.6	0.5	186.0	11.6
BR2: 0-2 cm	679.3	70.7	63.0	146.4	7.5	21.7	19.3	117.8	9.2	0.6	101.5	70.1	1.3	0.9	256.7	33.0
BR2: 2-4 cm	557.3	55.2	49.8	75.8	5.5	16.0	15.2	91.8	6.7	0.8	51.6	26.0	0.8	0.7	120.6	13.5
BR2: 4-6 cm	721.8	66.6	61.3	133.9	6.6	19.4	18.1	111.0	8.4	0.7	92.8	69.3	1.0	0.9	245.5	16.8
BR2: 6-8 cm	729.2	69.7	61.9	141.0	7.0	20.4	18.8	111.3	8.3	0.5	100.1	66.8	1.1	0.9	248.5	17.0
BR2: 8-10 cm	715.2	62.8	57.2	136.9	6.1	17.9	17.3	102.3	7.7	0.8	77.8	58.0	1.0	0.9	188.1	15.0
BR2: 12-14 cm	660.7	60.0	53.7	127.0	6.1	17.0	16.4	104.6	7.4	0.6	69.0	47.8	1.2	0.9	167.9	13.8
BR2: 16-18 cm	707.6	76.4	66.9	153.8	7.6	22.3	19.4	116.0	8.2	0.7	105.0	71.3	1.6	1.0	263.8	17.3
BR2: 20-22 cm	691.2	73.6	64.2	149.7	7.5	21.0	19.1	105.9	7.0	0.5	98.0	65.7	1.3	0.9	250.8	16.8
BR2: 24-26 cm	551.4	62.2	53.2	148.4	6.2	17.3	14.6	97.5	6.0	0.4	87.6	59.2	1.0	0.8	231.6	15.0
BR2: 28-30 cm	617.6	67.6	57.9	152.9	6.8	19.0	17.1	103.5	6.1	0.7	93.4	65.7	1.2	0.9	242.1	15.9
BR2: 32-34 cm	634.0	67.4	61.0	153.6	6.6	19.3	16.0	95.7	6.5	0.6	94.7	63.9	1.4	1.0	242.2	15.5
BR2: 38-40 cm	658.1	70.7	64.6	154.6	6.8	20.3	16.2	95.3	7.3	0.2	95.7	69.2	1.9	1.1	243.8	15.7
BR2: 44-46 cm	635.7	71.0	65.6	144.2	6.8	20.9	18.2	93.2	7.0	0.2	99.5	66.8	1.7	1.0	251.0	15.9
BR2: 50-52 cm	526.1	56.5	51.1	77.2	5.4	17.3	13.8	68.8	5.6	0.5	53.2	28.9	1.5	1.0	104.2	12.0
BR2: 58-60cm	628.4	62.9	59.0	147.0	6.0	18.1	16.0	89.0	5.8	0.4	89.4	59.6	1.2	0.9	225.5	14.4
BR2: 66-68 cm	731.5	77.3	70.2	157.7	7.9	22.8	25.0	103.9	8.7	0.4	103.5	80.4	1.8	1.4	251.5	18.0
BR2: 74-76 cm	540.4	67.8	61.9	151.6	6.9	20.2	16.3	75.0	7.5	0.7	91.1	91.0	2.0	1.3	241.1	16.3
BR3-B: 0-2 cm	458.6	29.2	23.6	192.3	2.6	5.3	7.2	45.7	2.9	0.8	31.3	38.0	0.3	0.3	112.9	7.5
BR3-B: 2-4 cm	589.1	35.3	31.0	208.8	3.2	6.5	8.1	62.4	3.7	0.1	43.0	51.1	0.4	0.5	162.3	9.5
BR3-B: 4-6 cm	663.3	37.2	31.4	225.6	3.4	6.9	8.7	65.2	4.3	0.3	38.1	44.2	0.4	0.4	137.7	9.9
BR3-B: 6-8 cm	641.1	32.7	26.5	184.2	3.0	6.0	7.3	56.5	3.5	0.2	33.0	41.6	0.3	0.4	139.0	8.6
BR3-B: 8-10 cm	542.8	35.9	29.0	157.9	3.4	6.9	9.1	54.7	3.3	0.3	34.1	37.3	0.4	0.5	142.4	9.0
BR3-B: 12-14 cm	621.9	37.2	31.1	169.6	3.3	7.0	8.4	58.8	3.1	0.3	43.8	48.6	0.3	0.5	163.0	10.0
BR3-B: 16-18 cm	557.3	34.3	29.1	142.6	3.0	6.2	7.5	53.6	2.6	0.4	37.8	44.0	0.3	0.3	151.3	8.8
BR3-B: 20-22 cm	508.5	37.8	31.8	159.0	3.6	7.7	10.2	69.1	3.1	0.8	45.4	49.8	0.4	0.5	167.1	10.4

Table I.K (cont.)

Sample ID	P	V	Cr	Mn	Co	Ni	Cu	Zn	As	Se	Rb	Sr	Mo	Cd	Ba	Pb
BR3-B: 24-26 cm	538.4	35.7	30.1	174.2	3.2	7.0	8.3	60.5	3.1	0.7	44.5	49.2	0.3	0.4	162.2	9.8
BR3-B: 28-30 cm	518.3	37.1	31.3	155.7	3.4	7.3	9.2	56.0	3.2	0.6	43.6	47.7	0.4	0.6	164.5	10.1
BR3-B: 34-36 cm	516.2	38.2	31.2	156.8	3.7	7.5	8.7	55.4	3.0	0.9	45.5	49.0	0.4	0.6	166.5	10.4
BR3-B: 40-42 cm	407.3	34.5	29.6	180.1	3.4	7.3	8.0	47.4	2.9	1.2	33.1	33.9	0.5	0.5	122.9	9.0
BR3-B: 46-48 cm	394.2	38.0	34.0	135.8	3.5	8.0	8.8	51.1	2.5	0.5	36.6	32.1	0.4	0.5	120.6	9.9
BR3-B: 50-51 cm	529.0	39.0	33.7	166.3	3.8	8.2	9.0	65.5	3.1	0.9	46.6	48.4	0.5	0.6	159.3	10.4

Table I.L Trace Element Concentrations – Mud Belt Sediment Cores (all data in ppm)

Sample ID	P	V	Cr	Mn	Co	Ni	Cu	Zn	As	Se	Rb	Sr	Mo	Cd	Ba	Pb
Geo8319: 0 - 2 cm		60.91	90.24	181.89	6.56	39.22	41.86	58.08	33.15	0.03	87.43	117.99	4.71	0.99	294.13	4.53
Geo8319: 2 - 4 cm		70.84	111.82	200.05	7.38	44.92	51.98	71.10	36.37	n.d.	97.05	121.05	5.65	1.26	312.59	6.75
Geo8319: 4 - 6 cm		70.43	127.41	194.69	7.36	46.58	31.38	65.12	38.73	0.49	98.01	120.25	5.64	0.95	309.52	4.04
Geo8319: 6 - 8 cm		66.64	114.96	189.44	6.83	43.25	33.81	56.39	32.55	0.92	91.07	113.87	5.68	1.03	288.04	3.53
Geo8319: 8 - 10 cm		65.57	112.79	184.74	6.70	42.71	27.42	52.31	29.01	n.d.	89.23	117.99	6.85	0.67	285.57	3.32
Geo8319: 10 - 12 cm		73.77	168.70	196.72	7.40	45.64	28.89	57.07	27.56	2.01	95.55	121.35	9.19	0.95	288.06	3.24
Geo8319: 12 - 14 cm		80.30	139.85	197.53	7.84	50.07	30.47	56.28	26.17	1.06	98.22	128.32	11.44	0.99	284.97	3.48
Geo8319: 15 - 17 cm		76.50	132.03	180.87	7.38	49.04	40.09	50.27	21.27	0.23	92.55	112.38	12.45	1.16	254.92	37.96
Geo8319: 18 - 20 cm		76.94	142.15	193.50	7.59	49.40	40.48	57.17	19.20	0.81	95.54	120.31	14.16	1.48	279.28	3.71
Geo8319: 21 - 23 cm		78.12	125.03	198.64	8.02	52.20	31.98	56.37	18.50	1.80	98.48	127.29	13.36	1.03	286.32	3.05
Geo8319: 24 - 26 cm		57.19	87.84	134.91	5.68	37.45	36.97	47.57	11.34	n.d.	74.72	75.14	11.74	1.48	155.36	3.96
Geo8319: 27 - 29 cm		54.55	88.21	139.69	5.64	39.30	33.04	52.51	10.56	1.21	80.21	80.28	10.88	1.59	181.14	17.97
Geo8322: 0 - 1 cm		101.92	156.77	254.13	11.89	79.55	38.54	74.00	14.64	0.52	117.69	190.78	4.68	0.17	311.25	1.89
Geo8322: 2 - 3 cm		97.06	150.67	232.91	11.31	76.38	41.14	74.08	10.89	1.01	116.23	178.18	4.80	0.18	303.89	1.78
Geo8322: 4 - 5 cm		110.66	173.70	287.74	13.07	86.20	64.65	90.24	12.98	n.d.	146.83	216.34	5.69	0.40	363.75	2.67
Geo8322: 6 - 7 cm		108.60	174.14	278.67	12.78	84.23	49.44	82.97	13.08	n.d.	133.02	202.61	6.55	0.27	364.07	2.18
Geo8322: 8 - 9 cm		114.60	187.79	294.31	13.64	90.41	52.53	95.99	13.71	0.25	129.14	228.31	7.36	0.14	402.26	3.57
Geo8322: 10 - 11 cm		115.67	190.32	296.47	13.52	90.64	52.13	88.63	14.07	n.d.	129.81	225.28	9.13	0.17	386.41	36.42
Geo8322: 13 - 14 cm		114.71	186.28	288.90	13.66	89.77	37.51	84.04	14.55	n.d.	135.62	231.19	12.53	0.17	388.25	2.47
Geo8322: 16 - 17 cm		119.17	190.69	289.97	13.79	92.38	39.49	85.55	16.18	n.d.	138.19	239.80	15.56	0.16	383.24	2.63
Geo8322: 19 - 20 cm		115.35	190.68	279.73	13.28	94.62	61.38	78.99	16.66	n.d.	106.13	253.72	17.51	0.14	400.84	6.17
Geo8322: 22 - 23 cm		117.35	196.84	277.41	13.78	99.79	38.00	79.91	15.94	n.d.	125.95	240.03	20.12	0.21	364.80	1.97
Geo8322: 25 - 26 cm		113.79	195.88	280.65	13.83	101.39	40.77	74.40	14.78	n.d.	124.42	225.72	17.66	0.18	373.55	2.18
Geo8322: 28 - 29 cm		108.50	201.46	277.69	13.37	103.04	59.18	78.91	12.28	0.32	119.41	230.77	14.62	0.31	372.28	21.79
Geo8322: 31 - 32 cm		111.44	202.02	282.41	13.46	104.59	57.13	75.39	14.55	n.d.	132.06	201.17	14.64	0.15	374.60	2.13
Geo8322: 34 - 35 cm		111.36	209.21	294.77	14.09	107.12	60.50	96.21	12.00	1.09	140.01	191.72	14.08	0.41	383.95	2.53
Geo8322: 37 - 38 cm		110.73	210.53	290.52	13.85	106.30	53.76	86.37	11.78	1.67	132.11	211.68	13.98	0.25	375.40	2.30
Geo8322: 40 - 41 cm		110.63	213.88	312.77	14.04	107.84	48.83	84.90	11.36	1.14	130.65	232.36	19.28	0.28	378.65	2.49

Table I.M – ICP-MS Major Elements results - Mud Belt cores

Sample ID	Mg	Al	K	Ca	Fe
Geo8319: 0 - 2 cm	10527	49959	18358	10288	24240
Geo8319: 2 - 4 cm	11938	55482	19210	10919	27586
Geo8319: 4 - 6 cm	11778	55341	17750	10190	28329
Geo8319: 6 - 8 cm	11314	50987	16397	10641	24893
Geo8319: 8 - 10 cm	11239	50684	16400	11724	24172
Geo8319: 10 - 12 cm	11759	53896	17349	12251	26299
Geo8319: 12 - 14 cm	12632	55576	16324	13542	26956
Geo8319: 15 - 17 cm	11849	48938	14871	11944	25089
Geo8319: 18 - 20 cm	12014	52836	17906	11369	26801
Geo8319: 21 - 23 cm	12389	55127	18122	12496	28561
Geo8319: 24 - 26 cm	9002	34886	10377	7525	19153
Geo8319: 27 - 29 cm	10277	39009	11605	7543	19083
Geo8322: 0 - 1 cm	19247	70569	19274	24014	45645
Geo8322: 2 - 3 cm	17268	63006	20386	23213	42149
Geo8322: 4 - 5 cm	20660	82755	25934	24838	49266
Geo8322: 6 - 7 cm	18766	75305	24997	24618	48306
Geo8322: 8 - 9 cm	21372	86207	25800	27946	53276
Geo8322: 10 - 11 cm	21395	84517	24042	28640	52777
Geo8322: 13 - 14 cm	20879	85147	24332	30583	51949
Geo8322: 16 - 17 cm	21086	85390	24653	32175	52780
Geo8322: 19 - 20 cm	19680	80413	25598	31965	52115
Geo8322: 22 - 23 cm	21808	82003	23194	32739	53532
Geo8322: 25 - 26 cm	21958	81828	23066	29581	53388
Geo8322: 28 - 29 cm	21785	78270	21961	30558	52305
Geo8322: 31 - 32 cm	22251	79421	23208	23692	53033
Geo8322: 34 - 35 cm	22713	83612	24751	21658	56472
Geo8322: 37 - 38 cm	22713	82994	24732	25793	55685
Geo8322: 40 - 41 cm	22391	83973	23547	31242	54885

Table I.N – Olifants River Estuary Sediment C:H:N Analyses

	Total			Organic		
Sample ID	C	H	N	C	H	N
OE2-A: 0-2 cm	1.7	0.3	0.1	1.0	0.7	0.6
OE2-A: 2-4 cm	1.3	0.2	0.1	0.4	0.3	0.1
OE2-A: 4-6 cm	1.4	0.3	0.1	0.6	0.2	0.1
OE2-A: 6-8 cm	1.1	0.1	0.0	0.2	0.1	0.0
OE2-A: 8-10 cm	1.3	0.1	0.1	0.3	0.1	0.1
OE2-A: 10-12 cm	1.1	0.2	0.1	0.3	0.4	0.1
OE2-A: 14-16.5 cm	1.3	0.2	0.1	0.2	0.1	0.0
OE2-A: 19-22 cm	1.2	0.2	0.1	0.3	0.2	0.1
OE3-B: 0-2 cm	0.2	0.1	0.0	0.3	0.3	0.3
OE3-B: 2-4 cm	0.1	0.1	0.0	0.3	0.3	0.2
OE3-B: 4-6 cm	0.2	0.1	0.0	0.5	0.4	0.4
OE3-B: 6-8 cm	0.1	0.1	0.0	0.3	0.2	0.2
OE3-B: 8-10 cm	0.1	0.1	0.0	0.2	0.2	0.1
OE3-B: 12-14 cm	0.1	0.1	0.0	0.3	0.2	0.1
OE3-B: 16-17 cm	0.1	0.1	0.0	0.3	0.3	0.3
OE4-A: 0-2 cm	1.1	0.8	0.2	1.2	0.7	0.7
OE4-A: 2-4 cm	1.0	0.8	0.2	1.3	1.0	1.1
OE4-A: 4-6 cm	0.8	0.7	0.1	0.9	0.9	0.6
OE4-A: 6-8 cm	0.7	0.7	0.1	1.0	0.9	0.6
OE4-A: 8-10 cm	0.7	0.6	0.1	0.9	0.8	0.6
OE4-A: 12-14 cm	0.9	0.7	0.1	0.8	0.7	0.3
OE4-A: 16-18 cm	0.8	0.7	0.1	0.9	0.8	0.4
OE4-A: 20-22.5 cm	0.9	0.7	0.1	1.0	0.9	0.5
OE6: 0-2 cm	0.9	0.4	0.1	0.9	0.5	0.4
OE6: 2-4 cm	0.8	0.4	0.1	1.1	0.6	0.4
OE6: 4-6 cm	0.9	0.4	0.1	1.0	0.6	0.5
OE6: 6-8 cm	0.8	0.4	0.1	0.9	0.7	0.5
OE6: 8-10 cm	0.7	0.4	0.1	0.9	0.6	0.4
OE6: 12-14 cm	0.9	0.5	0.1	0.8	0.6	0.2
OE6: 16-18 cm	0.8	0.5	0.1	0.9	0.6	0.3

Table I.O. – Berg River Estuary Sediment C:H:N Analyses

	Total			Organic		
Sample ID	C	H	N	C	H	N
BR1-A: 0-2 cm	2.5	0.7	0.3	1.9	1.0	0.5
BR1-A: 2-4 cm	1.7	0.7	0.2	1.2	0.6	0.2
BR1-A: 4-6 cm	2.3	0.8	0.3	1.1	0.7	0.2
BR1-A: 6-8 cm	1.4	0.5	0.2	0.8	0.3	0.1
BR1-A: 8-10 cm	1.4	0.6	0.2	1.1	0.6	0.3
BR1-A: 12-14 cm	1.2	0.4	0.1	0.8	0.3	0.1
BR1-A: 16-18 cm	1.2	0.4	0.1	0.7	0.3	0.1
BR1-A: 20-22 cm	1.1	0.5	0.1	0.7	0.3	0.1
BR1-A: 24-26 cm	1.2	0.7	0.1	0.7	0.3	0.1
BR1-A: 28-30 cm	1.2	0.7	0.1	0.7	0.3	0.1
BR1-A: 34-36 cm	1.5	0.8	0.2	0.9	0.5	0.1
BR1-A: 40-42 cm	1.2	0.7	0.1	0.7	0.4	0.1
BR1-A: 46-48 cm	1.1	0.6	0.1	0.6	0.3	0.1
BR1-A: 52-55 cm	0.9	0.5	0.1	0.5	0.3	0.1
BR2: 0-2 cm	1.4	0.8	0.2	1.8	0.8	0.3
BR2: 2-4 cm	1.1	0.7	0.1	1.0	0.8	0.4
BR2: 4-6 cm	1.2	0.7	0.2	1.0	0.8	0.3
BR2: 6-8 cm	1.2	0.6	0.2	1.3	0.9	0.4
BR2: 8-10 cm	1.1	0.6	0.1	1.2	0.8	0.4
BR2: 12-14 cm	1.1	0.6	0.1	0.8	0.6	0.3
BR2: 16-18 cm	1.3	0.6	0.2	1.1	0.8	0.3
BR2: 20-22 cm	1.0	0.7	0.1	0.9	0.7	0.3
BR2: 24-26 cm	0.9	0.6	0.1	0.9	0.7	0.3
BR2: 28-30 cm	1.0	0.6	0.1	0.9	0.7	0.3
BR2: 32-34 cm	1.0	0.7	0.1	0.9	0.7	0.3
BR2: 38-40 cm	1.1	0.7	0.1	0.9	0.7	0.4
BR2: 44-46 cm	1.1	0.6	0.2	1.1	0.8	0.4
BR2: 50-52 cm	1.0	0.6	0.1	1.1	0.8	0.4
BR2: 58-60cm	1.0	0.6	0.1	0.9	0.7	0.3
BR2: 66-68 cm	1.3	0.8	0.2	1.3	0.9	0.4
BR2: 74-76 cm	1.6	0.7	0.1	1.2	0.8	0.3
BR3-B: 0-2 cm	0.5	0.3	0.1	0.4	0.3	0.1
BR3-B: 2-4 cm	0.4	0.2	0.0	0.3	0.1	0.1
BR3-B: 4-6 cm	0.5	0.3	0.1	0.4	0.3	0.1
BR3-B: 6-8 cm	0.4	0.2	0.0	0.3	0.2	0.1
BR3-B: 8-10 cm	0.5	0.3	0.1	0.4	0.2	0.1
BR3-B: 12-14 cm	0.5	0.3	0.0	0.4	0.3	0.2
BR3-B: 16-18 cm	0.4	0.2	0.0	0.3	0.2	0.1
BR3-B: 20-22 cm	0.4	0.3	0.0	0.5	0.1	0.1
BR3-B: 24-26 cm	0.4	0.2	0.0	0.3	0.2	0.1
BR3-B: 28-30 cm	0.4	0.2	0.0	0.3	0.2	0.1
BR3-B: 34-36 cm	0.4	0.3	0.0	0.4	0.3	0.1
BR3-B: 40-42 cm	0.5	0.3	0.1	0.4	0.3	0.1
BR3-B: 46-48 cm	0.4	0.3	0.0	0.4	0.3	0.1
BR3-B: 50-51 cm	0.5	0.3	0.1	0.4	0.2	0.1

Table I.P. Mud Belt Sediment C:H:N Analyses

	Total			Organic		
Sample ID	C	H	N	C	H	N
Geo8319-1: 0 - 2 cm	4.1	5.7	0.6	4.5	2.2	1.0
Geo8319-1: 2 - 4 cm	4.8	-0.6	0.6	5.4	8.4	1.3
Geo8319-1: 4 - 6 cm	4.5	-0.8	0.6	4.3	1.2	0.8
Geo8319-1: 6 - 8 cm	4.4	0.7	0.6	4.3	1.5	0.9
Geo8319-1: 8 - 10 cm	4.7	0.5	0.6	4.4	2.6	1.8
Geo8319-1: 10 - 12 cm	4.6	0.7	0.6	4.3	2.5	0.8
Geo8319-1: 12 - 14 cm	4.7	0.7	0.6	4.3	1.2	0.8
Geo8319-1: 15 - 17 cm	4.8	0.1	0.6	5.4	4.3	1.0
Geo8319-1: 18 - 20 cm	4.8	0.3	0.6	4.2	2.2	0.7
Geo8319-1: 21 - 23 cm	5.0	1.0	0.6	5.3	2.4	0.9
Geo8319-1: 24 - 26 cm	4.3	0.9	0.5	4.2	2.1	0.7
Geo8319-1: 27 - 29 cm	4.1	0.4	0.5	3.8	2.0	7.7
Geo8322-1: 0 - 1 cm	6.9	-3.5	0.9	8.2	5.4	1.7
Geo8322-1: 2 - 3 cm	7.0	-8.1	0.9	8.3	5.2	1.7
Geo8322-1: 4 - 5 cm	7.1	-3.6	0.9	8.1	5.6	1.6
Geo8322-1: 6 - 7 cm	7.4	-16.1	0.9	8.1	16.0	1.6
Geo8322-1: 8 - 9 cm	7.3	-8.5	0.9	8.0	6.4	1.7
Geo8322-1: 10 - 11 cm	7.2	-8.9	0.9	8.1	5.8	1.5
Geo8322-1: 13 - 14 cm	7.2	-9.9	0.9	7.9	8.1	1.7
Geo8322-1: 16 - 17 cm	7.1	-2.0	0.9	7.9	16.4	2.3
Geo8322-1: 19 - 20 cm	7.4	-9.3	0.9	8.0	9.1	1.7
Geo8322-1: 22 - 23 cm	7.5	-2.9	0.9	8.5	9.2	1.7
Geo8322-1: 25 - 26 cm	7.3	-1.2	0.9	8.4	7.9	1.7
Geo8322-1: 28 - 29 cm	7.4	-13.8	0.9	8.7	11.4	2.4
Geo8322-1: 31 - 32 cm	7.0	-2.0	0.9	8.6	11.2	2.1
Geo8322-1: 34 - 35 cm	7.3	-12.1	0.9	8.6	7.0	1.9
Geo8322-1: 37 - 38 cm	7.5	-13.9	0.9	8.9	10.4	1.9
Geo8322-1: 40 - 41 cm	7.1	-6.9	0.8	8.6	10.4	1.7

Table I.Q. Data Quality for Surface Water Samples
(values in ηmol/L unless specified otherwise)

Element	# of standards	# of duplicates	Mean Value Recorded	Mean Error	S.T.D. of Errors
Mg (mmol/L)	1	8	50371	11503	8306
Al (mmol/L)	1	8	2.02	0.94	1.46
Si (mmol/L)	1	8	32.83	6.24	6.63
P (mmol/L)	1	8	4.46	1.90	2.00
K (mmol/L)	1	8	7680	1672	1131
Ca (mmol/L)	1	8	5511	1092	701
V	1	8	977	355	425
Cr	1	8	172	226	360
Mn	1	8	492	59	56
Fe (mmol/L)	1	8	16.50	3.55	2.86
Co	1	8	11.18	2.32	1.84
Ni	1	8	190	40	45
Cu	1	8	719	309	331
Zn (mmol/L)	1	8	1.941	1.303	2.244
As (mmol/L)	1	8	0.887	0.161	0.172
Se	1	8	1567	284	162
Rb	1	8	820	162	137
Sr (mmol/L)	1	8	63.1	12.1	8.5
Mo	1	8	82.2	15.4	9.8
Cd	1	8	1.645	0.707	1.099
Ba	1	8	129.40	15.42	8.66
Pb	1	8	5.93	7.89	11.85

Appendix II

Table 1. Analytical conditions for determination of major elements using a Philips PW1480 WDXRF spectrometer.

Element /line	Collimator	Crystal	Detector	PHS LWL	PHS UPL	Counting time (s)	Concentration range **	RMS	Lower limits of determination*	No. of standards
NiKα	F	LiF(220)	FS	22	70	100	0 - 0.48	0.003	0.004	11
FeKα	F	LiF(220)	FL	16	68	100	0 - 17	0.069	0.019	20
MnKα	F	LiF(220)	FL	15	66	100	0 - 0.27	0.004	0.014	22
CrKα	F	LiF(220)	FL	14	70	100	0 - 3.5	0.011	0.008	11
TiKα	F	LiF(200)	FL	32	68	100	0 - 3.9	0.022	0.023	22
CaKα	F	LiF(200)	FL	30	76	50	0 - 77	0.102	0.004	21
KKα	F	LiF(200)	FL	32	74	100	0 - 15.5	0.037	0.003	21
S Kα	C	GE(111)	FL	32	74	100	0 - 53.5	0.112	0.100	11
P Kα	C	GE(111)	FL	34	74	100	0 - 3.4	0.011	0.008	16
SiKα	C	PE(002)	FL	26	80	100	0 - 100	0.215	0.052	20
AlKα	C	PE(002)	FL	26	80	100	0 - 100	0.084	0.074	21
MgKα	F	PX-1	FL	36	68	100	0 - 85	0.141	0.102	20
NaKα	F	PX-1	FL	30	78	100	0 - 9.1	0.065	0.17	12

** all concentrations expressed as wt% oxide; S as SO_3

* = 10 H lower limit of detection, expressed as wt% oxide

From Willis, 1999.

Table II.B – Sediment Trace Element Concentrations for Duplicates (ppm)

Sample ID	P	V	Cr	Mn	Co	Ni	Cu	Zn	As	Se	Rb	Sr	Mo	Cd	Ba	Pb
OE3-B: 2 – 4cm DUP	363	61.8	92.3	372	9.61	19.64	11.65	59.0	2.87	0.53	51.1	94.0	0.281	0.034	301.6	9.76
OE4-A: 16 - 18cm DUP	703	106.6	83.2	862	17.02	32.57	46.18	150.4	9.05	0.48	103.2	141.9	0.852	0.156	397.3	19.61
OE6: 0 - 2cm DUP	387	52.8	39.5	161	7.18	14.37	18.30	80.5	5.12	0.62	44.7	56.8	0.714	0.171	170.9	11.22
BR1-A: 0 – 2cm DUP	1215	72.8	76.6	101	6.25	23.44	19.11	98.8	9.86	1.10	83.4	89.7	0.703	1.572	170.7	16.36
BR1-A: 34 - 36cm DUP	655	55.3	51.3	103	4.88	16.74	15.24	78.0	7.05	1.18	76.4	85.5	1.805	1.117	195.5	13.58
BR2 4 – 6cm DUP	861	75.6	62.8	142	6.83	19.59	17.95	105.7	8.57	0.64	85.6	63.6	1.012	0.918	225.5	16.40
BR2 12 - 14cm DUP	862	72.5	61.6	153	6.84	18.79	18.03	102.0	7.94	0.60	88.2	68.5	1.244	0.908	233.4	15.57
BR3-B: 4 – 6cm DUP	914	42.3	33.8	258	3.64	7.24	7.78	91.1	4.41	0.38	43.7	51.9	0.414	0.445	159.3	10.46